



**UNIVERSIDADE FEDERAL DO PARÁ
INSTITUTO DE GEOCIÊNCIAS
PROGRAMA DE PÓS-GRADUAÇÃO EM GEOLOGIA E GEOQUÍMICA**

DISSERTAÇÃO DE MESTRADO Nº 546

**ESTRATIGRAFIA E PALEOAMBIENTE DA FORMAÇÃO
PASTOS BONOS, JURÁSSICO-CRETÁCEO DA BACIA DO
PARNAÍBA**

Dissertação apresentada por:

ALEXANDRE RIBEIRO CARDOSO

Orientador: Prof. Dr. Afonso César Rodrigues Nogueira (UFPA)

**BELÉM
2019**

Dados Internacionais de Catalogação e Publicação (CIP)

Biblioteca do Instituto de Geociências

Cardoso, Alexandre Ribeiro 1994-

Estratigrafia e paleoambiente da Formação Pastos Bons, Jurássico-Cretáceo da Bacia do Parnaíba. – 2019.

xv, 93: il ; 30 cm

Inclui bibliografias

Orientador: Afonso César Rodrigues Nogueira

Dissertação (Mestrado) – Universidade Federal do Pará, Instituto de Geociências, Faculdade de Geologia, Belém, 2019.

1. Paleoambiente. – 2. Sistema lacustre. – 3. Formação Pastos Bons. – 4. Jurássico-Cretáceo. I. Título.

CDD 22 ed.: 552.509813



Universidade Federal do Pará
Instituto de Geociências
Programa de Pós-Graduação em Geologia e Geoquímica

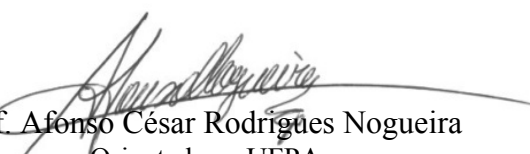
**ESTRATIGRAFIA E PALEOAMBIENTE DA FORMAÇÃO
PASTOS BONS, JURÁSSICO-CRETÁCEO DA BACIA DO
PARNAÍBA**

**DISSERTAÇÃO APRESENTADA POR:
ALEXANDRE RIBEIRO CARDOSO**

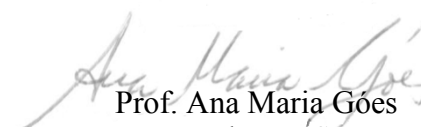
**Como requisito parcial à obtenção do Grau de Mestre em Ciências na Área de
GEOLOGIA**

Data de Aprovação: 06 / 03 / 2019

Banca Examinadora:


Prof. Afonso César Rodrigues Nogueira
Orientador – UFPA


Prof. Joelson Lima Soares
Membro – UFPA


Prof. Ana Maria Góes
Membro - USP

Aos meus pais,
minhas forças motrizes.

AGRADECIMENTOS

Agradeço aos meus pais, Cintia Ribeiro e Azarias Cardoso, pelo apoio, investimentos e ensinamentos. Obrigado por me abrirem o mundo, por me incentivarem em todas as horas, por serem meus exemplos de pessoas e por entenderem a minha ausência em muitos momentos.

Ao meu irmão, Alessandro Cardoso, e aos meus avós, Ruth e Virgílio Cardoso; José Ribeiro e Amparo Rufino; a minha avó de coração – Vó Pastora (*in memorian*), pelo carinho e palavras de confiança.

Ao Prof. Dr. Afonso Nogueira, pela amizade, pelas oportunidades, por me inserir na ciência e pelas infundáveis e divertidas discussões geológicas.

Aos Profs. Drs. Joelson Soares e José Bandeira, pelas sugestões e solicitude sempre que preciso.

Ao CNPq, PPGG e à Universidade Federal do Pará, pelo suporte financeiro e estrutural durante o desenvolvimento desta pesquisa. O presente trabalho foi realizado com apoio da Coordenação de Aperfeiçoamento de Pessoal de Nível Superior – Brasil (CAPES) – Código de Financiamento 001.

Aos amigos do GSED, Cleber Rabelo, Guilherme Raffaeli, Pedro Augusto, Walmir Lima, Isabella Miranda, Hudson Santos, Renato Sol, Luiz Saturnino, Roberto Araújo, Raphael Araújo, Isaac Salém, Taynara Martins, Mateus Xavier, Eduardo Santos, Fernando Andrade, Raíza Renné, Lucas Chelsea, Renan Fernandes, Alexandre Castelo e Gabriel Leal. Obrigado pelas risadas, desabafos, pelos infinitos copos de café e por sempre estarem disponíveis a tirar dúvidas, ajudar com textos, imagens e processos laboratoriais. Obrigado pela oportunidade de aprender diariamente com vocês, por me inspirarem com seu esforço e brilhantismo, por me ajudarem a sempre procurar o meu melhor, por serem exemplos de pesquisadores e pessoas.

Em especial, agradeço ao Cleber Rabelo (braço direito) pela parceira em etapas de campo, produções textuais e elaboração de imagens. Ao Guilherme Raffaeli (oráculo do GSED), pelos inúmeros conselhos, pelo apoio durante a geoquímica e análise de fósseis, por me incentivar a pensar “fora da caixa” e por elevar o nível deste trabalho. Ao Walmir Lima pela tentativa trabalhosa (e infelizmente infrutífera) de achar palinórfos. À Raíza Renné, pelo auxílio na aquisição das imagens de catodoluminescência.

Agradeço aos técnicos Everaldo Cunha (Laboratório de Sedimentologia); Joelma Soares (Laboratório de Laminação); à Prof. Dra. Simone Paz, ao técnico Aldemir Sotero e ao bolsista Wesley Achilles (Laboratório de Difração de Raios-X).

Aos Profs. Drs. Michel Sauma (UFRA) e Francisco Abrantes (UNICAMP) pela amizade, apoio e incentivo.

Aos amigos de graduação, por tornarem esta caminhada mais fácil. Em especial, agradeço Williamy Felix, Danilo Cruz, Daniela Soares, Ivinny Barros, Paulo Ronny, Vitor Centeno, Layse Hollanda, Paulo Faro, Malu Ferreira, Enzo Venturieri e João Paulo. Aos amigos de fora da geologia, Lana Castro, Brenda Moreira, Fernanda Fonseca, Bruna Adriele, Marcelo Assunção, Alexandre Dias e Evelyn Melo.

Agradeço a todos que, direta ou indiretamente, me auxiliaram a iniciar e concluir este trabalho, cujos nomes não caberiam em poucas páginas.

“Corre, desenha, enfeita a imagem,
A ideia veste,
Cinge-lhe ao corpo a ampla roupagem,
Azul-celeste.
Torce, aprimora, alteia, lima
A frase; e, enfim,
No verso de ouro engasta a rima,
Como um rubim.
(...)
E horas sem conto passo, mudo,
O olhar atento,
A trabalhar, longe de tudo,
O pensamento.
Porque o escrever – tanta perícia,
Tanta requer,
Que ofício tal... Nem há notícia
De outro qualquer.”

Olavo Bilac – Profissão de Fé

RESUMO

A transição Jurássico-Cretáceo foi marcada pela fragmentação do supercontinente Gondwana Oeste e consequente abertura do Oceano Atlântico. Os estágios pré-ruptura foram caracterizados por soerguimentos epirogênicos associados a acumulações volumosas de magma na infracrosta. Adicionalmente, derrames vulcânicos expressivos ocorreram na porção central do Gondwana Oeste, compondo a *Central Atlantic Magmatic Province* (CAMP). Um estágio de subsidência térmica pós-CAMP permitiu a instalação de extensos lagos coincidentes com depocentros da Bacia do Parnaíba, registrado em camadas jurássico-cretáceas da Formação Pastos Bons (FPB). A FPB é constituída, predominantemente, por espessos folhelhos avermelhados intercalados a arenitos tabulares. A porção basal é constituída por folhelhos pretos fossilíferos, denominados de Folhelho Muzinho. Devido a exposições descontínuas e deslocamentos por falhas, a estratigrafia do Mesozoico da Bacia do Parnaíba permanece pouco compreendida e existe a necessidade de trabalhos faciológicos e estratigráficos de detalhe. Neste sentido, esta pesquisa realizou uma releitura destes depósitos para elucidar o paleoambiente e as implicações paleogeográficas da FPB no contexto do supercontinente Gondwana, com base na análise de fácies e cicloestratigrafia. A proveniência desta sucessão foi investigada a partir de diagramas de composição de arenitos, catodoluminescência de quartzo e análise de minerais pesados. As camadas intituladas Folhelho Muzinho foram avaliadas através de petrografia, DRX e MEV/EDS. A FPB é composta por cinco associações de fácies, interpretadas como lacustre central (AF1), *sheet-like delta front* (AF2), lacustre marginal (AF3) e canais fluviais efêmeros (AF4). A AF1 é composta por ciclos de ressecamento/raseamento ascendente, definidos por folhelhos pretos milimetricamente intercalados a carbonatos, que gradam para folhelhos avermelhados alternados a arenitos estratificados/laminados. Os folhelhos são compostos por quartzo, illita, esmectita e calcita. Os níveis fossilíferos incluem macroformas jovens e adultas no mesmo horizonte, encapsuladas por lâminas crenuladas de Fe-esmectitas, ricas em matéria orgânica. A AF1 indica sedimentação no centro de lagos estratificados, em condições eutróficas e anóxicas. Eventos de mortandade em massa foram induzidos, provavelmente, pela contaminação da coluna d'água devido à liberação de H₂S por cianobactérias. A transição para pelitos e arenitos espessos reflete a evolução de lagos *underfilled* para *overfilled*, conforme houve o aumento no aporte de sedimentos e água. A AF2 é composta por arenitos tabulares em ciclos de espessamento ascendente, que registram desconfinamento do fluxo e preenchimento progressivo do lago, com consequente retrabalhamento do topo das camadas

por ação de ondas. A AF3 é constituída por ciclos de raseamento ascendente, demarcados por marcas onduladas, estruturas de adesão ou gretas de contração. A AF4 é definida por ciclos granodecrescentes ascendentes desenvolvidos por canais fluviais efêmeros, com conglomerados e arenitos que gradam para pelitos. Esta sucessão define lagos abertos e estratificados, dominados por processos de decantação e fluxos desconfinados, em regime hiperpicnal. O arcabouço estratigráfico da FPB é composto por quatro ciclos deposicionais, constituídos por ciclos centimétricos a métricos, limitados por superfícies de inundação. Estes ciclos definem um padrão retrogradacional-progradacional-retrogradacional, com aumento ascendente do espaço de acomodação condicionado por pulsos da subsidência térmica pós-CAMP e variações no suprimento sedimentar. A sucessão mesozoica sugere migração do Gondwana Oeste para zonas equatoriais no Jurássico-Cretáceo, com atenuação da aridez em relação ao Permiano-Triássico. Os arenitos da FPB indicam proveniência de orógenos reciclados e interior cratônico, enquanto que dados de catodoluminescência indicam fonte vulcânica predominante. Para testar possíveis correlações com unidades adjacentes, verificou-se que a assembleia de minerais pesados da FPB é muito similar a de depósitos eólicos da Formação Corda, e ambas diferem dos depósitos fluviais da Formação Grajaú. Os índices ZTR, GZi e RZi são mais altos para os arenitos da FPB e da Formação Corda, e baixos para a Formação Grajaú. Os depósitos fluviais distinguem-se, sobretudo, por exibirem sillimanita e alto teor de hornblenda (>50%). Estes dados indicam minerais policíclicos e fontes mistas para os arenitos mesozoicos da Bacia do Parnaíba. O Grupo Mearim exhibe contribuição vulcânica suprida por basaltos do CAMP e fonte metapelítica de baixo a médio grau metamórfico. Esta última, possivelmente, é representada por rochas neoproterozoicas do Domínio Médio Coreau, Província Borborema. Diferentemente, a Formação Grajaú foi suprida por granitos brasileiros tipo-I. Esta evolução geológica indica mudança de proveniência ou exumação de áreas fontes em comum durante o Mesozoico da Bacia do Parnaíba.

Palavras-Chave: Estratigrafia; Proveniência; Subsidência Térmica; Paleoambiente; Lacustre.

ABSTRACT

The Jurassic-Cretaceous transition was marked by the fragmentation of the West Gondwana supercontinent and consequent opening of the Atlantic Ocean. The pre-rupture stages were characterized by epeirogenic uplifts associated with voluminous magmatic accumulation in the infracrust. Additionally, expressive volcanic flows occurred in the central portion of the West Gondwana, composing the Central Atlantic Magmatic Province (CAMP). A post-CAMP thermal subsidence stage allowed the installation of massive lakes coincidentally with the depocenters of the Parnaíba Basin, which is recorded in the Jurassic-Cretaceous Pastos Bons Formation (PBF). The PBF is a predominantly constituted of thick reddish mudstones interbedded to tabular sandstones. The basal portion is composed of fossiliferous black shales, the Muzinho Shale. Due to discontinuous exposures and fault displacements, the stratigraphy of the Mesozoic of the Parnaíba Basin keeps poorly understood and there is a necessity for more detailed faciological and sedimentological studies. In this sense, this research performed a sedimentological lecture of these deposits in order to elucidate the paleoenvironment and Paleogeography of the PBF in the context of the West Gondwana, through outcrop-based facies analysis and cyclostratigraphy. The provenance of this succession was investigated through compositional sandstones diagram, quartz hot cathodoluminescence and heavy minerals analyses. The Muzinho Shale beds were evaluated through petrography, XRD and SEM/EDS. The PBF is composed of four facies associations, interpreted as central lake (FA1), sheet-like delta front (FA2), lakeshore (FA3) and ephemeral fluvial channels (FA4). FA1 is composed of drying/shallowing upward cycles, defined by millimeter-scale black shales interlayered with limestones, that grade to reddish shales and laminated/stratified sandstones. Shales are composed by quartz, illite, smectite and calcite. The fossiliferous levels include young and adult macroforms in the same horizon, sandwiched by crinkly laminations with organic rich Fe-smectites. FA1 indicate sedimentation in the center of the lakes, in eutrophic and anoxic conditions. Mass mortality events were probably induced by contamination of the water column due to H₂S release by cyanobacteria. The transition to mudstones and sandstones reflects the evolution of underfilled to overfilled lakes, as the sediment and water supply were increased. FA2 is composed of tabular sandstones in thickening upward cycles, which record unconfined flows and progressive lake filling, with consequent reworking of the top of the beds by wave action. FA3 is constituted of shallowing upward cycles, marked by wave marks, adhesion structures or mud cracks. FA4 is defined by fining upward cycles developed by ephemeral fluvial channels, with conglomerates and

sandstones grading to mudstones. This succession defines open and stratified lakes, dominated by settling and unconfined flows, in hyperpycnal regime. The stratigraphic framework of the PBF is composed of four depositional cycles, constituted of centimeter to millimeter-scale cycles, bounded by flooding surfaces and unconformities. These cycles define a retrogradational-progradational-retrogradational stacking pattern, with increasing accommodation space upward conditioned by post-CAMP thermal subsidence pulses and variations in sediment supply. The Mesozoic succession suggests migration of the West Gondwana toward Equatorial regions during Jurassic-Cretaceous, with aridity attenuation relatively to the Permian-Triassic. The sandstones of the PBF indicate provenance from recycled orogens and craton interior, whereas cathodoluminescence data indicate predominantly volcanic sources. In order to test possible correlations with adjacent units, we verified the heavy minerals assemblage of the PBF is very similar to the Corda Formation, and both differ from the fluvial deposits of the Grajaú Formation. The ZTR, GZi and RZi indexes are higher for sandstones of the PBF and Corda Formation, and lower for the Grajaú Formation. The fluvial deposits distinguish mainly by sillimanite and high hornblende content (>50%). These data indicate polycyclic minerals and mixed sources for sandstones of the Parnaíba Basin. The Mearim Group exhibits volcanic contribution supplied by CAMP basalts and low to medium grade metapelitic sources. This last was possibly supplied by Neoproterozoic rocks of the Médio Coreau Domain, Borborema Province. Differently, the Grajaú Formation was supplied by type-I Brazilian granites. This geological evolution indicates change in provenance areas or exhumation of common source areas during the Mesozoic of the Parnaíba Basin.

Keywords: Stratigraphy; Provenance; Thermal Subsidence; Paleoenvironment; Lake.

LISTA DE ILUSTRAÇÕES

Figura 1 – A. Mapa de localização da Bacia do Parnaíba e contexto geotectônico (Modificado de Schobbenhaus et al, 1984; Santos e Carvalho, 2004). B. Localização da área de estudo. -----	2
Figura 2 – Paleogeografia mesozoica. A. Triássico Inferior a Médio. B. Jurássico Médio. C. Cretáceo Superior. -----	6
Figura 3 – Caracterização paleoclimática, composição atmosférica, eventos de colocação de LIPs, impactos de meteoros e intensidade das extinções durante a Era Mesozoica. -----	7
Figura 4 – Histórico de estudos sobre a estratigrafia do Mesozoico da Bacia do Parnaíba, com destaque para a Formação Pastos Bons. -----	13

ARTIGO 1

Figure 1 – Location map of the study area. A. Central Atlantic Magmatic Province distribution in West Gondwana (from Torsvik and Cocks, 2013). B. Detailed occurrence of CAMP-related volcanic rocks in West Gondwana (Modified from Schaller et al, 2012). C. Parnaíba Basin, northeastern Brazil and main geotectonic boundaries (modified from Schobbenhaus et al, 1984; Santos and Carvalho, 2004). D. Study area, southeastern Parnaíba Basin. -----	19
Figure 2 – Stratigraphic relations of the Upper Jurassic lacustrine deposits. A. Sardinha Formation dykes, crosscutting Pastos Bon Formation (Scale: 34 cm). B. Sedimentary dyke filled by fluvial deposits of the Grajaú Formation in the top of Pastos Bons beds (Scale: 34 cm). C. Fluvial deposits (Grajaú Formation) unconformably overlying Pastos Bons Formation (Scale: 1.70 m). D. Graben structures in the Parnaíba Basin, with Paleozoic basement topographically higher than Mesozoic deposits (Scale: 1.85 m).-----	23
Figure 3 – Stratigraphic relations of the Upper Mesozoic succession of the Parnaíba Basin.	24
Figure 4 – Stratigraphic logs of the studied succession. -----	28
Figure 5 – Central lake and sheet-like delta front deposits. -----	31
Figure 6 – Lakeshore and ephemeral fluvial channel deposits.. -----	35
Figure 7 - High-frequency lacustrine cycles and fluvial cycles.. -----	37
Figure 8 - A. General profile, stacking patterns, trends, Fischer plots and depositional cycles. B. Sequence stratigraphic stages and depositional cycles of the lacustrine system	

(CI-CIV – depositional cycle; lfs – lacustrine flooding surface; U1 – unconformity 1; U2 – unconformity 2; UL – underfilled lake phase; OL – overfilled lake phase).-----41

ARTIGO 2

- Figure 1** – Stratigraphic proposals for Mesozoic of Parnaíba Basin, highlight for Pastos Bons and Corda formations (Modified from Rabelo and Nogueira, 2015).-----49
- Figure 2** – A. Localization map and geotectonic contextualization of Parnaíba Basin (Modified from Schobbenhaus et al, 1984; Santos and Carvalho, 2004). B. Localization map of the study area. -----49
- Figure 3** – Stratigraphic logs of the studied succession and samples positioning.-----54
- Figure 4** – Petrographic aspects of Upper Mesozoic sandstones from Parnaíba Basin..-----56
- Figure 5** – Tectonic discrimination diagrams for Upper Mesozoic sandstones of the Parnaíba Basin. -----58
- Figure 6** – Petrographic aspects of quartz grains from lacustrine (A-E) and aeolian (F-I) deposits. -----59
- Figure 7** – Quartz cathodoluminescence from lacustrine (A-D) and aeolian (E-F) deposits.- 60
- Figure 8** - Quartz provenance of lacustrine and eolian deposits, according to ternary provenance discrimination diagram (Bernet and Basset, 2005).-----61
- Figure 9** – Heavy minerals from lacustrine succession (Pastos Bons Formation). -----64
- Figure 10** - Heavy minerals from aeolian succession (Corda Formation). -----66
- Figure 11** - Heavy minerals from fluvial deposits (Grajaú Formation). -----68
- Figure 12** - ZTR index of aeolian, lacustrine and fluvial deposits from Upper Mesozoic Parnaíba Basin.-----70
- Figure 13** – Proportion between GZi and RZi indexes according to the facies associations in the lacustrine, aeolian and fluvial deposits. -----71

SUMÁRIO

DEDICATÓRIA	iv
AGRADECIMENTOS	v
EPÍGRAFE	vii
RESUMO	viii
ABSTRACT	x
LISTA DE ILUSTRAÇÕES	xii
1 INTRODUÇÃO	iv
1.1 APRESENTAÇÃO-----	iv
2 OBJETIVOS	3
3 MESOZOICO	4
4 CONTEXTO GEOLÓGICO REGIONAL	8
4.1 BACIA DO PARNAÍBA -----	8
4.2 GRUPO MEARIM -----	8
4.3 FORMAÇÃO PASTOS BONS-----	9
4.3.1 Conteúdo Fossilífero e Idade da Formação Pastos Bons-----	11
5 MATERIAIS E MÉTODOS	14
5.1 ANÁLISE DE FÁCIES-----	14
5.2 ESTRATIGRAFIA DE SEQUÊNCIAS-----	14
5.3 CICLOESTRATIGRAFIA -----	14
5.4 PETROGRAFIA DE ARENITOS-----	15
5.5 CATODOLUMINESCÊNCIA-----	15
5.6 MINERAIS PESADOS-----	15
5.7 DIFRAÇÃO DE RAIOS-X-----	16
 ARTIGO 1 Lake cyclicality as response to thermal subsidence: a post-CAMP scenario in the Parnaíba Basin, NE Brazil	17
1 INTRODUCTION	17
2 GEOLOGICAL SETTING	19
3 METHODS	21
4 RESULTS	21
4.1 GENERAL ASPECTS -----	21
4.2 FACIES ASSOCIATION -----	29
5 CYCLOSTRATIGRAPHY	36

5.1	LACUSTRINE CYCLES-----	36
5.2	EPHEMERAL FLUVIAL CHANNEL CYCLES-----	37
6	THE ROLE OF THERMAL SUBSIDENCE IN LAKE CYCLES.....	38
7	THE JURASSIC-CRETACEOUS HISTORY OF THE WEST GONDWANA	42
8	CONCLUSIONS.....	42

ARTIGO 2 Multi-approach provenance in stratigraphy: implications for the Upper Mesozoic evolution of the Parnaíba Basin, NE Brazil

1	INTRODUCTION	48
2	GEOLOGICAL SETTING.....	49
2.1	CRITICAL ANALYSIS OF THE STRATIGRAPHIC PROPOSALS -----	50
3	METHODS.....	51
4	SANDSTONES OF THE MEARIM GROUP	52
4.1	PETROGRAPHIC FEATURES OF QUARTZ GRAINS-----	56
4.1.1	Lacustrine Succession (Pastos Bons Formation)-----	56
4.1.2	Aeolian Succession (Corda Formation) -----	56
4.2	QUARTZ CATHODOLUMINESCENCE -----	57
5	HEAVY MINERALS of the upper mesozoic parnaíba basin	61
5.1	HEAVY MINERALS OF THE MEARIM GROUP -----	61
5.1.1	Lacustrine Succession (Pastos Bons Formation)-----	61
5.1.2	Aeolian Succession (Corda Formation) -----	64
5.2	FLUVIAL SUCCESSION (GRAJAÚ FORMATION)-----	67
5.3	ZTR and GZi x RZi Indexes-----	69
6	HEAVY MINERAL ASSEMBLAGES OF THE UPPER MEZOSOIC SANDSTONES	71
6.1	UPPER MESOZOIC PROVENANCE EVOLUTION OF THE PARNAÍBA BASIN -----	73
7	CONCLUSIONS.....	74
	REFERÊNCIAS	80
	APÊNDICE A – TABELAS DE CONTAGEM	90

1 INTRODUÇÃO

1.1 APRESENTAÇÃO

O Mesozoico foi marcado pela reorganização de massas continentais em resposta à fragmentação do supercontinente Pangea e, posteriormente, do supercontinente Gondwana, com drásticas consequências paleoclimáticas, geológicas e biológicas a níveis globais (Torsvik & Cocks 2013; Holz 2015). Na Bacia do Parnaíba, o Mesozoico (pré-Albiano) é documentado principalmente por estratos siliciclásticos continentais, depositados sob condições áridas/semiáridas. Este registro consiste em sucessões desértico-lacustres (Formação Motuca) (Abrantes *et al* 2016), desérticas (Formação Sambaíba) (Abrantes & Nogueira 2012), flúvio-lacustres (Formação Pastos Bons) (Romero Bállen 2012), flúvio-eólicas (Formação Corda) (Rabelo e Nogueira 2015), além de derrames vulcânicos das formações Mosquito e Sardinha (Uchupi & Emery 1991; Merle *et al* 2011; Oliveira *et al* 2018).

Apesar dos avanços recentes, a estratigrafia do Mesozoico da Bacia do Parnaíba permanece problemática, de modo que muitos autores sugerem a necessidade de estudos detalhados, sobretudo nos depósitos jurássico-cretáceos da Formação Pastos Bons (Caldasso 1978; Caldasso & Hama 1978; Góes & Feijó 1994; Vaz *et al* 2007). Os trabalhos acerca desta unidade consistem em análises paleontológicas (Lima & Campos 1980; Gallo & Figueiredo 2004; Gallo 2005; Petra 2006; Montefeltro *et al* 2013), mapeamentos regionais (Lima & Leite 1978; Góes & Feijó 1994; Vaz *et al* 2007) e análises faciológicas pontuais (Romero Bállen 2012; Cardoso *et al* 2017), e ainda carecem de uma discussão conjunta destes dados. Ademais, a definição da distribuição, dinâmica deposicional e contextualização da Formação Pastos Bons quanto à estratigrafia de sequências são enfoques inéditos na literatura especializada. Neste sentido, este trabalho utilizou a análise de fácies, cicloestratigrafia e estratigrafia de sequências de alta resolução para determinar os paleoambientes e controles deposicionais da Formação Pastos Bons, assim como as implicações paleogeográficas destes depósitos no contexto do supercontinente Gondwana Oeste. Adicionalmente, pretende-se integrar os dados paleontológicos e estratigráficos, a partir do posicionamento dos fósseis descritos na literatura, e discutir os fatores que influenciam na estratigrafia de sequências de ambientes lacustres sem conexão marinha. O posicionamento estratigráfico desta unidade em relação, principalmente, às formações Corda e Grajaú, é discutida com base em análises de discriminação tectônica de arenitos, catodoluminescência de quartzo e proveniência de

minerais pesados. A área de estudo está situada na porção sudeste da Bacia do Parnaíba, abrangendo os estados do Maranhão e Piauí, Nordeste do Brasil (Fig. 1).

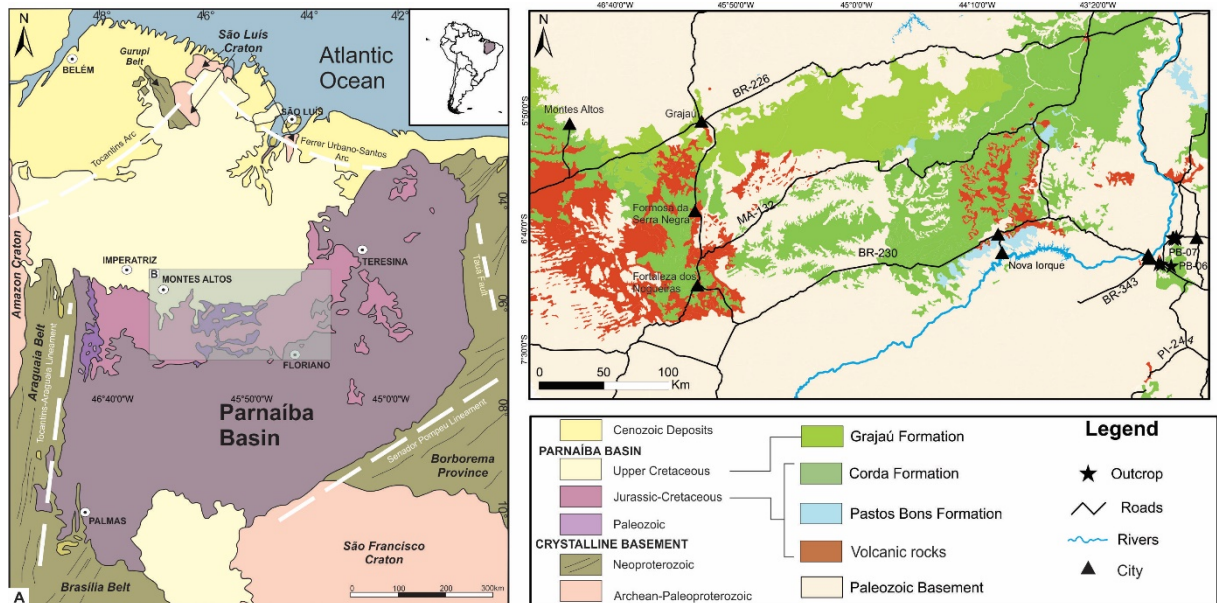


Figura 1 – A. Mapa de localização da Bacia do Parnaíba e contexto geotectônico (Fonte: Modificado de Schobbenhaus *et al*, 1984; Santos & Carvalho, 2004). B. Localização da área de estudo.

2 OBJETIVOS

Os objetivos deste trabalho incluem a determinação da origem dos ciclos deposicionais da Formação Pastos Bons e a definição da evolução paleoambiental destes depósitos na região sudeste da Bacia do Parnaíba, assim como elucidar os principais fatores atuantes na deposição desta unidade. Este trabalho é uma oportunidade de discutir a aplicação da estratigrafia de sequências e Fischer Plots em ambientes exclusivamente continentais. Adicionalmente, pretende-se refinar as relações estratigráficas da Formação Pastos Bons com as unidades adjacentes, principalmente com a Formação Corda, e compreender as implicações paleogeográficas desta sucessão no contexto do supercontinente Gondwana Oeste.

3 MESOZOICO

A Era Mesozoica, compreendida entre 251 e 66 Ma, foi marcada pela fragmentação do supercontinente Pangea, com amplas consequências paleogeográficas, paleoclimáticas, geológicas e biológicas. Subdivide-se nos períodos Triássico (251 – 201 Ma), Jurássico (201 – 145 Ma) e Cretáceo (145 – 65,5 Ma) (*International Union on Geological Sciences – IUGS*, 2013). No Triássico Inferior houve a separação do Pangea entre Laurásia e Gondwana e consequente abertura do Oceano Índico. No Triássico Médio a Superior iniciou-se a quebra do Gondwana, com a separação de Antártica e Austrália em relação à América do Sul e África, enquanto a Índia se movimentava em direção ao norte. A transição para o Jurássico foi marcada pela separação entre a América do Norte e América do Sul (Fig. 2a; Wicander & Monroe 2013; Holz 2015). No Jurássico ocorreu a abertura do Oceano Atlântico Norte, a partir da separação da África e da América do Norte e início da abertura do Oceano Atlântico Sul (Fig. 2b). Esta abertura foi finalizada no Cretáceo Inferior, com a separação da América do Sul e África, enquanto o mar de Tethys era progressivamente fechado. A América do Norte e a Groenlândia passaram por processos de fissão continental e abertura de um mar restrito. No Cretáceo Superior, Austrália e Antártica migraram para o hemisfério sul, próximo a linha do Equador (Fig. 2c; Veevers 2004; Holz 2015).

A temperatura média global do Mesozoico era de $\sim 25^{\circ}\text{C}$ (6 - 9°C acima da atual), com oscilações de condições *greenhouse* quentes a frias, e alguns intervalos curtos de *hothouse*, comumente associados à colocação de LIPs (*large igneous provinces*) (Fig. 3; Holz 2015). O clima da Terra era controlado, principalmente, pela 1) redistribuição paleogeográfica dos continentes; 2) erupções vulcânicas associadas ao rifteamento do supercontinente Pangea; e 3) liberação de metano em erupções vulcânicas (Wicander & Monroe 2013). Esta tendência ao aumento global da temperatura foi esporadicamente revertida por invernos de impacto (*impact winters*), ocasionados pela queda de meteoros e a consequente ascensão de nuvens de poeira, responsáveis pelo bloqueio temporário de raios solares. Pelo menos nove grandes crateras de impacto (diâmetro > 20 km) são datadas como mesozoicas (Rajmon 2009).

O Mesozoico, de modo geral, foi caracterizado pelo nível elevado do mar, a exceção do Induano Inferior (Triássico Inferior), Hettangiano/Sinemuriano (Jurássico Inferior) e Valangiano (Cretáceo Inferior) (Holz 2015). A separação das massas continentais resultou na migração das linhas de costas, formação de mares epíricos e aceleração dos padrões de circulações oceânicas/atmosféricas (Wicander & Monroe 2013). O conteúdo de O_2 atmosférico chegou a valores de 15% no Triássico Inferior, com aumento gradual e ápice em

25 – 30% no Cretáceo Superior (Holz 2015). O teor de CO₂ é estimado em 1200 – 4800 ppm, 4 a 16 vezes acima do valor atual (Fig. 3; Steinthorsdottir *et al* 2011; Holz 2015).

A transição Permiano/Triássico foi marcada por uma extinção em massa propiciada por alterações climáticas extremas (Fig. 3) (Twitchett 2006; McElwain & Punyasena 2007; Callegaro *et al* 2014). No final do Triássico Superior, os invertebrados marinhos repovoaram os oceanos e mares, no entanto, com baixa diversidade de espécies. Esta diversidade foi expandida no Triássico Superior, com maior proliferação de espécies escavadoras. A ictiofauna era dominada por teleósteos, mas também houve a elevação no número de espécies cartilaginosas (Wicander & Monroe 2013). Os continentes eram amplamente dominados por répteis gigantes, principalmente os dinossauros, surgidos no Triássico Superior, com epíbole no Jurássico (Bardet *et al* 2014; Holz 2015). A transição Triássico/Jurássico também registrou a evolução de répteis mamaliformes (terapsídeos e cinodontes), enquanto que o Cretáceo documentou o aparecimento das primeiras espécies de mamíferos. Quanto à flora, predominavam plantas sem sementes e gimnospermas no Triássico/Jurássico, o que mudou com o surgimento das angiospermas no Jurássico Superior/Cretáceo Inferior (Wicander & Monroe 2013).

O final do Cretáceo foi marcado pela sazonalidade climática, o que exigiu uma grande capacidade adaptativa dos organismos da época (Holz 2015). A extinção em massa ocorrida na transição Cretáceo/Paleoceno (Fig. 3) decorreu de impactos extraterrestres, os quais geraram grandes nuvens de poeira que bloquearam a luz solar, fato que afetou intensamente a fotossíntese, com consequências catastróficas para a cadeia alimentar (Veevers 2004; McElwain & Punyasena 2007; Callegaro *et al* 2014). Houve a vaporização das rochas e consequente liberação dos ácidos sulfúrico e nítrico, que resultaram em chuvas ácidas. Além disso, ocorreu a diminuição abrupta da temperatura superficial e vulcanismo intenso (Wicander & Monroe 2013).

Os principais recursos econômicos do Mesozoico são depósitos de carvão (e.g. Bacia de Kaitanga, Austrália); petróleo e gás natural (e.g. Bacia de Indus, Paquistão; Bacia de San Juan, México); urânio, potássio e vanádio (e.g. Platô do Colorado, EUA). Kimberlitos diamantíferos estão presentes, principalmente no Platô Iramba (África do Sul), além de BIFs restritas, como na Bacia de Lorraine (Luxemburgo). *Placers* de ouro são comuns nas Montanhas Klamath (EUA) e depósitos porfiríticos de cobre ocorrem em maior quantidade no *Copper Belt* dos Andes (Peru e Chile) (Wicander & Monroe 2013).

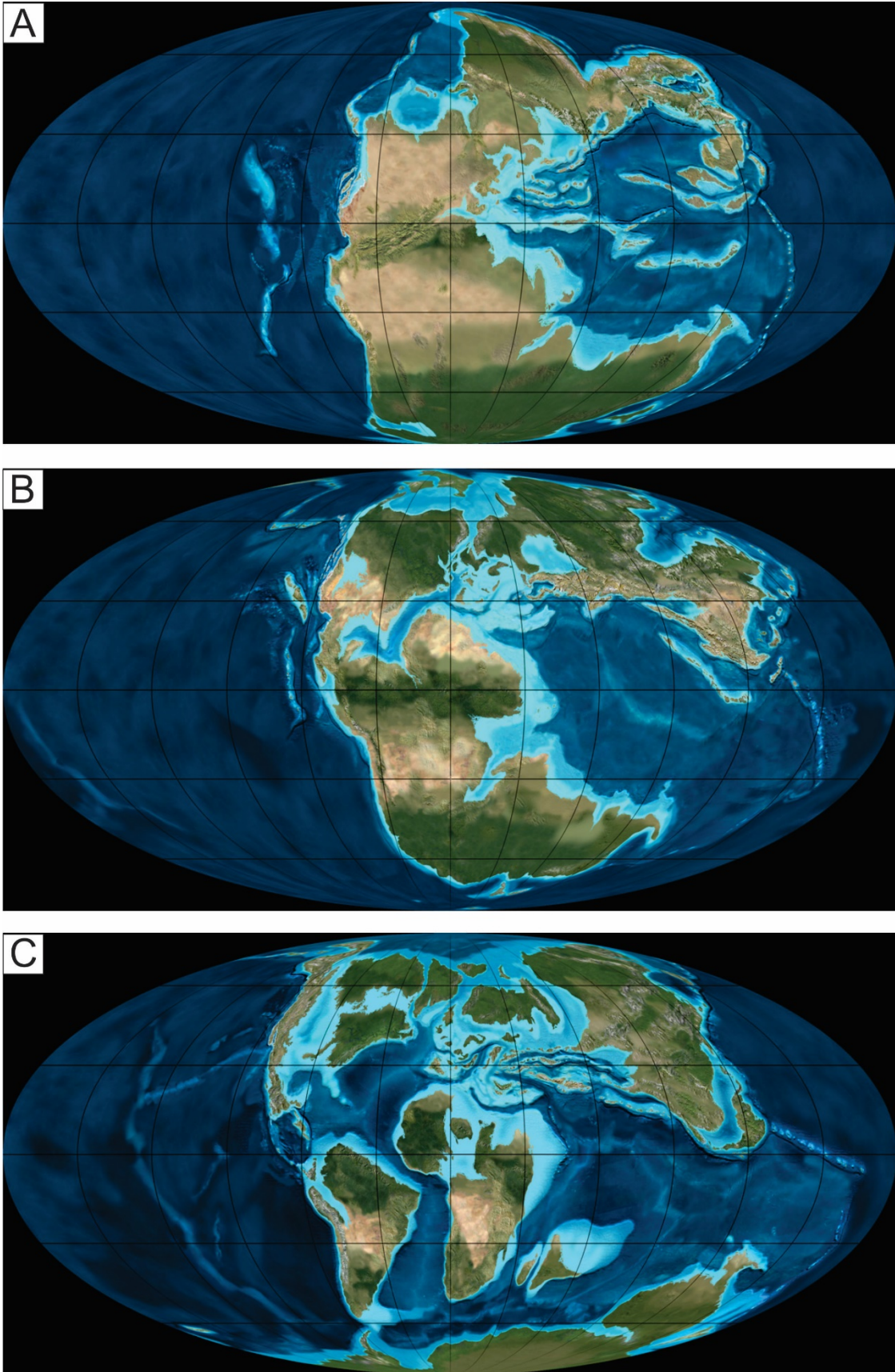


Figura 2 - Paleogeografia mesozoica. A. Triássico Inferior a Médio. B. Jurássico Médio. C. Cretáceo Superior.

FORNTE: *Software Global Paleogeography* (Scotese, 2000).

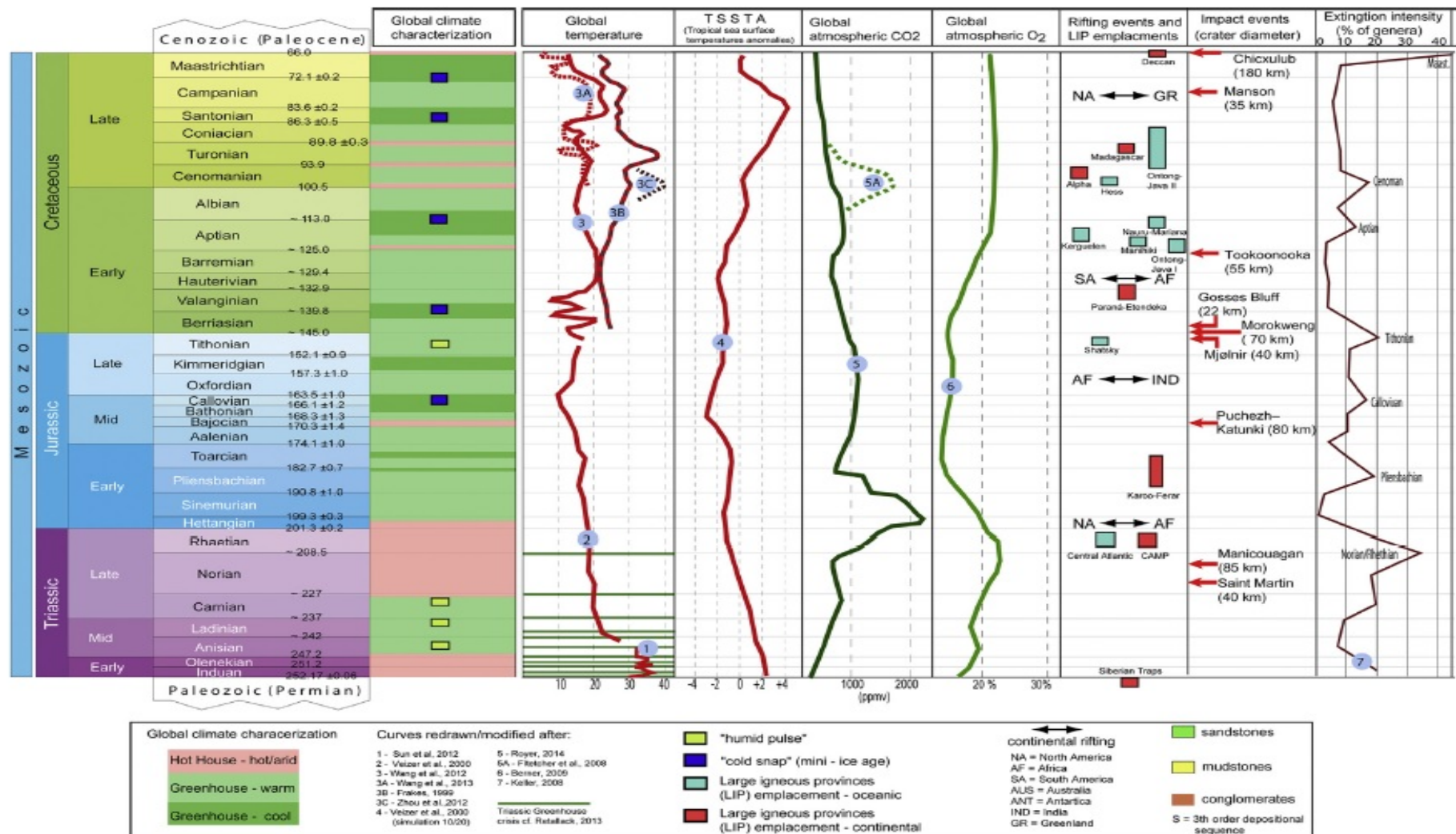


Figura 3 – Caracterização paleoclimática, composição atmosférica, eventos de colocação de LIPs, impactos de meteoros e intensidade das extinções durante a Era Mesozoica.

FONTE: Adaptado de Holz (2015).

4 CONTEXTO GEOLÓGICO REGIONAL

4.1 BACIA DO PARNAÍBA

A Bacia do Parnaíba é uma bacia intracratônica paleozoica, situada a norte da Plataforma Sul-Americana, Nordeste do Brasil, e estende-se pelos estados do Pará, Tocantins, Maranhão, Piauí, Ceará e Bahia (Aguiar 1969; Góes & Feijó 1994). Esta bacia, definida como do tipo *sag* (Daly *et al* 2014), abrange cerca de 600.000 km², e pode atingir de 3.4 a 3.5 km de espessura no seu depocentro (Caputo 1984; Vaz *et al* 2007). O embasamento é composto por rochas ígneas, metamórficas e sedimentares (Vaz *et al* 2007), pertencentes ao Cinturão Araguaia-Tocantins, crátons Amazônico e São Francisco, Província Borborema, além das bacias Riachão e Jaibaras (Victor Zálan 1991; Oliveira e Mohriak 2003; Castro *et al* 2014), com idades arqueanas a ordovicianas, formados e/ou retrabalhadas durante o Ciclo Brasileiro (Vaz *et al* 2007). O embasamento da Bacia do Parnaíba é composto por três domínios distintos, denominados bloco Amazônico/Araguaia, bloco Parnaíba e bloco Borborema (Daly *et al* 2014), além de um sistema de bacias pré-silurianas precursoras, representadas pelas bacias Riachão e Jaibaras (Castro *et al* 2014; Porto *et al* 2018).

A origem e evolução da Bacia do Parnaíba estão relacionadas, principalmente, a eventos tectonomagmáticos (Daly *et al* 2014). Lineamentos e dobramentos importantes foram gerados e/ou reativados por eventos de descompressão e resfriamento, com influência na formação de estruturas grabeniformes, sobretudo durante a fragmentação do supercontinente Gondwana (Schobbenhaus *et al* 1984). Vaz *et al* (2007) classificaram como estruturas principais da bacia os lineamentos Pico Santa-Inês, Marajó-Parnaíba e o Lineamento Transbrasileiro. Estas feições foram fundamentais nos estágios de geração da bacia, na evolução local e no direcionamento dos eixos deposicionais (Vaz *et al*, 2007). Góes & Feijó (1994) dividiram a estratigrafia desta bacia em cinco seqüências: Seqüência Siluriana; Seqüência Devoniana; Seqüência Carbonífero-Triássica; Seqüência Jurássica e Seqüência Cretácea. No entanto, na proposta mais atual, Vaz *et al* (2007) subdividiram a Bacia do Parnaíba em Seqüência Siluriana; Seqüência MesoDevoniana-EoCarbonífera; Seqüência NeoCarbonífera-EoTriássica; Seqüência Jurássica e Seqüência Cretácea.

4.2 GRUPO MEARIM

Lisboa (1914) criou os termos Série Mearim e Formação Corda, para basaltos e arenitos na parte superior (Triássico) do Rio Mearim, respectivamente. Este autor também

criou o termo Camadas Pastos Bons para designar folhelhos e calcários verdes a marrom-chocolate, os quais contêm lentes de opala, intercalados com arenitos brancos. Em seguida, o termo Grupo Mearim foi utilizado por Aguiar (1969), com o intuito de agrupar as formações Mosquito, Corda e Sardinha à então intitulada Formação Pastos Bons. Góes & Feijó (1994) detalharam o Grupo Mearim e sugeriram que este é constituído pelas formações Pastos Bons e Corda, interdigitadas e sobrepostas discordantemente sobre a Formação Mosquito e ao Grupo Balsas, além de serem sotopostas, em discordâncias, pelos depósitos cretáceos das formações Sardinha, Grajaú, Codó e Grupo Itapecuru. A partir de reavaliações feitas por Vaz *et al* (2007), a idade cretácea foi sugerida para a Formação Corda, o que deixou apenas a Formação Pastos Bons como representante do Jurássico na Bacia do Parnaíba. Romero Ballén (2012) e Rabelo & Nogueira (2015) discutem tal afirmação e sugerem que a Formação Corda é, também, jurássica.

A Formação Corda é composta por arenitos finos a médios, bimodais, cinza-esbranquiçados e avermelhados, com grãos arredondados e foscos de quartzo, com alguns níveis de sílex (Góes & Feijó 1994; Santos & Carvalho 2004). De acordo com Vaz *et al* (2007), a deposição dessa unidade foi influenciada pelo arqueamento Alto Parnaíba. O ambiente determinado foi desértico com subambientes flúvio-lacustres (Góes & Feijó 1994; Romero Ballén 2012; Rabelo & Nogueira, 2015).

4.3 FORMAÇÃO PASTOS BONS

A Formação Pastos Bons foi primeiramente definida por Lisboa (1914) como Camadas Pastos Bons, a qual designava a intercalação de calcários, folhelhos e arenitos entre a cidade homônima e o município de São João dos Patos, ambos no Estado do Maranhão. Apesar disto, muitos dos trabalhos posteriores não seguiram a proposta inicial que, aliada à complexidade das relações de contato da Formação Pastos Bons e unidades adjacentes, gerou divergências na estratigrafia do Mesozoico da Bacia do Parnaíba. Brazil *et al* (1948) posicionaram as camadas referentes às formações Motuca, Sambaíba e Pastos Bons na então denominada Formação Melancieiras. Campbell (1949), contudo, atribuiu as Camadas Pastos Bons à Formação Motuca. Mesner & Wooldridge (1964) elevaram as Camadas Pastos Bons ao nível de formação. Posteriormente, Aguiar (1969) utilizou esta denominação para referir-se à lamitos do vale do Rio Pedra de Fogo, ao sul da cidade de Pastos Bons. Em seguida, Cunha & Carneiro (1972) unificaram as formações Pastos Bons e Corda (Sistema Desértico Corda-Pastos Bons). Nunes (1973) reavaliou a estratigrafia da região entre Teresina-Jaguaribe e

incluiu as formações Pastos Bons e Motuca na Formação Pedra de Fogo e omitiu a Formação Corda. Tantas divergências estratigráficas (Fig. 4) e litológicas levaram alguns autores a recomendarem a redefinição ou a exclusão do termo “Formação Pastos Bons” (Caldasso 1978; Góes & Feijó 1994) e, mesmo em trabalhos mais recentes (Vaz *et al* 2007; Romero Bállen 2012; Rabelo & Nogueira 2015), ainda não existe consenso quanto ao posicionamento estratigráfico desta unidade.

A deposição da Formação Pastos Bons se deu ao longo da Estrutura de Xambioá, que se comportou como um baixo deposicional durante o Mesozoico (Hasui *et al* 1991). Trabalhos prévios interpretam que a sedimentação desta unidade foi localizada em paleodepressões, concentradas entre altos topográficos gerados por derrames magmáticos (Lima & Leite 1978; Góes & Feijó 1994; Vaz *et al* 2007). A Formação Pastos Bons apresenta 77 m de espessura no seu depocentro, e abrange folhelhos e arenitos esverdeados e marrom-avermelhados próximos ao município de Pastos Bons, localizado no Maranhão. Esta unidade representa a porção Jurássica Superior da Bacia do Parnaíba (Gallo 2005; Vaz *et al* 2007; Montefeltro *et al* 2013), e apresenta-se, de leste para oeste, em contato discordante com as Formações Poti, Piauí (entre Floriano e Monsenhor Gil - PI) (Santos & Carvalho 2004), Pedra de Fogo (no Riacho Pedra de Fogo - MA) e Motuca (Lima & Leite 1978); e concordante e gradacional com a Formação Corda (Aguiar 1971). A Formação Pastos Bons estende-se ao longo do vale do Rio Itapecuru e seus afluentes, no Estado do Maranhão até o Piauí, onde aflora de modo intermitente até a região de Floriano (PI) (Lima & Leite 1978).

Caputo (1984) subdividiu esta unidade em três partes: 1) a base é constituída por arenitos brancos com variações esverdeadas-amareladas, compostos por grãos de granulometria fina a média, subarredondados e, comumente, com estratificação plano-paralela e, pontualmente, lentes de calcário; 2) parte média, caracterizada por siltitos, folhelhos/argilitos cinza-esverdeados, com intercalações de arenitos; e 3) o intervalo superior contém arenitos vermelhos/rosados, de granulometria fina, que gradam para siltitos, com alguns níveis de folhelho. Embora o posicionamento estratigráfico da Formação Pastos Bons seja muito questionado, o paleoambiente desta unidade é definido pela maioria dos autores como lacustre com influência fluvial, em clima semiárido a árido (Mesner & Wooldridge 1964; Caputo 1984; Góes & Feijó 1994; Petra 2006; Vaz *et al* 2007; Romero Bállen *et al* 2013). Mais recentemente, Cardoso *et al* (2017) definiram um sistema de *flysch-like delta front* para esta unidade.

Romero Bállen (2012) sugere tectônica em blocos para a região entre Pastos Bons e Fortaleza dos Nogueiras, Estado do Maranhão, baseado na disposição de padrões

sedimentares, falhas de direção NNW-SSE nas margens oeste e sul do Alto do Itapecuru e na presença de uma janela da Formação Sambaíba na área da Serra das Alpercatas (Cunha & Carneiro 1972; Lima & Leite 1978). De acordo com Romero Bállen (2012), estas falhas afetaram principalmente as formações Pastos Bons e Corda e estariam associadas ao episódio distensivo que culminou na abertura do Oceano Atlântico Sul. Ainda segundo este autor, dados de paleocorrente indicam fluxo para oeste, com a fonte sedimentar representada pelo próprio Alto do Itapecuru. Estas evidências levaram Romero Bállen (2012) a subdividir duas sub-bacias, nomeadas com base nas cidades homônimas: a sub-bacia de Fortaleza dos Nogueiras (a oeste) e a sub-bacia de Pastos Bons (a leste).

4.3.1 Conteúdo Fossilífero e Idade da Formação Pastos Bons

O conteúdo fossilífero da Formação Pastos Bons é constituído, principalmente, por peixes, conchostráceos e palinórfos (Lima & Campos 1980; Gallo 2005) e sua unidade fossilífera principal é representada pelo Folhelho Muzinho. Nestas camadas foi encontrado o gênero *Lepidotes piauhyensis*, cuja idade sugerida inicialmente foi Cretáceo Superior (Roxo & Löefgren 1936). Posteriormente, Kegel (1956)* *apud* Caldasso (1978) utilizou a associação *Lepidotes* e *Semionotus* para atribuir idade triássica superior para estes folhelhos. Entretanto, o registro do gênero *Pholidophoridae* conduziu Santos (1953) a recomendar que estas camadas fossem posicionadas no Triássico Médio-Jurássico Superior. Em seguida, por intermédio de *Macrolimnadiopsis* que ocorrem no Folhelho Muzinho, Beurlen (1954) adotou idade triássica superior. Enquanto que Santos (1974) sugeriu idade jurássica média, a partir de *Pleurophoídeos* e *Macrosemiídeos*.

A partir da identificação de organismos lacustrinos pertencentes aos gêneros *Lioestheria*, *Macrolimnadiopsis*, ostracodes do gênero *Candona* e conchostráceos, a idade jurássica superior também foi proposta por Pinto & Purper (1974), que associaram estas ocorrências com a Formação Pastos Bons, assim como Plummer (1948) e Mesner & Wooldridge (1964). Contudo, os estudos palinológicos de Lima & Campos (1980) no Folhelho Muzinho indicaram idade eocretácea (Barremiano). Gallo (2005), em reavaliação do trabalho de Roxo & Löefgren (1936), atestou idade jurássica superior-cretácea inferior para a Formação Pastos Bons. Idade semelhante foi sugerida por Petra (2006) e Bernardes-de-Oliveira *et al* (2007), com base na descrição de peixes e palinórfos mesofíticos, respectivamente, estes últimos possivelmente correlatos ao Andar Dom João. Outra ocorrência importante nesta unidade é o registro de uma nova espécie de crocodiliano

(*Batrachomimus pastosbonensis*; Montefeltro *et al* 2013), pertencente ao Jurássico Superior, único representante dos *Paralligatoridae*, grupo anteriormente reconhecido apenas na Ásia.

*Kegel, W; 1956. As inconformidades na Bacia do Parnaíba e zonas adjacentes. Rio de Janeiro, DNPM/DMG, Boletim 141, 46p, 1956.

	Mesner e Wooldridge (1964)	Aguiar (1969)	Cunha e Carneiro (1972)	Góes (1990)	Góes et al (1993)	Góes e Feijó (1994)	Rezende (2002)	Vaz et al (2007)	Romero et al (2013)	Rabelo e Nogueira (2015)
Cretáceo	Fm. Codó	Fm. Codó	Fm. Codó	Fm. Codó	Fm. Itapecuru	Fm. Itapecuru	Fm. Itapecuru	Fm. Itapecuru	Grupo Itapecuru	
		Fm. Grajaú	Fm. Sardinha	Fm. Grajaú			Fm. Codó	Fm. Codó		
		Fm. Sardinha	Fm. Grajaú	Fm. Sardinha	Fm. Sardinha	Fm. Sardinha	Fm. Sardinha	Fm. Sardinha	Fm. Sardinha	Fm. Grajaú
Jurássico	Fm. Corda	Fm. Corda	Fm. Corda	Fm. Corda	Fm. Corda	Fm. Corda	Fm. Sardinha	Fm. Pastos Bons	Fm. Sardinha	Fm. Sardinha
	Basaltos/Diabásios	Fm. Pastos Bons	Fm. Pastos Bons	Fm. Pastos Bons	Fm. Mosquito	Fm. Pastos Bons	Fm. Mosquito	Fm. Mosquito	Fm. Mosquito	Fm. Mosquito
	Fm. Sambaíba	Fm. Mosquito	Fm. Mosquito	Fm. Mosquito	Fm. Sambaíba	Fm. Mosquito	Fm. Sambaíba	Fm. Sambaíba	Fm. Sambaíba	Fm. Sambaíba
Triássico	Fm. Pastos Bons	Fm. Sambaíba	Fm. Sambaíba	Fm. Sambaíba	Fm. Sambaíba	Fm. Sambaíba	Fm. Sambaíba	Fm. Motuca	Fm. Sambaíba	Fm. Sambaíba

Figura 4 - Histórico de estudos sobre a estratigrafia do Mesozoico da Bacia do Parnaíba, com destaque para a Formação Pastos Bons. FONTE: Modificado de Romero Bállen (2012) e Rabelo & Nogueira (2015).

5 MATERIAIS E MÉTODOS

5.1 ANÁLISE DE FÁCIES

Esta etapa teve como base a técnica de modelamento de fácies sugerida por Walker (1992), constituída pela: 1) individualização e descrição de fácies, com o objetivo de caracterizar a mineralogia, textura e aspectos geométricos, bem como as estruturas sedimentares, conteúdo fóssilífero e padrões de paleocorrente presentes; 2) a compreensão dos processos sedimentares que atuaram na formação das fácies e 3) associação de fácies, com base em fácies contemporâneas e cogenéticas, as quais permitem a definição de diferentes ambientes e sistemas deposicionais. Este método foi utilizado em campo e auxiliado por seções panorâmicas e perfis colunares confeccionados em afloramentos.

5.2 ESTRATIGRAFIA DE SEQUÊNCIAS

Neste trabalho, utilizou-se a estratigrafia de sequências de alta resolução (Vail & Posamentier 1988; Van Wagoner *et al* 1990; Posamentier *et al* 1988; Mitchum & Van Wagoner 1991; Posamentier & James 1993; Kerans & Tinker 1997; Ribeiro 2001; Catuneanu 2006). Este método permitiu a reconstituição dos fatores controladores da sedimentação e sua relação com a formação de superfícies deposicionais. A determinação de “ordens” (*i.e.* terceira, quarta, quinta; Goldhammer *et al* 1993) é usada com restrições devido a subjetividade dos limites de tempo que separam as várias escalas de ciclicidade e o menor período de formação das sequências lacustres em comparação às sequências marinhas.

5.3 CICLOESTRATIGRAFIA

A delimitação de superfícies-chave na escala de afloramento foi utilizada na localização dos ciclos. Utiliza-se, neste trabalho, a definição de Kerans & Tinker (1997), na qual um ciclo de escala métrica representa superfícies de quarta a quinta ordem. Esta proposta é similar a definição de parassequência (Spence & Tucker 2007), que corresponde a sucessões sedimentares regionais, de escala métrica, com fácies que indicam raseamento ascendente, aprofundamento seguido de raseamento ascendente, agradação ou espessura constante da lâmina d'água. Ciclos recorrentes serão subdivididos em sequências deposicionais (e.g. Vail 1987), as quais constituem uma ferramenta fundamental na análise de alta resolução,

sobretudo na definição de tratos de sistema e oscilações do nível de base. Neste sentido, *Fischer Plots* foram utilizados para avaliar as variações de ciclicidades (mudanças de fácies, espessura, frequência/padrão) e determinação de superfícies-chave (Fischer 1964; Sadler *et al* 1993; Bosence *et al*, 2009). Esta metodologia compara o desvio cumulativo a partir da espessura média dos ciclos e o número de ciclos, no intuito de modelar a taxa de criação de espaço de acomodação relacionada às variações do nível de base. Nesta etapa, a extensão *Fischer Plot Excel* foi utilizada, conforme Husinec *et al* (2008).

5.4 PETROGRAFIA DE ARENITOS

A análise textural, mineralógica e diagenética foi feita a partir da confecção de lâminas delgadas e a contagem de, no mínimo, 300 pontos, com posterior classificação segundo a proposta de Folk (1968). O equipamento utilizado nesta etapa foi um microscópio petrográfico Axioskop polarizador e acessórios Zeiss, acoplado a uma câmera digital Sony CYBERSHOT, MPEG MOVIE EX, com 3.3 Mega Pixels e zoom de 6.0x em modo de cena, com a qual foram obtidas as fotomicrografias.

5.5 CATODOLUMINESCÊNCIA

A análise de catodoluminescência foi realizada em um CITL Cathodoluminescence Mk5-2. As imagens foram capturadas por uma câmera Leica DFC310 FX, acoplada a um microscópio Leica DM4500 P Led, posteriormente processadas no software LAS V4.4. O sistema foi operado com uma aceleração de voltagem de 15 Kv, corrente de 150 μ A e vácuo entre 0.003 e 0.05 Pa em tempo de exposição de 10 a 15 s e, em seguida, 50 s. Esta etapa contou com amostras de arenitos das formações Pastos Bons (8 amostras) e Corda (8 amostras). Critérios de definição da proveniência com base na luminescência do quartzo foram baseados em Augustsson & Bahlburg (2003), Bernet & Basset (2005) e Augustsson & Rekker (2012). Esta fase foi auxiliada por critérios petrográficos para a identificação de proveniência de quartzo, conforme Oliveira *et al* (2017).

5.6 MINERAIS PESADOS

A coleta sistemática de amostras foi realizada nos pacotes de arenito da sucessão estudada, cujas granulometrias variam de fina a média. Esta etapa foi seguida pela

desagregação e peneiramento a seco e a úmido. A determinação da assembleia de minerais pesados seguiu a metodologia clássica descrita por Morton (1985; 2012), de modo que os minerais pesados foram separados nas frações 0,062-0,125 mm e 0,125-0,250 mm, com a elutriação em bromofórmio (densidade 2,8 g/cm³) e posterior montagem em lâminas de vidro. Contagens de 100-300 grãos foram realizadas segundo a técnica de *ribbon counting* (Galehouse 1971). Para melhor restringir a proveniência com base em minerais pesado, Morton & Hallsworth (1994) sugeriram a contagem e cálculo da proporção de minerais com o mesmo comportamento hidráulico e diagenético. Neste sentido, os índices GZi e RZi também foram empregados para os depósitos estudados. Este trabalho contou com 14 amostras da Formação Pastos Bons, 10 amostras da Formação Corda e 4 amostras da Formação Grajaú. Amostras com concentração de pesados não-opacos e não-micáceos insuficientes para a análise quantitativa foram utilizadas apenas na identificação mineralógica e descrição dos principais aspectos morfológicos e texturais dos grãos.

5.7 DIFRAÇÃO DE RAIOS-X

As análises de difração de raios-X foram realizadas no Laboratório de Difração de Raios-X do Instituto de Geociências e aplicadas em seis amostras do “Folhelho Muzinho” (Roxo & Løefgren 1936). Nesta etapa, utilizou-se um Difratorômetro modelo Emyrean da PANalytical, com tubos de raios-X cerâmicos de anodo de Co ($K_{\alpha 1} = 1,789010 \text{ \AA}$), foco fino longo, filtro K_{β} de Fe, detector PIXCEL3D-Medpix3 1x1, no modo *scanning*, com voltagem de 40 kV, corrente de 35 mA, tamanho do passo 0.0262° em 2θ , varredura de 3.0072° a 94.9979° em 2θ , tempo/passo de 30,6 s, fenda divergente: $1/4^{\circ}$ e anti-espalhamento: $1/2^{\circ}$, máscara: 10 mm.

ARTIGO 1 – Lake cyclicality as response to thermal subsidence: a post-CAMP scenario in the Parnaíba Basin, NE Brazil

Cardoso¹, A. R.; Nogueira¹, A. C. R.; Rabelo¹, C. E. N.

¹Programa de Pós-Graduação em Geologia e Geoquímica – Universidade Federal do Pará

Abstract

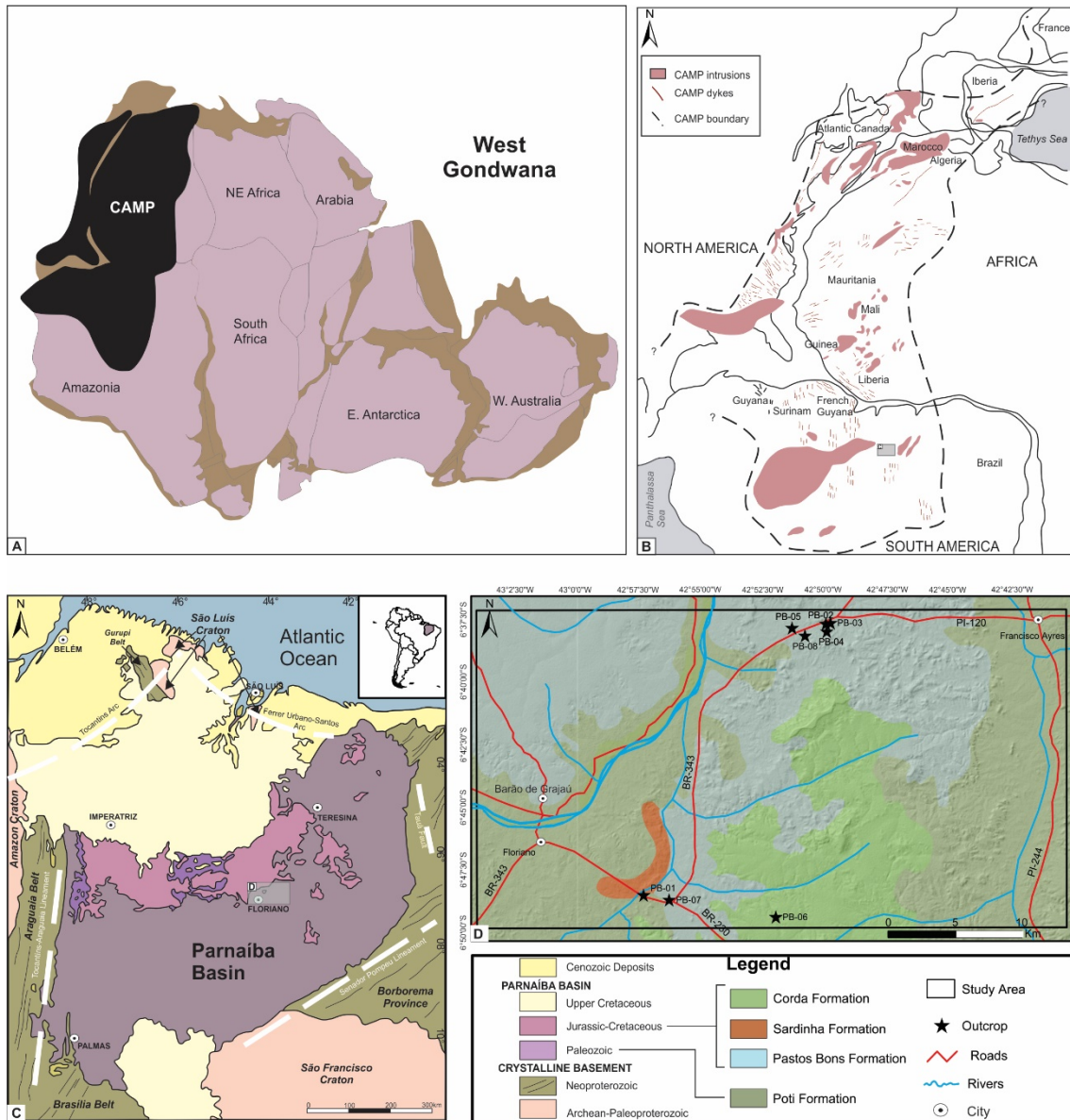
The Jurassic-Cretaceous transition was marked by the fragmentation of the West Gondwana supercontinent and consequent opening of the Atlantic Ocean. This event resulted in extensive lava flows in the central portion of West Gondwana, composing the Central Atlantic Magmatic Province. In the Parnaíba Basin (NE Brazil), a large lacustrine system succeeded this event, nevertheless, the post-CAMP scenario and the influence of the decreasing isotherms in the Mesozoic sedimentation are poorly understood. In this sense, cyclostratigraphy and outcrop-based facies analysis were carried out in the lacustrine stratigraphic record, allowing the recognition of four paleoenvironments: central lake, sheet-like delta front, lakeshore and ephemeral fluvial channels, mainly organized in shallowing upward cycles. The upsection transition of thin black shales and limestones to thick oxidized mudstones and stratified sandstones reflects the evolution of underfilled to overfilled lake settings. The lacustrine succession is organized in four major depositional cycles, characterized by millimeter to centimeter-scale cycles, bounded by unconformities or flooding surfaces. The cycles define a retrogradational-progradational-retrogradational stacking pattern, with random and frequent changes in lithology and cycle thickness. Subsidence was also influenced by crustal loading associated with thick subsurface Jurassic intrusions. Cyclostratigraphic data suggest that the upward increasing accommodation space was controlled by the post-CAMP thermal subsidence, as well as shifts in sedimentary supply and water inflow/outflow.

1 INTRODUCTION

The last depositional history in West Gondwana during terminal Jurassic times was concomitant to the subsidence that preceded the continental break up (Torsvik and Cocks, 2013). Short-lived asthenospheric upwelling beneath the plate is linked to basic intrusions that modified the Gondwana landmass organization and caused localized uplifts adjacent to extensive thermally subsiding regions (Klöcking *et al*, 2018). These subsiding zones allowed

the establishment of a large lacustrine setting coincident with the Mesozoic depocenters (Cardoso *et al*, 2017). This geological pathway is recorded in the Upper Jurassic-Lower Cretaceous lacustrine siliciclastic deposits of the Parnaíba Basin, Northeastern Brazil (Fig. 1). The most expressive magmatic event in West Gondwana is linked to the Central Atlantic Magmatic Province (CAMP), which comprises massive lava flows triggered by the Atlantic Ocean opening (Torsvik and Cocks, 2013; Oliveira *et al*, 2018).

Large magmatic accumulations concentrated on the northern Brazilian sedimentary basins comprise subvolcanic intrusions up to 700.000 km³, equivalent to 58-66% of the CAMP sill volumes worldwide (Svensen *et al*, 2018). In the Parnaíba Basin, these sills may reach up to 250 m-thick and hundreds of kilometers in extent (Trosdorf Jr. *et al*, 2018), although little is known about the post-magmatic stages. The influence of subsidence and extensional processes in lake generation is widely reported; nevertheless, the role of thermal subsidence in lacustrine depositional sequences is rarely addressed in previous works (e.g. Allen, 1997; Higgs, 1999; Abdullayev *et al*, 2018). This favors to consider the Mesozoic lacustrine siliciclastic succession as the prime candidate to evaluate the depositional history developed during Upper Jurassic-Lower Cretaceous in West Gondwana. The outcrop-based facies and stratigraphic analysis allowed identifying depositional sequences and different cycle patterns, providing a new stratigraphic lecture for this succession. Afterwards, we interpret the paleogeographic implications of these deposits in the context of the West Gondwana supercontinent. Furthermore, the cyclostratigraphic analysis of lacustrine deposits allowed including criteria to reach a more robust stratigraphic framework for Mesozoic Era of the Parnaíba Basin, as well as contributing to understand the post-CAMP events in the West Gondwana.



2 GEOLOGICAL SETTING

The Parnaíba Basin is a Paleozoic intracratonic basin, located in the northern South American Platform, northeastern Brazil (Aguiar, 1969; 1971; Góes and Feijó, 1994). This basin is defined as a sag-type (Daly *et al*, 2014), comprises approximately 600.000 km² and may reach 3.4 to 3.5 km-thick sediments in its center (Caputo, 1984; Vaz *et al*, 2007). The origin and evolution of the Parnaíba Basin are mainly related to tectonomagmatic events (Daly *et al*, 2014). Important lineaments and fold structures were generated and/or reactivated

by decompression and cooling events, which influenced in grabens formation, especially during the Gondwana fragmentation (Schobbenhaus *et al*, 1984). The basement is represented by crystalline rocks of the Araguaia-Tocantins Fold Belt, Borborema Province and pre-Silurian precursor basins (Riachão and Jaibaras basins) (Castro *et al*, 2014; Daly *et al*, 2014; Porto *et al*, 2018).

The Mesozoic Era was marked by the landmass reorganization due to the fragmentation of Pangea and, afterwards, of the Gondwana supercontinent resulting in drastic ecological and geological consequences on a global scale (Torsvik and Cocks, 2013; Holz, 2015). In the Parnaíba Basin, this scenario is documented by continental strata deposited in arid/semiarid conditions recording desertic-lacustrine (Motuca Formation) (Abrantes *et al*, 2016), desertic (Sambaíba Formation) (Abrantes and Nogueira, 2012), fluvial-lacustrine (Pastos Bons Formation) (Romero Bállen, 2012; Cardoso *et al*, 2017), fluvial-aeolian (Corda Formation) (Rabelo and Nogueira, 2015), fluvial-deltaic (Grajaú Formation) (Góes and Rossetti, 2001) and extensive volcanic plains (Merle *et al*, 2011; Oliveira *et al*, 2018). The magmatic events are mainly subdivided in two stages, generated during the Lower Jurassic and Upper Cretaceous (Veevers, 2004; Torsvik and Cocks, 2013; Merle *et al*, 2011; Heilbron *et al*, 2018). The first event is accurately related to the Central Atlantic Magmatic Province (CAMP), a massive outpouring of lava flows concomitant to the opening of the Atlantic Ocean, whereas the origin of the second stage, as well as the possible occurrence of a third stage, remain debatable (Heilbron *et al*, 2018; Klöcking *et al*, 2018; Oliveira *et al*, 2018).

The lacustrine succession of the Pastos Bons Formation, focus of this work, is positioned in the Jurassic Sequence of the Parnaíba Basin. The deposition of this unit occurred through the Xambioá Structure, which behaved as a depression during the Mesozoic (Hasui *et al*, 1991). Many authors consider that this deposition was concentrated in paleodepressions, located between topographic highs formed by lava flows (Lima and Leite, 1978; Góes and Feijó, 1994; Vaz *et al*, 2007). These deposits unconformably overlie Paleozoic successions of Poti, Piauí, Pedra de Fogo and Motuca formations (from east to west) and present concordant to gradational contacts with Corda Formation (Aguiar, 1971; Lima and Leite, 1978; Santos and Carvalho, 2004). Pastos Bons Formation is defined as a fluvial-influenced lacustrine setting in arid/semiarid climate, with local occurrence of deltaic deposits (Mesner and Wooldridge, 1964; Caputo, 1984; Góes and Feijó, 1994; Petra, 2006; Vaz *et al*, 2007; Romero Bállen, 2012; Cardoso *et al*, 2017).

3 METHODS

Facies analysis followed the facies modeling suggested by Walker (1992), constituted by facies individualization and description, comprehension of depositional processes and assembly of cogenetic/contemporaneous facies. X-ray diffraction followed total rock method and was applied in black shales to improve the mineralogical characterization. Cyclostratigraphy, based on the delimitation of key surfaces in outcrop scale, was applied in the identification and positioning of the individual cycles. In this work, we use the definition of Kerans and Tinker (1997), in which metric cycles represent fourth and fifth order processes. This proposal is similar to the parasequence definition, which corresponds to genetically related sedimentary successions, bounded by flooding surfaces (Spencer and Tucker, 2007; Catuneanu *et al.*, 2009). Recurrent cycles were subdivided in depositional cycles (Vail and Posamentier, 1987), which constitute a fundamental tool in high-resolution analyses, in this case considering the base level oscillations of the lake. In this sense, in order to evaluate cyclicity variations (facies changes, thickness, frequency/pattern) and define key-surfaces, we used the *Fischer Plots* extension (Fischer, 1964; Sadler *et al.*, 1993; Bosence *et al.*, 2009). This methodology compares the cumulative departure from average cycle thickness and the cycle number to estimate the accommodation space creation rate related to base level variations (Husinec *et al.*, 2008).

4 RESULTS

4.1 GENERAL ASPECTS

The Pastos Bons Formation is exposed throughout road cuts, dried drainage beds and small hills with exposures that reach up to 30 m-thick. Composite profiles indicate approximately 50 m-thick for the entire studied succession (Fig. 2). Intrusive basaltic dykes related to Cretaceous magmatism form bodies with tabular to irregular geometry reaching 30-50 cm-thick and oriented towards N-S and NE-SW (Fig. 2a). Cemented sandstones and gray and green-colored mudstones occur in the contact aureoles of these intrusions. Other diagenetic or hydrothermal features are calcite druses and calcite veins. Polymictic clast-supported conglomerate and coarse-grained sandstone from mid-Cretaceous Grajaú Formation unconformably overlies the studied succession, interpreted as fluvial deposits with migration to NW (Fig. 2c). Grajaú deposits contain basalt clasts suggesting a post-magmatic deposition. Coarse-grained fluvial sandstones of the Grajaú Formation fill metric dykes that

cut the top of Pastos Bons Formation (Fig. 2b). These clastic dykes can be considered as a fracturing or geomorphological readjustment coeval with the deposition of Grajaú Formation. Graben-like structures present ENE-WSW and NW-SE trends and occur in a stepped-like setting throughout approximately 200 km-width, as indicated by geophysical and stratigraphic data (Meju *et al*, 1999; Ballén, 2012). This extensional faulting affected the Paleozoic basement, Mesozoic succession (Mosquito and Pastos Bons formations) and Cenozoic lateritic levels in the topmost Pastos Bons beds, such that this unit may be topographic below or in lateral contacts with Paleozoic units (Fig. 2d).

The stratigraphic relations of the Pastos Bons deposits are summarized in Fig. 3. The outcrop-based facies analysis identified seventeen siliciclastic and chemical facies representative of a lacustrine system grouped in four facies associations: FA1 – central lake; FA2 – sheet-like delta front; FA3 – lakeshore; and FA4 – ephemeral fluvial channels (Table 1; Fig. 4).

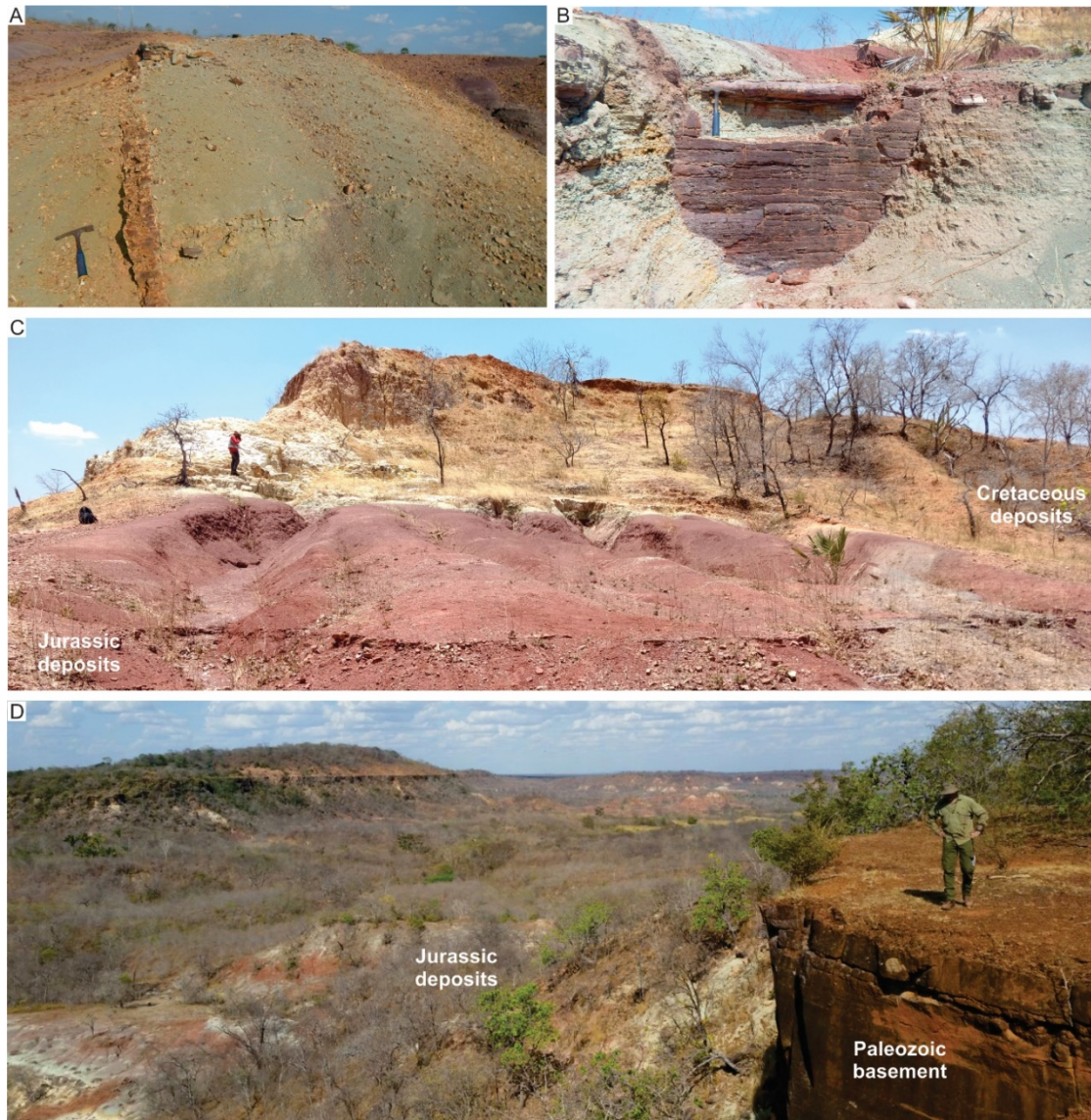


Figure 2 – Stratigraphic relations of the Upper Jurassic lacustrine deposits. A. Sardinha Formation dykes, crosscutting Pastos Bons Formation (Scale: 34 cm). B. Sedimentary dyke filled by fluvial deposits of the Grajaú Formation in the top of Pastos Bons beds (Scale: 34 cm). C. Fluvial deposits (Grajaú Formation) unconformably overlying Pastos Bons Formation (Scale: 1.70 m). D. Graben structures in the Parnaíba Basin, with Paleozoic basement topographically higher than Mesozoic deposits (Scale: 1.85 m).

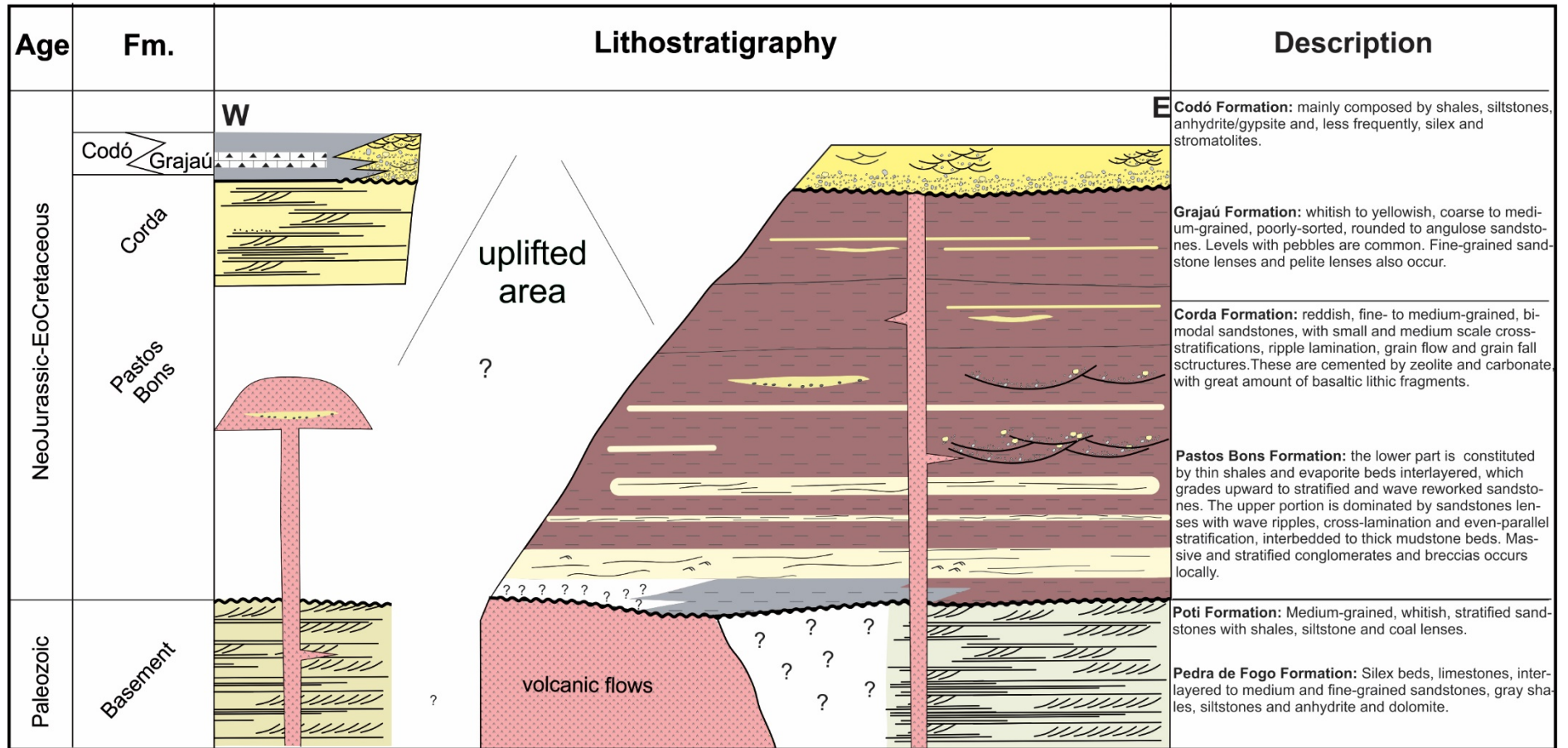


Figure 3 – Stratigraphic relations of the Upper Mesozoic succession of the Parnaíba Basin.

Table 1 – Facies, facies associations and depositional processes of Upper Mesozoic lacustrine succession of the Parnaíba Basin, Northeastern Brazil.

Facies	Description	Depositional Processes
Laminated Limestone (Ll)	Milimeter to centimeter-scale tabular beds composed by fibrous calcite crystals.	Lake water drop, Ca and CO ² saturation and consequent chemical precipitation in a low energy environment.
Fossiliferous Shale (Sf)	0.2-5 m-thick black shales, with tabular geometry and even-parallel lamination. Fossils of <i>Lepidotes piauhyensis</i> occur throughout the beds.	Transportation through suspension and deposition through fall-out in shallow water, high organic matter preservation in anoxic environment and with low sedimentary supply.
Laminated Mudstone (Ml)	Reddish, afossiliferous mudstone beds, with tabular geometry, 0.5-7 m-thick, laterally continuous. It presents even-parallel lamination to massive structure.	Transportation through suspension and deposition through fall-out with subordinated traction.
Mudstone with mudcracks (Mmc)	Centimeter-scale mudstone beds (<10 cm), with red color and quadratic mudcracks.	Low energy sedimentation and posterior subaerial exposure in semiarid/arid climate. Exposure and desiccation of muds.
Massive Siltstone (Sim)	2 m-thick massive to laminated siltstone beds, with grayish color Sandstone lenses occur locally and exhibit undulose laminations.	Transport through suspension and deposition through fall-out. Combined flow occurred subordinately.
Massive Sandstone (Sm)	Fine-grained, greenish to whitish sandstones, with massive to even-parallel structures. Cementation by carbonates.	Rapid sand deposition by traction, with consequent liquefaction. Cementation by diagenetic fluids.
Sandstone with supercritically climbing ripple cross-lamination (Scr)	Fine-grained sandstones, with subrounded and well-sorted grains, whitish to yellowish, and supercritically climbing ripple cross-laminations, capped by clay films. Beds are 0.3-2.5 m-thick.	Predominantly tractive transportation with high sedimentary supply rate.

Sandstone with adherence structures (Sa)	Fine-grained sandstones, with well-sorted and rounded to subrounded grains. These layers exhibit adherence warts and adherence laminations.	Subaereal exposure of a humid sandy substrate and aeolian reworking.
Sandstone with even-parallel stratification (Sep)	Tabular yellowish sandstone beds, 0.2-1.5 m-thick, with rounded to subrounded, moderately-sorted grains. These strata are fine to medium-grained, with even-parallel stratification and normal-to-reverse grading. Contacts may be marked by ball and pillow and flame structures.	Bedforms with straight crest transported by traction and predominance of upper flow regime. Unconfined and wax-wane flow.
Sandstone with trough cross-stratification (St)	Fine to medium-grained sandstone beds, with trough cross-stratification, in irregular beds, 0.5-1 m-thick.	Transportation by traction of bedforms with sinuous crest and predominance of lower flow regime.
Sandstone with incipient cross-stratification (Si)	Sandstones with medium-scale incipient cross-stratifications are up to 3 m-thick and exhibit irregular morphology. Abundant mica and quartz clasts in the sandstone. Paleocurrents indicate migration towards N/NE.	Transportation by traction of bedforms with sinuous crest and predominance of lower flow regime.
Sandstone with wave structures (Sw)	Irregular beds up to 5 m-thick, with undulose lamination, pinch and swell and wave ripples, which are capped by clay films. Contacts with adjacent facies may be marked by ball and pillow and flame structures.	Predominance of combined flow in shallow lake water. Plastic adjustment by liquefaction.
Sandstone with wave marks (Swm)	Fine-grained, well-sorted sandstones, with rounded grains in beds with 0.3-0.5 m-thick. Asymmetrical wave marks.	Decrease of water level accompanied by increase of sediment supply, shoaling and oscillatory flow reworking.
Stratified Breccia (Bs)	Tabular to base-truncated beds, 0.2-2 m-thick, consisting in large	Deposition by traction in a high energy environment with

		floating clasts (0,5-17 cm) in a coarse-grained matrix. Siliceous sandstone, mudstone and quartz clasts are common. Medium-scale tangential cross-stratification is present. These beds are cemented by carbonate.	substrate reworking by fluvial channels.
Massive Conglomerate (Cm)		Tabular, brown to greyish conglomerate beds, up to 1 m-thick, composed by clast- and matrix supported massive conglomerates with predominance of quartz clasts.	Rapid sedimentation by fluvial channels, with predominance of unidirectional bed-load currents.
Cross-stratified Conglomerate (Cs)		Clast- to matrix-supported conglomerates, with greyish colored beds, tabular to irregular geometry and 0.5-1.5 m-thick. These strata present medium-scale trough cross-stratification. Mudstone and quartz clasts (< 4 cm). are disseminated in the coarse-grained matrix.	High energy deposition by fluvial channels, with predominance of bedload unidirectional currents.

SW

NE

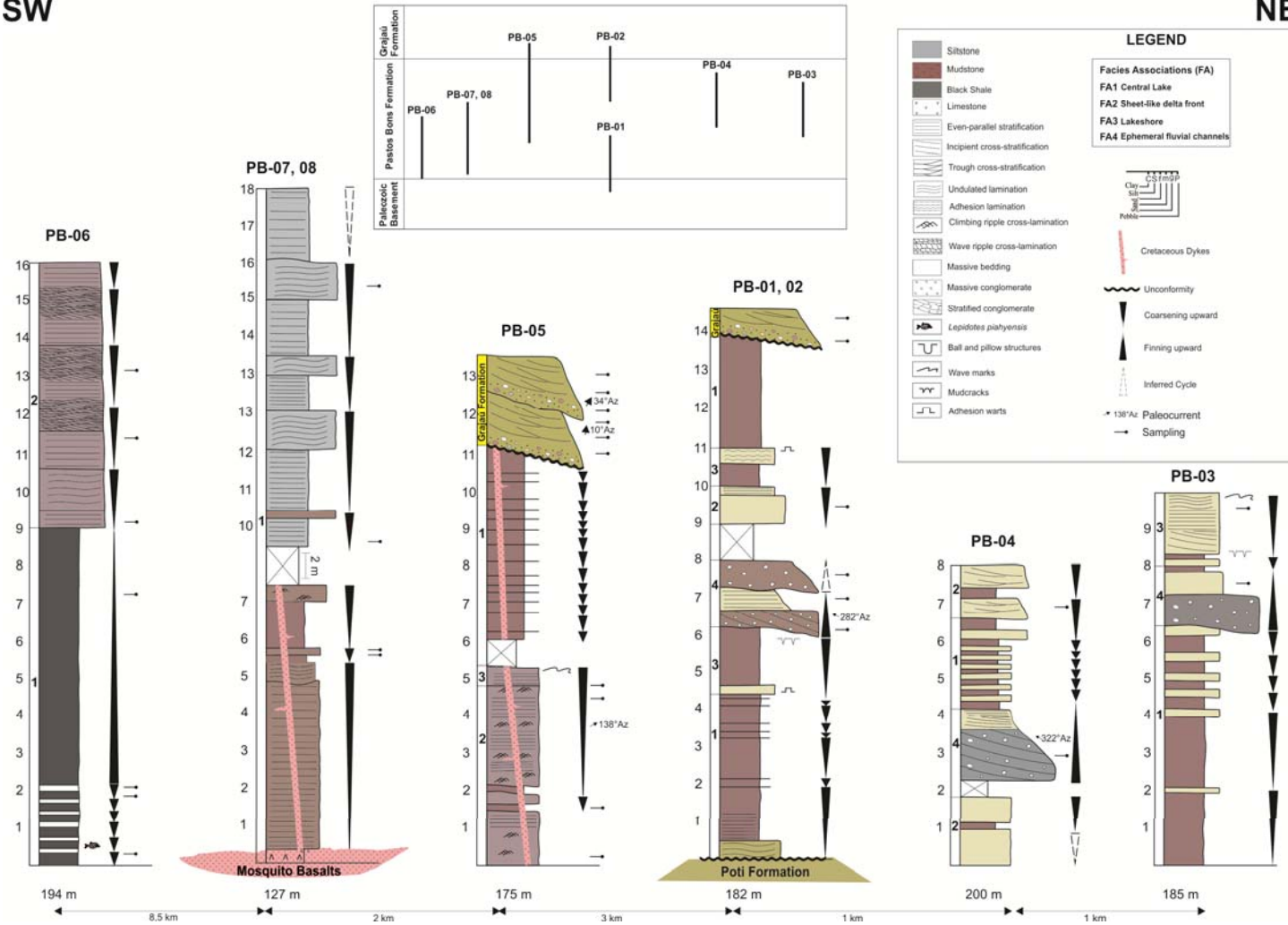


Figure 4 – Stratigraphic logs of the studied succession.

4.2 FACIES ASSOCIATION

FA1 – Central Lake

The FA1 is constituted by fossiliferous shale (Sf), laminated limestone (Ll), laminated mudstone (Ml), laminated siltstone (Sl), sandstone with supercritically climbing ripples lamination (Src) and massive bedding (Sm). Shales and limestones are organized in shallowing/salinization upward cycles in the base of this succession and upsection occurs a thickening upward of mudstone (Fig. 5a). The facies Sf is constituted of tabular, pyrite-bearing black shales with even-parallel lamination associated with abundant *Lepidotes piauhyensis* fossils (Fig. 5b). Several specimens of adult and young individuals with different sizes are well-preserved. X-ray diffraction in black shales indicate predominance of smectite, illite, calcite and quartz. Thin horizons define small-scale (<0.3 m) shallowing/salinization upward cycles with Ll facies in the top constituted of fibrous calcite crystals, forming tabular and irregular layers, laterally continuous for dozens of meters. These packages grade vertically to laminated or massive, oxidized, afossiliferous and relatively thick (~7 m) mudstone (Ml facies), locally with sandstone lenses (Fig. 5c, d). Massive to even-parallel laminated siltstone are up to 6 m-thick and can be continuously correlated for hundreds of meters along of the studied area.

The upper portion of FA1 is characterized by centimeter to millimeter-thick beds of massive to laminated sandstone interbedded with mudstone (Sm and Src facies). This association consists in tabular to irregular strata formed by small-scale thickening upward cycles with predominance of mudstone beds. Facies Src presents pervasive calcite cement and, locally, veins filled by spar calcite. The upper contact with FA2 is sharp and occasionally exhibits deformational structures.

Interpretation: FA1 records two different lacustrine phases. The first phase includes facies Sf and Ll, organized in millimeter to centimeter-scale shallowing/salinization upward cycles. Pyrite-bearing black shales and the whole-body-fossil of *Lepidotes piauhyensis* indicate low energy and anoxic conditions related to the central portions of the lake. We considered an active thermocline, such that the deepest portions of the lake were protected from oxygen replenishment. Unselective mass mortality was probably caused by thermocline demise and abrupt changes in oxygenation, such that the thanatocoenosis is constituted by a polytypical fossil assemblage containing individuals of variable sizes, with juvenile and old specimens in the same horizon (Petra, 2006). Additionally, the anoxia is corroborated by

specimens with tetany, back-arching and gasping fish fossils (Grogan and Lund, 2002; Petra, 2006). Fossils preservation was probably enhanced by rapid burial, high nutrient content and anoxic conditions (e.g. Carroll and Bohacs, 1999; Bohacs *et al*, 2000, 2003; Retallack, 2011). According to Petra (2006), Pastos Bons lake was characterized by temperatures of 20-30°C and saline water, under arid to semi-arid climate during the Mesozoic Era in West Gondwana (Holz, 2015). The contraction phase in the lake is evidenced by shallowing/salinization cycles formed by increase of evaporation (outflow) associated with low pluvial precipitation and reduced riverine inflow. In these conditions, the kinetic precipitation of Ca^{+2} and CO_2 saturation led to lime mud accumulation. Fibrous calcite associated with lime muds may represent a secondary phase, with pseudomorphs after gypsum crystals. The upper portion of the FA1 marks the second phase defined by lake expansion, which was caused by increasing water and sediment supply and characterized by mud deposition in the distal portions (M1 and S1 facies). Interbedded mudstones and massive to laminated fine-grained sandstones suggest variation of suspension and siliciclastic underflows. Apparently, the expansion and contraction phases did not modify the water stratification in the central lake setting.

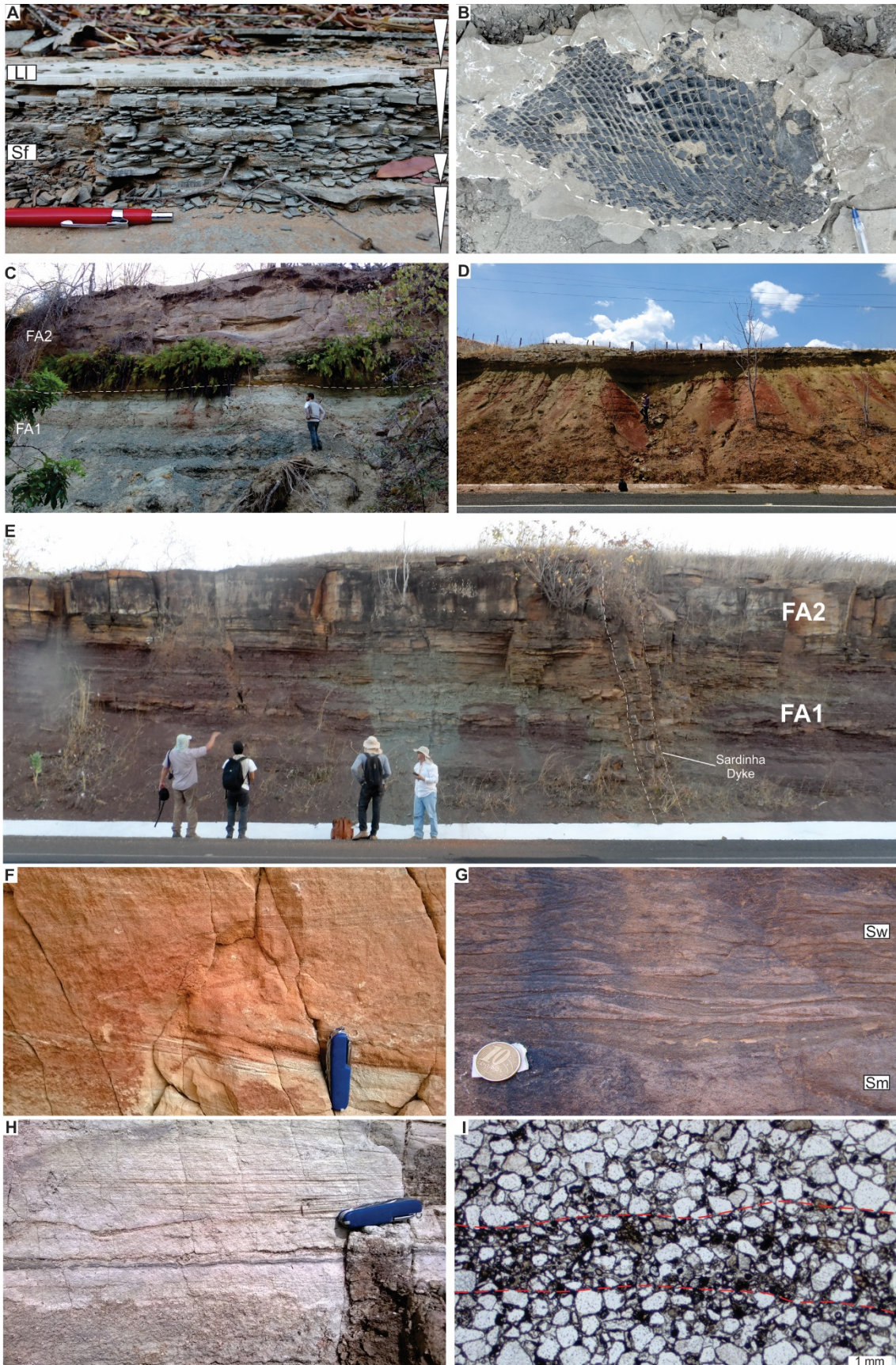


Figure 5 – Central lake and sheet-like delta front deposits. **A.** Interlayering of black shales and limestone beds organized in shallowing/salinization upward cycles (Scale: 1.70 m). **B.** Well-preserved *Lepidotes piauhyensis* specimen (Scale: 2 cm). **C.** Sharp contacts between FA1 and FA2 (Scale: 1.70 m). **D.** Upper part of FA1, with reddish mudstones interlayered with sandstone beds (Scale: 1.70 m). **E.** Abrupt contact between FA1

and FA2. Cretaceous basaltic dykes crosscut these packages (Scale: 1.80 m). **F.** Incipient cross-stratification in sandstones (Scale: 10 cm). **G.** Pinch and swell structures (Scale: 1 cm). **H.** Sandstone with even-parallel and low-angle cross-stratifications (Scale: 10 cm). **I.** Thin section of sandstone with even-parallel stratification showing normal-to-reverse grading.

FA2 – Sheet-like Delta Front

The FA2 is constituted mainly by sandstone with trough cross-stratification (St), even-parallel lamination (Sep), wave structures (Sw) and massive bedding (Sm). This FA occurs in sharp contacts with FA1 and composes shallowing upward and thickening upward cycles (Fig. 5e). These packages crop out in 12 m-thick successions with lateral continuity for hundreds of meters. Small-scale sets of trough cross-stratification comprise tabular beds with 0.5-1 m-thick exhibiting migration to NW and SE (Fig. 5f). Facies St is associated with tabular to irregular fine-grained sandstone beds and internally exhibit wave ripples, undulated and pinch and swell laminations marking the topmost of shallowing upward cycles (Fig. 5g). The even-parallel stratification (Sep facies) generally is defined by normal-to-reverse grading included in 0.2-1.5 m-thick strata (Fig. 5h, i). The contact with FA1 is marked by deformational features, such as ball and pillow and flame structures. Low-angle cross-lamination and massive beds (Sm) occur locally.

Interpretation: FA2 occurs as laterally extensive tabular beds, which compose flatbeds deposited in lower (St facies) to upper (Sep facies) flow regime (e.g. Olariu *et al*, 2010). These deposits record unconfined flows supplied by intermittent fluvial channels that spread in the marginal lacustrine system, probably during flash floods (e.g. Della Fávera, 2001; Olariu *et al*, 2010). The hyperpycnal sedimentary load deposition over a pre-lithified clay-rich substrate possibly hindered the friction causing underflows that reached deep portions of the lake (e.g. Reading, 1984; Andrade *et al*, 2014). The rapid deposition resulted in the construction of an unconventional delta front (e.g. Olariu *et al*, 2010) and can explain the predominantly sharp contacts between FA1 and FA2.

The increasing sediment supply into the lake promoted the progressive reduction of accommodation space, recorded by thickening upward cycles of sandy beds. The progressive shoaling caused the water level fall which allowed the reworking by oscillatory flow (Sw facies) (e.g. Dumas *et al*, 2005; Lamb *et al*, 2008; Bouma, 2008; Luca and Basilici, 2013). Rapid deposition over relatively water-saturated beds triggered syndimentary deformation (liquefaction), indicated by soft-sediment deformation (e.g. Owen and Moretti, 2011; Owen *et al*, 2011). Although this succession presents similarities with the Bouma Sequence, some differences are outstanding. Some examples are normal-to-reverse grading in the same beds,

as well as the interlayering of even-parallel stratified and wave rippled sandstones (e.g. Olariu *et al*, 2010), which indicate wax-wane flow (*sensu* Lamb *et al*, 2008; North and Davidson, 2012). Paleocurrent data reflect the variable sedimentary sources, supplied by multiple ephemeral fluvial channels.

FA3 – Lakeshore

The 1.5 m-thick succession of FA3 is organized in shallowing upward cycles that include sandstone with wave structures (Sw facies) and even-parallel laminations (Sep facies) which vertically grades to sandstones with adhesion structures (Sa facies) and massive to laminated mudstones (Ml facies). Complete, non-orthogonal and non-oriented mud cracks occur in mudstone whose contact with sandstone are marked by load cast (Mmc facies). Raindrops are imprinted on even parallel planes superimposing parting lineation (Fig. 6a-e). The limits of the cycles gently dip (2-4°) composing a large scale bedform with lateral continuity for dozens of meters.

Interpretation: FA3 represents the marginal portion of the lake, whose deposition was predominantly in low energy conditions. The seasonal variation of riverine sand discharge promoted the modification of the shoreface/foreshore profile (Ilgar and Nemec, 2005; Nichols, 2009). The successive phases of shoaling caused exposure of the lake margin, and laminated sands forming a humid substrate (Sep and Sw facies) sporadically reworked by wind (Sa facies) (e.g. Davis Jr., 1992). The sands were deposited by upper flow regime in the lake margin and frequently exposed and marked by sporadic rains. The cracked muds deposited in ponds confirm the frequently exposure of the lakeshore.

FA4 – Ephemeral Fluvial Channels

The FA4 is constituted of matrix-supported stratified breccia (Bs), massive conglomerate (Cm), trough cross-stratified conglomerate (Ct), sandstone with trough cross-stratification (St), massive bedding (Sm) and even-parallel stratification (Sep), as well as laminated mudstone (Ml). FA4 deposits exhibit irregular geometry and are organized in small-scale fining upward cycles with medium to coarse-grained facies (Bs, Cm, Ct and St facies) to mudstone beds (~5 cm; Ml facies). Bs, Cm and Ct facies consists in meter-scale massive to tangential cross-stratified layers, with medium coarse-grained sandy matrix with rounded to subrounded grains, rich in opaque minerals. The clasts present 0.5 to 17 cm-length

and are constituted of silex and, subordinately, sandstone, mudstone and quartz fragments (Fig. 6f). The massive to stratified conglomerates (Cm and Ct facies) exhibit scoured bases and trough cross-stratified sandstone (St) forms sets up to 1 m-thick (Fig. 6g, h). These beds grade upsection to tabular, fine to medium-grained sandstone with even-parallel stratification or massive bedding (Sep and Sm facies). Supercritically climbing ripple cross-lamination occurs associated in the toe set of trough cross bedding (St facies). The sandy facies generally include fine to medium-grained, rounded and well-sorted grains. Small-scale cross-stratifications migrate to NNW, NNE and SW. These deposits overlap FA1 with predominantly erosive contacts (Fig. 6i).

Interpretation: stratified breccias and massive to stratified conglomerates (Bs, Cm and Ct facies) indicate tractive, high-energy currents forming gravel bars, during ephemeral fluvial channel migration enhanced by flash floods (Davis Jr., 1992; Nichols, 2009). Tabular, laterally extensive beds organized in fining upward cycles up to 2 m-thick indicate high lateral migration in reduced accommodation space for sedimentation (Davis Jr., 1992). Transition to massive or trough cross-stratified sands suggests decreasing energy flow, with migration of straight (Sep facies) and sinuous (St facies) crest bedforms in predominantly lower flow regime (Nichols, 2009). The waning of the riverine inflow generated slack water with deposition of muds (Ml facies).



Figure 6 – Lakeshore and ephemeral fluvial channel deposits. **A.** Undulated laminations covered by clay films (Scale: 5 cm). **B.** Asymmetrical wave ripples (Scale: 5 cm). **C.** Adhesion warts (Scale: 5 cm). **D.** Mudcracks from facies Mmc (Scale: 34 cm). **E.** Sandstone with parting lineation and raindrops filled by calcite (Scale: 34 cm). **F.** Facies Cm, with clasts up to 17 cm-length (Scale: 5 cm). **G.** Sandstones with small-scale trough cross-stratification (Scale: 34 cm). **H.** Sharp contacts between FA1 and FA4 (Scale: 34 cm). **I.** Massive conglomerate from facies Cm (Scale: 5 cm).

5 CYCLOSTRATIGRAPHY

In this work, we applied Kerans and Tinker (1997) definition, which proposed “small-scale cycles” to designate parasequence-scale deposits. These are composed of meter-scale cycles, which record up to 10^4 - 10^5 years coastline shifts, defining fourth to fifth order successions. This terminology was originally applied in marine settings; however, its definition allows the use of this concept in continental environments with some restrictions due to smaller timescales in lacustrine coastlines oscillations. The Pastos Bons Formation consists in a retrogradational lacustrine system, whose stratigraphic record reaches approximately 50 m-thick and comprises black to brown-red-colored shales, sandstones, as well as conglomerates and limestones. These deposits are organized in shallowing/salinization, thickening, thinning and fining upward small-scale cycles, bounded by unconformities and/or flooding surfaces. These cycles are detailed below, according to the facies association(s) in which they occur.

5.1 LACUSTRINE CYCLES

Shallowing/salinization upward cycles occur in central lake deposits and are denominated by Cycle Type 1 (underfilled lake cycles). These are constituted of millimeter to centimeter-scale black shales and limestone beds, symmetrically repeated exclusively in the base of FA1 (Fig. 7a). The Cycle Type 1 is aggradational, bounded by a lacustrine flooding surface, which marks the transition to thickening upward cycles of shale beds and disappearance of limestone laminae. These deposits grade vertically to massive sandstones and thick massive to laminated, oxidized mudstone layers (~7 m) which compose thickening upward cycles (Cycle Type 2; overfilled lake cycles). Cycle Type 2 is asymmetrical and exhibits an aggradational to retrogradational pattern (Fig. 7b).

The transition of FA1 to FA2 is marked by a maximum lacustrine flooding surface, with mudstone beds overlain by stratified sandstones, grouped in shallowing and thickening upward cycles (Cycle Type 3; sheet-like delta front cycles) (Fig. 7c). These cycles are 10 m-thick, asymmetrical, progradational, and the upper boundary is marked by wave rippled sandstones. Contacts between facies associations may be characterized by soft sediment deformation structures (ball and pillow and flame structures). Cycle Type 4 (lakeshore cycles), predominantly asymmetrical, defines shallowing upward cycles, restricted to FA3. These are constituted by massive to laminated sandstones which grade to sandstones with wave marks, followed by sandstones with adhesion structures and mudstones with mudcracks, which is the upper limit of the cycles (Fig. 7d).

5.2 EPHEMERAL FLUVIAL CHANNEL CYCLES

Cycle Type 5 (ephemeral fluvial channel cycles) occurs asymmetrically in FA4 in up to 0.5-2 m-thick successions. These are fining upward cycles, defined by massive to stratified breccias and conglomerates, overlain by medium to fine-grained sandstones and thin pelites (Fig. 7e). These cycles may also start with coarse-grained sandstones with trough cross-stratification or massive bedding and are restricted to the intermediary portion of the lacustrine succession.

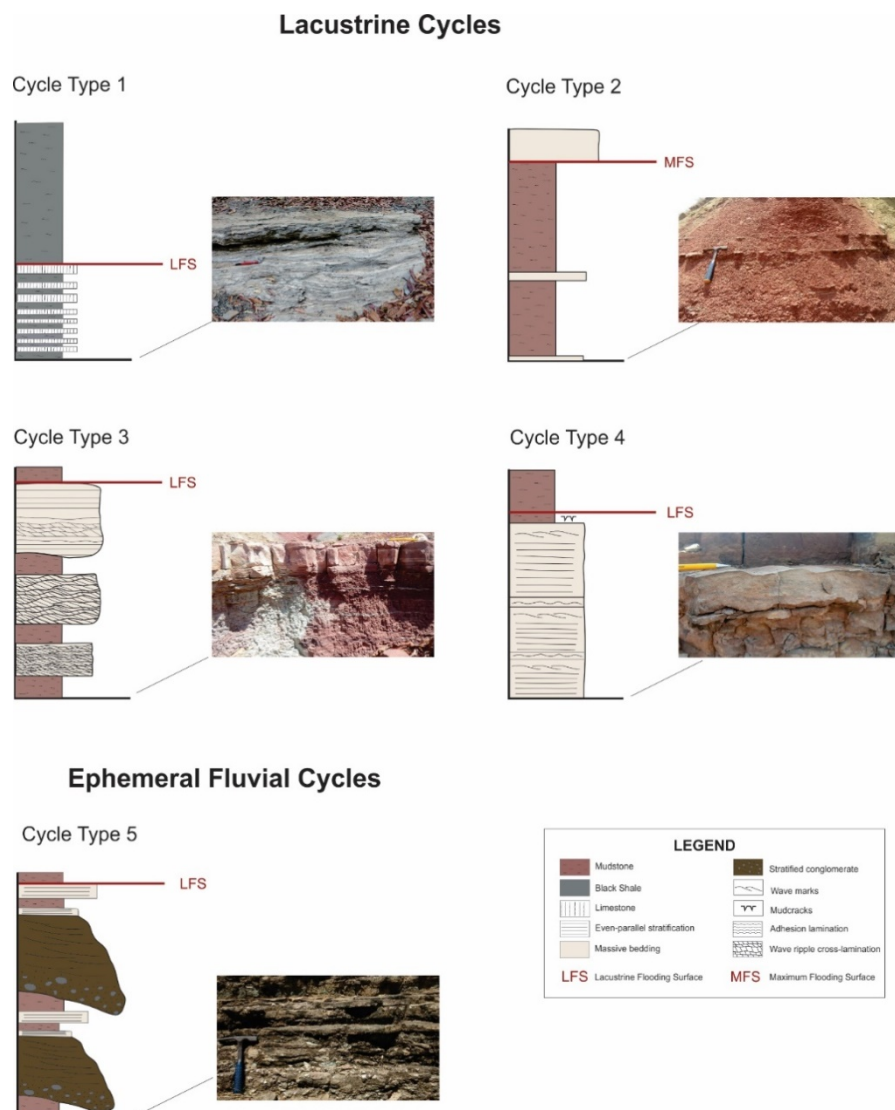


Figure 7 - High-frequency lacustrine cycles and fluvial cycles. Cycle type 1 – underfilled lake; Cycle type 2 – overfilled lake; Cycle type 3 – sheet-like delta front; Cycle type 4 – lakeshore; Cycle type 5- ephemeral fluvial channel.

6 THE ROLE OF THERMAL SUBSIDENCE IN LAKE CYCLES

The Upper Jurassic-Lower Cretaceous lacustrine succession of the Parnaíba Basin is mainly constituted of shallowing upward cycles. The lower portion is constituted by black shales and laminated limestones (FA1) which indicate high evaporation rate, low siliciclastic supply and low energy. These packages compose the depositional cycle 1 (CI), limited at the base by an unconformity of Pastos Bons Formation over a Paleozoic basement, as well as Jurassic volcanic rocks. The upper portion is outlined by a lacustrine flooding surface (LFS), which marks the upward lake deepening. The LFS delimitates the depositional cycle 2 (CII), constituted of massive to laminated mudstones interbedded with thin sandstone beds. The retrogradational pattern reflects the lake widening, increasing accommodation space and changes in sedimentary pattern due to the sporadic water and sediments inflow, probably supplied by ephemeral fluvial channels. This sequence is bounded upsection by a maximum flooding surface (MFS), positioned between FA1 and FA2.

Depositional cycle 3 (CIII) is progradational, marked by the lakeward shift of sedimentary facies, mainly provoked by lake water drop, probable remobilization of sediments in the lakeshore, as well as high sedimentation rates triggered by unconfined flows. This relation is indicated by sharp contacts between FA1 and FA2 and small-scale scours in the lakeshore (FA4; e.g. Keighley *et al*, 2003). CIII is constituted of thickening upward cycles, with predominantly flatbeds and evidences of wave reworking. Sandstones with wave structures, adhesion laminations/warts and mudstones with mudcracks occur locally (FA3) and record the water level waning in the lakeshore. Nevertheless, the upsection transition of these deposits to thick mudstone beds (FA1) suggests a new lake water deepening (retrogradational pattern) in oxidizing conditions, interpreted as depositional cycle 4 (CIV). This unit was probably influenced by increasing water and sediment input rate.

The Mesozoic lacustrine deposits of the Parnaíba Basin record an evolution of an underfilled to overfilled lake system (e.g. Carroll and Bohacs, 1999; Bohacs, 1999; Bohacs *et al*, 2000; 2003). This framework indicates the transition of closed saline lakes, in the lower succession, to open freshwater lakes upsection. Fischer Plots evidence this trend, with the upward increase of the cycles thickness and accommodation space (Fig. 8). Individual cycles exhibit lithological variability, as well as random and frequent changes in cycle thickness. These aspects are typically associated with subsidence pulses, since climate-influenced cycles are characterized by rhythmic lithology and regular thickness (Benvenuti, 2003; Paz and Rossetti, 2005; Nichols, 2009).

Recently acquired wide-angle reflection-refraction data identified increasing mantle and lowermost crust P-velocities toward the western portion of the Parnaíba Basin, which are directly linked to massive basic intrusions related to Jurassic magmatism (Soares *et al*, 2018). Although large lineaments occur in the eastern portion of the Parnaíba Basin, the uppermost crust was only weakly affected by Mesozoic extensional tectonics and the Neoproterozoic-Cambrian rifts underlying the basin had little effects on the Mesozoic evolution (Tozer *et al*, 2017; Soares *et al*, 2018). Therefore, the increasing accommodation space trend of the lacustrine system may be interpreted as a result of a slow and large-scale thermal subsidence that affected the Parnaíba Basin during the Upper Mesozoic (e.g. Hamdani *et al*, 1991; Hamdani *et al*, 1994; Klöcking *et al*, 2018; Soares *et al*, 2018). These events were probably caused by the decreasing isotherms temperature in consequence of the post-magmatic cooling (Jurassic CAMP magmatism). Depocenter shifts followed this thermal subsidence phase, controlled drainage systems, sediment/water input and probably triggered the evolution of the Pastos Bons lakes in the Parnaíba Basin (Fig. 9). This interpretation is coherent with the wide distribution (~550 km) and low maximum thickness of the Jurassic-Cretaceous lacustrine succession (~80 m). Linkages between large igneous provinces (LIP) and significant subsidence over long time spans have been mathematically modeled by Leng and Zhang (2010). These authors suggest that LIP-induced subsidence may occur even before and during magmatic emplacements. Some examples include Siberian, Columbia River and Emeishan LIPs (Leng and Zhang, 2010). Similarly, transient environments from shallow (Early Permian) to deep (Late Permian) water are recorded underlying the Wrangellia flood basalts (Richards *et al*, 1991).

Although CAMP magmatism is mainly concentrated in the western portion of the basin, the crustal loading and subsequent flexural effects must have influenced a much larger area (e.g. Klöcking *et al*, 2018). This tectonic stage probably affected the whole basin, as indicated by Moho as deep (or deeper) beneath the center than in the flanks of the Parnaíba Basin (Tozer *et al*, 2017; Soares *et al*, 2018). Similar interpretations were obtained by Tozer *et al* (2017), which used seismic and gravity data to suggest that viscoelastic stress relaxation probably followed a massive crustal loading triggered by volcanic rocks. Subsidence spans that extend geological periods, sometimes during hundreds of million years, are characteristic of cratonic basins, such as the Parnaíba Basin itself (Allen and Armitage, 2011). A coupled mechanism of thermal subsidence and crustal loading also influenced the sedimentation of lacustrine settings in the South Caspian Basin from Jurassic to Tertiary times (Abdullayev *et al*, 2018). In this sense, we evaluate that the thermal subsidence triggered by the CAMP

magmatism was occurring during or even before the deposition of the Jurassic-Cretaceous lacustrine sediments and may have ceased before the Cretaceous magmatism (~200 Ma – 115 Ma), which probably induced an epeirogenic uplift in the Parnaíba Basin (Klöcking *et al*, 2010). This is also supported by water-loaded subsidence curves presented by Rodríguez Tribaldos and White (2018) that suggest thermal time constants between 68 and 100 Ma.

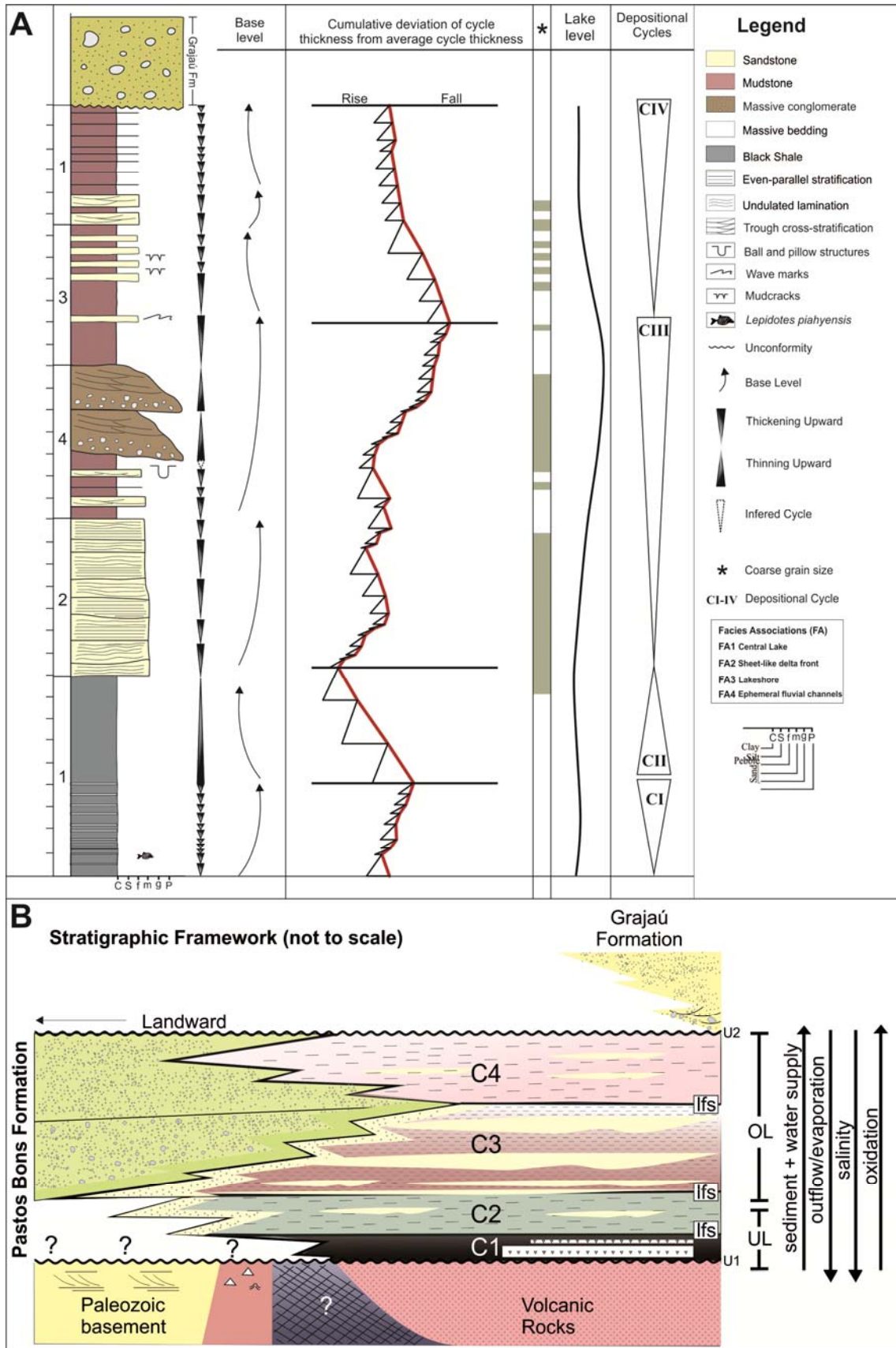


Figure 8 - A. General profile, stacking patterns, trends, Fischer plots and depositional cycles. **B.** Sequence stratigraphic stages and depositional cycles of the lacustrine system (CI-CIV – depositional cycle; lfs – lacustrine flooding surface; U1 – unconformity 1; U2 – unconformity 2; UL – underfilled lake phase; OL – overfilled lake phase).

7 THE JURASSIC-CRETACEOUS HISTORY OF THE WEST GONDWANA

The Lower Mesozoic succession of the Parnaíba Basin consists in the extremely arid desertic deposits overlying saline sabkha and lacustrine strata. This framework has been interpreted as the record of the Pangea assembly and regional uplift of the central and equatorial regions of this supercontinent, confining restricted seas or large lakes during Triassic (Abrantes *et al*, 2016). Previous plate reconstructions highlight that this stage marks a rapid rotation phase during Permian-Triassic transition, reaching the equatorial zone in the end-Triassic (Jaju *et al*, 2018). Afterwards, extensional forces caused the Pangea breakup triggering massive lava flows related to the Central Atlantic Magmatic Province (CAMP) (Veevers, 2004; Torsvik and Cocks, 2013; Svensen *et al*, 2018). Short-lived asthenospheric upwelling caused localized uplifts in the central region of the West Gondwana, adjacent to thermally subsiding areas (Klöcking *et al*, 2018). These depocenters allowed the implantation of a relatively shallow and large-scale lacustrine system in the central-southeastern Parnaíba Basin, coeval with wet desertic environments in the western margin (Rabelo and Nogueira, 2015).

New data presented in this work suggest that the paleogeographic rotation of the West Gondwana toward equatorial zones continued during the Upper Jurassic-Lower Cretaceous times. Nevertheless, large freshwater lakes and a wet desertic system evidence decreasing aridity conditions (Cardoso *et al*, 2017), possibly provoked by greenhouse upturns (e.g. Holz, 2015). Terminal opening stages of the Atlantic Ocean resulted in rifting processes and marine transgressions, causing subsequent environmental and climatic shifts in West Gondwana. This pathway is recorded by braided fluvial systems connected to shallow sea siliciclastic-evaporitic deposits (e.g. Góes and Rossetti, 2001; Paz and Rossetti, 2005). Cretaceous magmatism event (~126 Ma) dates the final Gondwana fragmentation, whereas a debatable third magmatic event (~118 Ma) in the Parnaíba Basin has been associated with the development of rift basins in western African and eastern Brazilian equatorial margins (Heilbron *et al*, 2018).

8 CONCLUSIONS

This work investigated the Upper Mesozoic depositional history after the massive emplacement and extrusion of basalts related to the CAMP in West Gondwana. Detailed outcrop-based stratigraphic and cyclostratigraphic analysis supported by Fischer Plots were performed in order to evaluate the influence of this thermal event in the sedimentary pathway

of the Parnaíba Basin, northeastern Brazil. The post-CAMP effects are better indicated by the Upper Jurassic-Lower Cretaceous lacustrine succession of the Pastos Bons Formation. This unit consists in central lake (FA1), sheet-like delta front (FA2), lakeshore (FA3) and ephemeral fluvial channels (FA4) deposits, mainly organized in shallowing upward cycles. The stratigraphic framework exhibits a retrogradational-progradational-retrogradational pattern, which is mainly defined by four depositional cycles (CI-CIV), bounded by lacustrine flooding surfaces and unconformities.

The lake evolution may be subdivided in two phases – underfilled and overfilled phases – with increasing accommodation space, mainly influenced by subsidence pulses and increasing water/sediment supply. A thermal subsidence stage in the Parnaíba Basin during the Jurassic-Cretaceous is indicated by lithological variability, random and frequent changes in cycle thickness, wide distribution (~550 km) and low thickness (~80 m) of the lacustrine succession, as well as weak or absent evidence of extensional tectonics in the upper crust. Additionally, voluminous subsurface intrusions in the northern South American Platform during Jurassic times may have induced rock loading and flexural effects in the Parnaíba Basin.

Acknowledgements

We are very grateful to National Council for Scientific and Technological Research (CNPq) for funding this research with a fellow scholarship (CNPq - 130823/2017-1) conceded to the first author, and to the Programa de Pós-Graduação em Geologia e Geoquímica (PPGG) of the Federal University of Pará (UFPA). We also thank Werner Truckenbrodt and Raphael Araújo for helpful suggestions. The first author also acknowledges the continuous contributions of the GSED Research Group members.

REFERENCES

- ABDULLAYEV, N. A.; KADIROV, F.; GULIYEV, I. S., 2018. Subsidence history and basin-fill evolution in the South Caspian Basin from geophysical mapping, flexural backstripping, forward lithospheric modeling and gravity modeling. *The Geological Society, London, Special Publications*, 472: 175-196.
- ABRANTES JR., F. R.; NOGUEIRA, A. C. R., 2012. Reconstituição paleoambiental das formações Motuca e Sambaíba, Permo-Triássico da Bacia do Parnaíba no sudoeste do Estado do Maranhão, Brasil. *Geol. USP, Sér. Cient.*, 13(3): 65-82.
- ABRANTES JR., F. R.; NOGUEIRA, A. C. R.; SOARES, J. L. Permian paleogeography of West-Central Pangea: reconstruction using sabkha-type gypsum-bearing deposits of Parnaíba Basin, Northern Brazil. *Sedimentary Petrology*, n. 341, p. 175-188, 2016.

- AGUIAR, G.A. de. Bacia do Maranhão: geologia e possibilidades de petróleo. Belém: PETROBRAS, 1969, p. 55-106. (Relatório Técnico, n. 371).
- AGUIAR, G.A. de. Revisão geológica da bacia paleozoica do Maranhão. In: CONGRESSO BRASILEIRO DE GEOLOGIA, 25, 1971, São Paulo. Anais... São Paulo: SBG, 1971. v.3, p. 113-122.
- ANDRADE, L.S.; NOGUEIRA, A.C.R.; BANDEIRA, J., 2014. Evolução de um Sistema Lacustre Árido Permiano, parte Superior da Formação Pedra de Fogo, Borda Oeste da Bacia do Parnaíba. *Geologia USP: Série Científica* 14 (4): 39–60.
- ALLEN, M. B.; MACDONALD, D. I. M.; XUN, Z.; VINCENT, S. J.; BROUET-MENZIES, C., 1997. Early Cenozoic two-phase extension and late Cenozoic thermal subsidence and inversion of the Bohai Basin, northern China. *Marine and Petroleum Geology*, n. 7/8 (14): 951-972.
- BENVENUTI, M. 2003. Facies analysis and tectonic significance of lacustrine fan-deltaic successions in the Pliocene–Pleistocene Mugello Basin, Central Italy. *Sedimentary Geology* 157: 197–203.
- BOHACS, K.M., 1999. Sequence stratigraphy of lake basins; unraveling the influence of climate and tectonics: *American Association of Petroleum Geologists Bulletin*, v. 83, p. 1878.
- BOHACS, K.M.; CARROLL, A.R.; NEAL, J.E., 2003. Lessons from large lake systems – Thresholds, nonlinearity, and strange attractors: *Geological Society of America Abstracts with Programs*, v. 32, no. 7, p. A-312.
- BOHACS, K.M.; CARROLL, A.R.; NEAL, J.E.; MANKIEWICZ, P.J., 2000. Lake-basin type, source potential, and hydrocarbon character: An integrated sequence stratigraphic – geochemical framework. In: Gierlowski-Kordesch, E., and Kelts, K., eds., *Lake basins through space and time: American Association of Petroleum Geologists Studies in Geology* v. 46, p. 3–37.
- BOSENCE, D., PROCTER, E., AURREL, M., KAHLA, A.B., BOUDAGHER-FADEL, M., CASAGLIA, F., CIRILLI, S., MEHDIE, M., NIETO, L., REY, J., SCHERREIKS, R., SOUSSI, M., WALTHAM, D., 2009. A dominant tectonic signal in high-frequency, peritidal carbonate cycles? A region analysis of Liassic platforms from western Thetys. *J. Sediment. Res.* 79, 389-475.
- BOUMA, A. H., 2008. Coarse-grained and fine-grained turbidite systems as end-member models: applicability and dangers. *Marine and Petroleum Geology*; 17: 137 – 143.
- CAPUTO, M.V. Stratigraphy, tectonics, paleoclimatology and paleogeography of Northern Basins of Brazil. 1984. xx, 583f. Tese (Doutorado) - University of California, Santa Barbara, USA: 1984.
- CARDOSO, A. R.; NOGUEIRA, A. C. R.; ABRANTES JR, F. R. A.; RABELO, C. E. N., 2017. Mesozoic lacustrine system in the Parnaíba Basin, northeastern Brazil: paleogeographic implications for West Gondwana. *Journal of South American Earth Science*. 74: 41-53.
- CARROLL, A.R.; BOHACS, K.M. Stratigraphic classification of ancient lakes: balancing tectonic and climatic controls. *Geology*, v. 27, p. 99-102, 1999.
- CASTRO, D.L., FUCK, R.A., PHILLIPS, J.D., VIDOTTI, R.M., BEZERRA, F.H.R., DANTAS, E.L., 2014. Crustal structure beneath the Paleozoic Parnaiba basin revealed by airborne gravity and magnetic data, Brazil. *Tectonophysics* 614, 128–145.
- CATUNEANU, O., ABREU, V.; BATTACHARYA, J.P.; BLUM, M.D.; DALRYMPLE, R.J.; ERIKSSON, P.G.; FIELDING, C.R.; FISHER, W.L.; GALLOWAY, W.E.; GIBLING, M.R.; GILES, K.A.; HOLBROOK, J.M.; JORDAN, R.; KENDAL, C.G.St.C.; MACURDA, B.; MARTINSEN, O.J.; MIAL, A.D.; NEAL, J.E.; NUMMEDAL, J.; POMAR, L.; POSAMENTIER, H.W.; PRATT, B.R.; SARG, J.F.; SHARLEY, K.W.; STEEL, R.J.; STRASSER, A.; TUCKER, M.E.; WINKER, C., 2009. Towards the standardization of sequence stratigraphy. *Earth-Science Reviews*, 92: 1-33.
- DALY, M. C.; ANDRADE, V.; BAROUSSE, C. A.; COSTA, R.; MCDOWELL, K.; PIGGOTT, N.; POOLE, A. J., 2014. Brasiliano crustal structure and the tectonic setting of the Parnaíba basin of NE Brazil: results of a deep seismic reflection profile. *Tectonics*, 33: 1-19.
- DAVIS, R. A. *Depositional systems: an introduction to sedimentology and stratigraphy*. Englewood Cliffs, NJ, Ed. Prentice Hall, 1992.
- DELLA FÁVERA, J. C. *Fundamentos de estratigrafia moderna*. Ed. Moderna. Rio de Janeiro, 2001.
- DUMAS, S.; ARNOTT, R.W.C.; SOUTHARD, J.B., 2005. Experiments on oscillatory flow and combined-flow bed forms: implications for interpreting parts of the shallow marine sedimentary record. *Journal of Sedimentary Research*, 75, 501-513.
- FISCHER, A.G., 1964. The Lofer cyclothems of the Alpine Triassic. In: Merriam, D.F. (Ed.), *Symposium on Cyclic Sedimentation*, 169: 107-149. *Kansas Geological Survey, Bulletin*.
- GÓES, A. M.; ROSSETTI, D. F. 2001. Gênese da Bacia de São Luís-Grajaú, Meio-Norte do Brasil. In: *O Cretáceo na Bacia de São Luís-Grajaú* (eds. D. F. Rossetti, A. M. Góes and W. Truckenbrodt), pp. 15–29. Coleção Friedrich Katzer. Belém: Museu Paraense Emílio Goeldi.
- GÓES, A.M.O.; FEIJÓ, F.J. A Bacia do Parnaíba. *Boletim de Geociências da Petrobras*, p. 57-67, 1994.
- GROGAN, E.D.; LUND, R., 2002. The geological and biological environment of the Bear Gulch Limestone (Mississippian of Montana) and a model for its deposition. *Geodiversitas* 24: 295–315.

- HAMDANI, Y.; MARESCHAL, J.-C.; ARKANI-HAMED, J., 1991. Phase changes and thermal subsidence in intracontinental sedimentary basins, *Geophys. J. Int.*, 106: 657-665.
- HAMDANI, Y.; MARESCHAL, J.-C.; ARKANI-HAMED, J., 1994. Phase changes and thermal subsidence of the Williston basin. *Geophys. J. Int.*, 116: 585-597.
- HASUI, Y.; COSTA, J.B.S.; BORGES, M.S.; ASSIS, J.F.P.; PINHEIRO, R.V.L.; BARTORELLI, A.; PIRES NETO, A.G.; MIOTO, J.A. A borda sul da Bacia do Parnaíba no Mesozóico. In: 3º Simpósio Nacional De Estudos Tectônicos, Rio Claro. Boletim, Rio Claro, SBG – Núcleo de São Paulo: v. 8, n. 1, p. 93-95, 1991.
- HEILBRON, M.; GUEDES, E.; MANE, M.; VALERIANO, C. M.; TUPINAMBÁ, M.; ALMEIDA, J.; SILVA, L. G. E.; DUARTE, B. P.; DELLA FÁVERA, J. C.; VIANA, A. Geochemical and temporal provinciality of the magmatism of the eastern Parnaíba Basin, NE Brazil. *The Geological Society of London, Special Publications*, 472, 251-278.
- HIGGS, R. Gravity anomalies, subsidence history and the tectonic evolution of the Malay and Penyu Basins (offshore Peninsula Malaysia). *Basin Research*, 11: 285-290.
- HOLZ, M. Mesozoic paleogeography and paleoclimate – a discussion of the diverse greenhouse and hothouse conditions of an alien world. *Journal of South American Earth Sciences*, v. 61, p. 91-107, 2015.
- HUSINEC, A., BASCH, D., ROSE, B., READ, J.F., 2008. FISCHERPLOTS: an excel spreadsheet for computing Fischer plots of accommodation change in cyclic carbonate successions in both the time and depth domains. *Comput. Geosci.* 34: 269-277.
- JAJU, M. M.; MORT, H. P.; NADER, F. H.; FILHO, M. L.; MACDONALD, D. I. M., 2018. Paleogeographical and paleoclimatic evolution of the intracratonic Parnaíba Basin, NE Brazil using GPlates plate tectonic reconstructions and chemostratigraphic tools. *The Geological Society of London, Special Publications* 472: 199-222.
- KEIGHLEY, D.; FLINT, S.; HOWELL, J.; MOSCARIELLO, A., 2003. Sequence stratigraphy in lacustrine basins: a model for part of the Green River Formation (Eocene), southwest Uinta Basin, Utah, U.S.A. *Journal of Sedimentary Research*, 73(6): 987-1006.
- KERANS, C.; TINKER, S.W., 1997. Sequence stratigraphy and characterization of carbonate reservoirs: *Society of Economic Paleontologists and Mineralogists Short Course Notes*, 40, 165 p.
- KLÖCKING, M.; WHITE, N.; MACLENNAN, J., 2018. Role of basaltic magmatism within the Parnaíba cratonic basin, NE Brazil. In: DALY, M. C., FUCHS, R. A., JULIÀ, J., MACDONALD, D. I. M. e WATTS, A. B. (eds) *Cratonic Basin Formation: A Case Study of the Parnaíba Basin of Brazil*. Geological Society, London, Special Publications, 472: 309-319.
- ILGAR, A.; NEMEC, W., 2005. Early Miocene lacustrine deposits and sequence stratigraphy of the Ermenek Basin, Central Taurides, Turkey. *Sedimentary Geology*, 173: 233-275.
- LAMB, M. P.; MYROW, P. M.; LUKENS, C.; HOUCK, K.; STRAUSS, J., 2008. Deposits from wave-influenced turbidites currents: Pennsylvanian Minturn Formation, Colorado, USA. *Journal of Sedimentary Research*, 78: 480-498.
- LIMA, E. A. M.; LEITE, J. F. Projeto de estudo global dos recursos minerais da Bacia Sedimentar do Parnaíba. Integração Geológico-Metalogenética: Relatório Final da Etapa III. Companhia de Pesquisa de Recursos Minerais. Recife, 212p, 1978.
- LUCA, P. H. V.; BASILICI, G., 2013. A prodeltaic system controlled by hyperpycnal flows and storm waves: reinterpretation of the Punta Negra Formation (Lower-Middle Devonian, Argentine Precordillera). *Brazilian Journal of Geology*, 43(4): 673-694.
- MANENTI, R. R.; SOUZA, W. E.; PORSANI, M. J., 2018. Reprocessing and interpretation of deep structures in a regional transect of the Parnaíba Basin, Brasil. *Geological Society of London, Special Publications*, 472: 101-107.
- MEJU, M. A.; FONTES, S.L.; OLIVEIRA, M.F.B.; LIMA, J.P.R.; ULUGERGERLI, E.U.; CARRASQUILLA, A.A., 1999. Regional aquifer mapping using combined VES-TEM-AMT/EMAP methods in the semiarid eastern margin of Parnaíba Basin, Brazil. *Geophysics*, 64(2): 337-356.
- MESNER, C. J.; WOOLDRIDGE, C. P. Maranhão Paleozoic basin and Cretaceous coastal basin, north Brazil. *Bulletin of the American Association of Petroleum Geologists*, v. 48, n. 9, p. 1475-1512, 1964.
- NICHOLS, G. *Sedimentary and stratigraphy*. Chichester, Ed. Wiley-Blackwel, Oxford. 2. ed., 2009.
- NORTH, C. P.; DAVIDSON S. K. Unconfined fluvial processes: recognition and interpretation of their deposits, and the significance for palaeogeographic reconstruction. *Earth-Science Reviews*, n. 111, p. 199-223, 2012.
- OWEN, G.; MORETTI, M.; ALFARO, P. Recognising triggers for soft-sediment deformation: current understanding and future directions. *Sedimentary Geology*, n. 235, p. 133-140, 2011.
- OWEN; G.; MORETTI, M. Identifying triggers for liquefaction-induced soft-sediment deformation in sands. *Sedimentary Geology*, n. 235, p. 141-147, 2011.
- PAZ, J.D.S.; ROSSETTI, D.F., 2005. Linking lacustrine cycles with syn-sedimentary tectonic episodes: an example from the Codó Formation (late Aptian), northeastern Brazil. *Geol. Mag.*, 142(3): 269-285.

- PETRA, M.S. Paleoiçtiofauna da Formação Pastos Bons (Bacia do Parnaíba) – Reconstituição Paleoambiental e Posicionamento Cronoestratigráfico. 2006. Dissertação (de Mestrado). Universidade do Estado do Rio de Janeiro, xvii, 141 f., 2006.
- PORTO, A.; DALY, M.C.; LA TERRA, E.; FONTES, S., 2018. The pre-Silurian Riachão Basin: a new perspective on the basement of the Parnaíba Basin, NE Brazil. In: DALY, M. C., FUCK, R. A., JULIÀ, J., MACDONALD, D. I. M. & WATTS, A. B. (eds) Cratonic Basin Formation: A Case Study of the Parnaíba Basin of Brazil. Geological Society, London, Special Publications, 472: 127-145.
- RABELO, C.N.; NOGUEIRA, A.C.R. O sistema desértico úmido do Jurássico Superior da Bacia do Parnaíba, na região entre formosa da Serra Negra e Montes Altos, Estado do Maranhão, Brasil. *Geol. USP, Séries Científicas*, v. 15, p. 3-21, 2015.
- READING, H.G. Sedimentary environment and facies. Blackwell Scientific Publicatoin. Oxford, 3. Ed., 1996.
- ROMERO BALLÉN, O. A. R. As sucessões sedimentares interderrames da Formação Mosquito, exemplo de um sistema eólico úmido, Província Parnaíba. Dissertação (de Mestrado). USP – Universidade de São Paulo, xix, 85 f, 2012.
- RETALLACK, G. J., 2011. Exceptional fOssil preservation during CO₂ greenhouse crisis?, *Palaeogeography, Palaeoclimatology, Palaeoecology*, 307: 59-74.
- SADLER, P.M., OSLEGER, D.A., MONTANEZ, I.P., 1993. On the labeling, length, and objective basis of Fischer plots. *J. Sediment. Petrol.* 63: 360-368.
- SANTOS M. E. C. M., CARVALHO M. S. S. Paleontologia das Bacias do Parnaíba, Grajaú e São Luís, Ed. 2, CPRM, Rio Janeiro, 212p, 2004.
- SCHALLER, M. F.; WRIGHT, J. D.; KENT, D. V.; OLSEN, P. E. Rapid emplacement of the Central Atlantic Magmatic Province as a net sink for CO₂. *Earth and Planetary Science Letters*, 323-324: 27-39.
- SCHOBHENHAUS, C., CAMPOS, D.A., QUEIROZ, E.T., WINGE, M., BERBERTBORN, M. (eds.). *Sítios Geológicos e Paleontológicos do Brasil*. Brasília, DNPM/CPRM, 1984.
- SOARES, J. E. P.; STEPHENSON, R.; FUCK, R. A.; LIMA, M. V. A. G.; ARAÚJO, V. C. M.; LIMA, F. T.; ROCHA, F. A. S.; TRINDADE, C. R., 2018. Structure of the crust and upper mantle beneath the Parnaíba Basin, Brazil, from wide-angle reflection-refraction data. *Geological Society of London, Special Publications*, 472: 67-82.
- SPENCE, G.H., TUCKER, M.E., 2007. A proposed integrated multi-signature model for peritidal cycles in carbonates. *J. Sediment. Res.* 77, 797-808.
- SVENSEN, H. H.; TORSVIK, T. H.; CALLEGARO, S.; AUGLAND, L.; HEIMDAL, T. H.; JERRAM, D. A.; PLANKE, S.; PEREIRA, E. Gondwana Large Igneous Provinces: plate reconstructions, volcanic basins and sill volumes. *Geological Society of London, Special Publications*, 472: 17-40.
- TORSVIK, T. H.; COCKS, L. R. M. Gondwana from top to base in space and time. *Gondwana Research*, n. 24, p. 999-1030, 2013.
- TROSDTORF JR., I.; MORAIS NETO, J. M.; SANTOS, S. F.; PORTELA FILHO, C. V.; DALL OGLIO, T. A.; GALVES, A. C. M.; SILVA, A. M., 2018. Phanerozoic magmatism in the Parnaíba Basin: characterization of igneous bodies (well logs and 2D seismic sections), geometry, distribution and sill emplacement patterns. *Geological Society of London, Special Publications*, 472: 321-340.
- VAZ, P.T.; REZENDE, N.G.A.M.; WANDERLEY FILHO, J.R.; TRAVASSOS, W.A.S. Bacia do Parnaíba. *Boletim de Geociências da Petrobras*, v. 15, n. 2, p. 253-263, 2007. VAIL, P.R., 1987. Seismic stratigraphy interpretation using sequence stratigraphy. In: Bally, W.A. (Ed.), *Atlas of Seismic Stratigraphy*. V 1, AAPG Studies Geology, 27: 1-10.
- VAIL, P.R.; POSAMENTIER, H, P. 1988, Principles of sequence stratigraphy: in James, D.P., and D.A. Leckie, (eds.), *Sequences, stratigraphy, sedimentology; surface and subsurface*, CSPG Memoir 15, p. 572.
- VEEVERS, J. J. Gondwanaland from 650-500 Ma assembly through 320 Ma merger in Pangea to 185-100 Ma breakup: supercontinental tectonics via stratigraphy and radiometric dating. *Earth-Science Reviews*, n. 68, p. 1-132, 2004.
- WALKER, R. G (ed.). Facies, facies models and modern stratigraphic concepts. In: R. G. WALKER, N. P. JAMES (eds.), *Facies Models - Response to Sea Level Change*. Ontario, Ed. Geological Association of Canada, Canada, v. 1, p. 1-14, 1992.

Artigo 2 – Multi-approach provenance in stratigraphy: implications for the Upper Mesozoic evolution of the Parnaíba Basin, NE Brazil

Cardoso¹, A. R.; Nogueira¹, A. C.R.; Rabelo^{1,2}, C. E. N.; Soares, J. L.¹

¹Programa de Pós Graduação em Geologia e Geoquímica – Universidade Federal do Pará

²Universidade da Amazônia

Abstract

Provenance analysis are highly affected by transport, depositional and diagenetic processes, as well as the grain size chosen for evaluation. In order to avoid misleading data, provenance research need multi-approach techniques. In this work, we test a set of widespread and low cost methods to investigate a debatable stratigraphic interval in the Parnaíba Basin, northeastern Brazil. Discontinuous exposures and fault displacements result in enigmatic stratigraphic relations in the Mesozoic portion of this basin. This succession consists in the lacustrine deposits of the Pastos Bons Formation and aeolian sandstones of the Corda Formation, composing the Mearim Group, and fluvial conglomerates and sandstones of the Grajaú Formation. The provenance of this succession was studied through sandstone petrography, quartz petrography, hot cathodoluminescence and heavy minerals analyses. Units from Mearim Group plotted in recycled orogenic and craton interior fields, whereas quartz petrography and cathodoluminescence constrain predominantly volcanic sources. The heavy minerals assemblages of the lacustrine and aeolian deposits are very similar, whereas the fluvial succession presents texturally immature grains and anomalous high hornblende content. Additionally, ZTR, GZi e RZi indexes are higher for lacustrine and aeolian deposits, and lower for fluvial beds. These data indicate polycyclic minerals and mixed sources for Mesozoic sandstones of the Parnaíba Basin. The Mearim Group presents both volcanic contribution, probably supplied by CAMP basalts, and low to medium-grade metapelitic heavy minerals assemblage. Heavy minerals were probably supplied by Neoproterozoic metapelites from the Ceará Central Domain (Ceará Group?), Borborema Province. Conversely, the Grajaú Formation was supplied by I-type Brazilian granites, incompatible with the Mearim Group. These data provided new stratigraphic relations for the Mesozoic deposits of the Parnaíba Basin and implications for the evolution of this basin.

Keywords: Provenance; Stratigraphy; Heavy minerals; Cathodoluminescence; Parnaíba Basin.

1 INTRODUCTION

Provenance analysis of sedimentary rocks has been challenged over the last years. The complexity in sedimentary provenance studies arises, mainly, from modifications that affect sedimentary rock components during the transport and physical-chemical processes acting at the depositional site (Boggs Jr., 2009; Sevastjanova *et al*, 2012; Garzanti, 2016). Additionally, burial and diagenetic modifications may hide or obliterate grains character and important informations about source lithology are lost, whereas track sedimentary recycling may be a difficult task (Morton and Hallsworth, 1994; Tucker, 1991; Nichols, 2009). Another problem is the limitation of analysis according to the grain size chosen for evaluation, which also may be complicated by the hydraulic behavior of the minerals, sensibility to chemical weathering or intrastratal leaching (Morton and Hallsworth, 1994, 1999; Andò *et al*, 2012; Morton, 2012). In this sense, a combination of a diverse set of techniques is recommended to avoid misleading data and get as close as possible of the true source(s) (Najman, 2006; Morton *et al*, 2011; Garzanti, 2016). Therefore, this work aims to evaluate stratigraphic issues based on a multi-approach provenance analysis, focusing on bulk-sediment (framework sandstone petrography), multi-minerals (heavy minerals petrography) and single-mineral (hot cathodoluminescence and quartz petrography) techniques. These analyses were carried out in a debatable stratigraphic succession, the Mearim Group, which represents the Upper Jurassic-Lower Cretaceous of the Parnaíba Basin, northeastern Brazil (Góes and Feijó, 1994). This group lacks widely distributed biostratigraphic data, which hamper accurate correlations and stratigraphic positioning.

Recently, the knowledge about the Mesozoic stratigraphy of the Parnaíba Basin has been significantly increased, although, this interval continues enigmatic, mainly due to fragmentary stratigraphic record. For this reason, many authors suggest the necessity of detailed studies, emphasizing the Jurassic-Cretaceous deposits of the Mearim Group (Caldasso, 1978; Caldasso and Hama, 1978; Góes and Feijó, 1994; Rezende, 1998; Vaz *et al*, 2007; Romero Bállen *et al*, 2013). This group is constituted by lacustrine and aeolian deposits, represented by the Pastos Bons and Corda formations, respectively (Góes and Feijó, 1994; Romero Bállen, 2012); however, the stratigraphy, contact relations and age of these deposits are not consensual (Fig. 1). According to Cunha and Carneiro (1972), these units compose an integrated depositional system, denominated Corda-Pastos Bons Desertic System. Nevertheless, other authors dissociated these deposits and suggested different ages (Vaz *et al*, 2007) or the presence of structural highs that separated the sedimentation in distinct sub-

basins (Romero Bállen, 2012). Due to these conflicts, the present work evaluates and compares the provenance of these deposits, situated in the central-southwestern portions of Parnaíba Basin, northeastern Brazil (Fig. 2).

	Mesner and Woolridge (1964)	Aguiar (1969)	Cunha and Carneiro (1972)	Góes (1990)	Góes et al (1993)	Góes and Feijó (1994)	Rezende (2002)	Vaz et al (2007)	Romero et al (2013)	Rabelo and Nogueira (2015)
Cretaceous	Codó Fm.	Codó Fm.	Codó Fm.	Codó Fm.	Itapecuru Fm.		Itapecuru Fm.	Itapecuru Fm.	Grupo Itapecuru	
		Grajaú Fm. Sardinha Fm.	Sardinha Fm. Grajaú Fm.	Grajaú Fm. Sardinha Fm.	Codó Fm. Grajaú Fm.	Grajaú Fm. Codó Fm.	Codó Fm. Grajaú Fm.	Codó Fm. Grajaú Fm.	Grajaú Fm. Codó Fm.	Grajaú Fm. Codó Fm.
Jurassic	Corda Fm.	Corda Fm.	Corda Fm.	Corda Fm.	Corda Fm.	Corda Fm.	Sardinha Fm.	Pastos Bons Fm.	Sardinha Fm.	Sardinha Fm.
	Basalts/Diabases	Pastos Bons Fm.	Pastos Bons Fm.	Pastos Bons Fm.	Pastos Bons Fm.	Pastos Bons Fm.	Mosquito Fm.	Mosquito Fm.	Mosquito Fm.	Mosquito Fm.
Triassic	Sambaiba Fm.	Mosquito Fm.	Mosquito Fm.	Mosquito Fm.	Sambaiba Fm.	Mosquito Fm.	Pastos Bons Fm.	Sambaiba Fm.	Sambaiba Fm.	Sambaiba Fm.
	Pastos Bons Fm.	Sambaiba Fm.	Sambaiba Fm.	Sambaiba Fm.	Sambaiba Fm.	Sambaiba Fm.	Sambaiba Fm.	Moluca Fm.	Sambaiba Fm.	Sambaiba Fm.

Figure 1 – Stratigraphic proposals for Mesozoic of Parnaíba Basin, highlight for Pastos Bons and Corda formations (Modified from Rabelo and Nogueira, 2015).

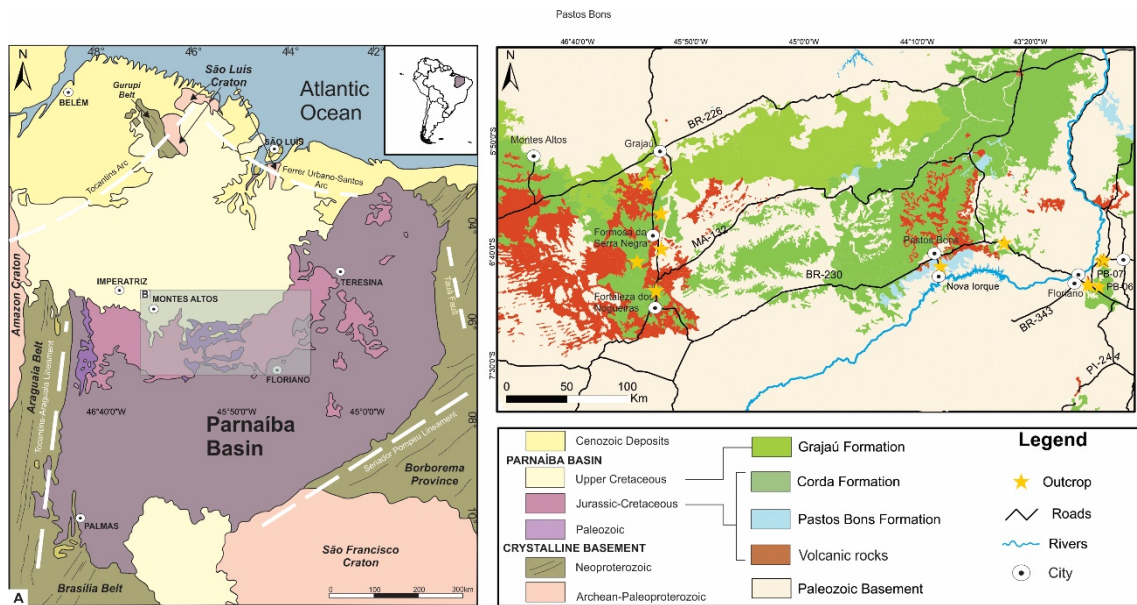


Figure 2 – A. Localization map and geotectonic contextualization of Parnaíba Basin (Modified from Schobbenhaus *et al*, 1984; Santos and Carvalho, 2004). B. Localization map of the study area.

2 GEOLOGICAL SETTING

The Parnaíba Basin is a Paleozoic intracratonic basin, located in the South American Platform, in northeastern Brazil (Aguiar, 1969; Góes and Feijó, 1994). This basin, defined as sag type, comprises approximately 600.000 km², and may achieve 3.4 to 3.5 km-thick in its depocenter (Caputo, 1984; Vaz *et al*, 2007; Daly *et al*, 2014). The basement is composed by

igneous, metamorphic and sedimentary rocks of the Araguaia-Tocantins Belt, Amazonian and São Francisco cratons, Borborema Province, as well as Riachão and Jaibas basins (Victor Zálan, 1991; Oliveira and Mohriak, 2003; Castro *et al*, 2014; Porto *et al*, 2018). These include Archean to Ordovician units with genesis and/or reworking associated with the Brasiliano Cycle (Vaz *et al*, 2007). According to Daly *et al* (2014), the basement of the Parnaíba Basin is compartmentalized in distinct domains, denominated as Amazonian/Araguaia block, Parnaíba block and Borborema block.

Góes and Feijó (1994) divided the sedimentary filling of the Parnaíba Basin in five sequences: Silurian; Devonian; Carboniferous-Triassic; Jurassic and Cretaceous sequences. Nevertheless, in the most recent proposal, Vaz *et al* (2007) subdivided the Parnaíba Basin in Silurian; MesoDevonian-EoCarboniferous; NeoCarboniferous-EoTriassic; Jurassic and Cretaceous supersequences. The Upper Mesozoic of the Parnaíba Basin is composed by lacustrine shales and sandstones of Pastos Bons Formation, aeolian sandstones of Corda Formation, fluvial sandstones and conglomerates of Grajaú Formation and lacustrine to marine shales and evaporites of Codó Formation (Góes and Feijó, 1994; Góes and Rossetti, 2001; Paz and Rossetti, 2005; Vaz *et al*, 2007).

2.1 CRITICAL ANALYSIS OF THE STRATIGRAPHIC PROPOSALS

According to Góes and Feijó (1994), Pastos Bons and Corda formations compose the Mearim Group, which represents the Jurassic Sequence of the Parnaíba Basin. Differently, Vaz *et al* (2007) positioned exclusively the Pastos Bons Formation in the Jurassic Supersequence and Corda Formation in the Cretaceous Supersequence, the latter with diachronic contacts with Codó and Grajaú deposits. However, the criteria applied to define these contacts were not mentioned. Furthermore, field relations evidence that fluvial sandstones of Grajaú Formation unconformably overlie the deposits of the Mearim Group (Cardoso *et al*, unpublished). In addition, Corda Formation is sharply overlaid by lacustrine and marine black shales from Codó Formation (Rabelo *et al*, 2018), which is defined as Cretaceous based on *Sergipea varirerrucata* palynomorphs (Batista, 1992). In this sense, the stratigraphic positioning of Mesozoic units, mainly the Mearim Group (Jurassic Sequence), is frequently questioned, such that faciological and detailed stratigraphic studies are recommended by many authors, in order to elucidate problems that persist since the last century (Caldasso, 1978; Caldasso and Hama, 1978; Góes and Feijó, 1994; Rezende, 1998; Vaz *et al*, 2007; Romero Bállen *et al*, 2013; Rabelo and Nogueira, 2015).

The deposition of Pastos Bons Formation occurred throughout the Xambioá Structure, which behaved as a crustal depression during the Mesozoic (Hasui *et al*, 1991). Previous works interpreted that this sedimentation was concentrated in paleodepressions, located between topographic highs generated by magmatic flows (Lima and Leite, 1978; Góes and Feijó, 1994; Vaz *et al*, 2007). Pastos Bons Formation presents 77 m-thick in its depocenter and comprises shales and greenish to brown-reddish sandstones, which compose a fluvial-lacustrine system (Vaz *et al*, 2007; Romero Bállen, 2012; Cardoso *et al*, 2017). This unit represents the Upper Jurassic-Lower Cretaceous of the Parnaíba Basin (Gallo, 2005; Vaz *et al*, 2007; Montefeltro *et al*, 2013), and unconformably overlies, from east to west, Poti, Piauí, Pedra de Fogo and Motuca formations (Lima and Leite, 1978; Santos and Carvalho, 2004). Corda Formation conformably to gradational overlies the Pastos Bons Formation (Aguiar, 1971). This unit includes the Muzinho Shale beds, which consist in black shales and limestones interbedding, with great fossil content represented by fishes, conchostracea and palynomorphs (Roxo and Löefgren, 1936; Santos, 1953; Gallo, 2005; Petra, 2006; Bernades-de-Oliveira *et al*, 2007).

Corda Formation is constituted by fine to medium-grained, gray-whitish and reddish sandstones, with rounded and matte quartz grains, interpreted as a wet desertic system (Góes and Feijó, 1994; Santos and Carvalho, 2004; Romero Bállen *et al*, 2013; Rabelo and Nogueira, 2015). Following Vaz *et al* (2007), the deposition of this unit was influenced by the Parnaíba High arching occurred during the Cretaceous. According to Romero Bállen (2012), the sedimentation of Pastos Bons and Corda formations was separated by structural highs in two sub-basins, western and eastern of Parnaíba Basin, respectively. While other authors consider that these units were connected, composing the Corda-Pastos Bons Desertic System (Cunha and Carneiro, 1972; Rezende, 1998).

3 METHODS

The systematic sampling was carried out in fine to medium-grained sandstones of the studied succession. Sandstones classification followed Folk (1968) proposal and, afterwards, the data were plotted in QtFLt and QmFLt diagrams from Dickinson (1985). The samples were imaged by hot cathodoluminescence analyses, carried out for Pastos Bons and Corda sandstones in a CITL Cathodoluminescence Mk5-2. The system was operated with an acceleration voltage of 15 Kv and 150 μ A current, vacuum between 0.003 and 0.05 Pa, exposure time firstly of 10 to 15 s and, afterwards, 50 s. Images were captured by a Leica

DFC310 FX camera, coupled to a Leica DM4500 P Led microscope, which afterwards were processed using LAS V4.4 software. Quartz provenance definition was supported by petrographic analyses and luminescence standards (Augustsson and Rekker, 2012; Oliveira *et al.*, 2017), and posteriorly, the data were plotted in Bernet and Basset (2005) diagram. These analyses were not possible for Grajaú Formation, due to the predominance of friable sandstones.

Heavy minerals assemblage segregation followed the classic methodology described by Morton (1985), such that sandstone samples were disaggregated and sieved through humid and dry methods. Heavy minerals were separated in 0.062-0.125 mm and 0.125-0.250 mm sandy fractions through elutriation in bromophorm (density 2.8 g/cm³) and posterior production of glass thin sections. Ribbon counting technique was applied (Galehouse, 1971) with a minimum of 100 and a maximum of 300 grains counted. In order to distinguish the provenance based on heavy minerals, Morton and Hallsworth (1994) suggested defining the hydraulic and diagenetic equivalent minerals ratio. In this sense, GZi and RZi index were utilized for the studied deposits. In this stage, we used fourteen samples from Pastos Bons Formation, ten samples from Corda Formation and four samples from Grajaú Formation. Samples with insufficient content of non-micaceous and non-opaque minerals for quantitative analysis (<100 grains) were utilized only for mineralogical identification and description of the main textural and morphological aspects.

4 SANDSTONES OF THE MEARIM GROUP

Pastos Bons Formation represents a lacustrine system influenced by fluvial channels, with a succession composed mainly by mudstones and sandstones (Fig. 3). The latter are represented by fine to medium-grained quartzarenites and rarely by arkoses and greywackes, with even-parallel lamination, normal-to-reverse grading and normal grading (Fig. 4a,b). These lithotypes are cement-supported and cement-and-grains-supported, with rounded to subrounded and subordinately subangulose, well to moderately sorted grains. Such constituents float in poikilotopic calcite cement, except clay matrix-rich sandstones, which do not present cement (Fig. 4c). Cementation is most expressive throughout medium-grained sandy layers and below sequence boundaries, especially flooding surfaces. Sandstones exhibit open to normal packing, with predominance of grain-no grain, punctual, rectilinear and compromise contacts and, less frequently, concave-convex contacts.

The main depositional constituents include monocrystalline and, subordinately, polycrystalline quartz. Monocrystalline quartz grains are well-rounded, with abrupt extinction and, subordinately, weak to strong undulose extinction (Fig. 4d). Inherited silica overgrowth and fragmented grains occur locally, as well as fluid inclusions trails and vacuoles. Feldspar grains are present in lower proportions and are represented by microcline and plagioclase. Microcline is evidenced by multiple cross twinning, whereas plagioclase exhibits polysynthetic and albite-Carlsbad twinning. These are predominantly rounded to subrounded, commonly fragmented grains. Reliquiar features occur in some grains, mainly deformation lamellas, perthitic texture and myrmekitic intergrowth. Feldspars may be partially or completely replaced by sericite, calcite cement or clayminerals, the latter mainly throughout twinning plains. Lithic fragments are predominantly allogenic, subrounded to rounded grains, derived from metamorphic, igneous and sedimentary sources. Quartzite (Fig. 4d) and schists fragments occur locally, with elongated morphologies and subrounded boundaries. Volcanic lithic fragments are represented by rounded grains, commonly altered to clayminerals (Fig. 4e). Sedimentary lithic fragments include sandstone, pelite, pseudomatrix and undeformed to deformed chert fragments (Fig. 4f,g). Other depositional constituents include clayey matrix, contorted mica flakes and heavy minerals.

Cementation is one of the most important volumetric phases in lacustrine sandstones, with poikilotopic calcite crystals often in compromise contacts (Fig. 4h). The cement may be partially to completely replacing quartz and feldspar grains, respectively (Fig. 4i). Porosity is rare, defined by secondary pores, mainly moldic and intracrystalline porosity. Grains with corrosion features and sandstones with heterogeneous packing are common. Clays occur mainly as framework grains replacement, pseudomatrix and clay films. The latter marks the morphology of solved/replaced grains and, occasionally, it may border moldic porosity.

Corca Formation is composed by sublittarenites, quartzarenites and, subordinately, subarkoses, with higher concentration in dune field, sand sheets and wadi facies, respectively (Fig. 3). These lithotypes are grains-and-cement supported, fine to medium-grained, well-rounded, and moderately-sorted, with matte grains floating in poikilotopic zeolite and calcite cement. Lithic fragments include, mainly, angulose fragments of volcanic rocks, whereas feldspars are rare. Detailed petrographic description of these deposits is presented by Rabelo *et al* (2018). According to QtFLt and QmFLt, either lacustrine and fluvial-aeolian deposits from Pastos Bons and Corca formations, respectively, are plotted in craton interior and recycled orogenic fields (Fig. 5).

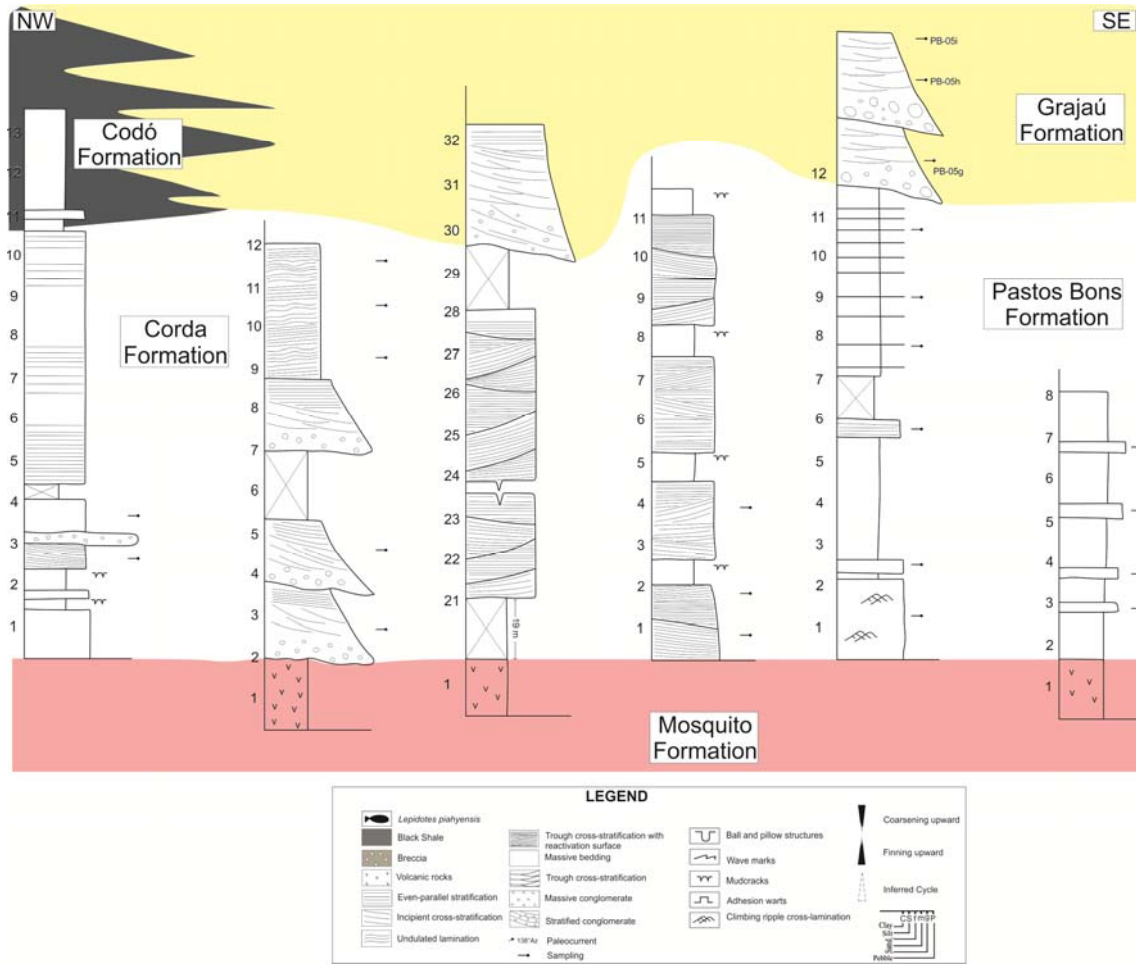


Figure 3 - Stratigraphic logs of the studied succession and samples positioning.

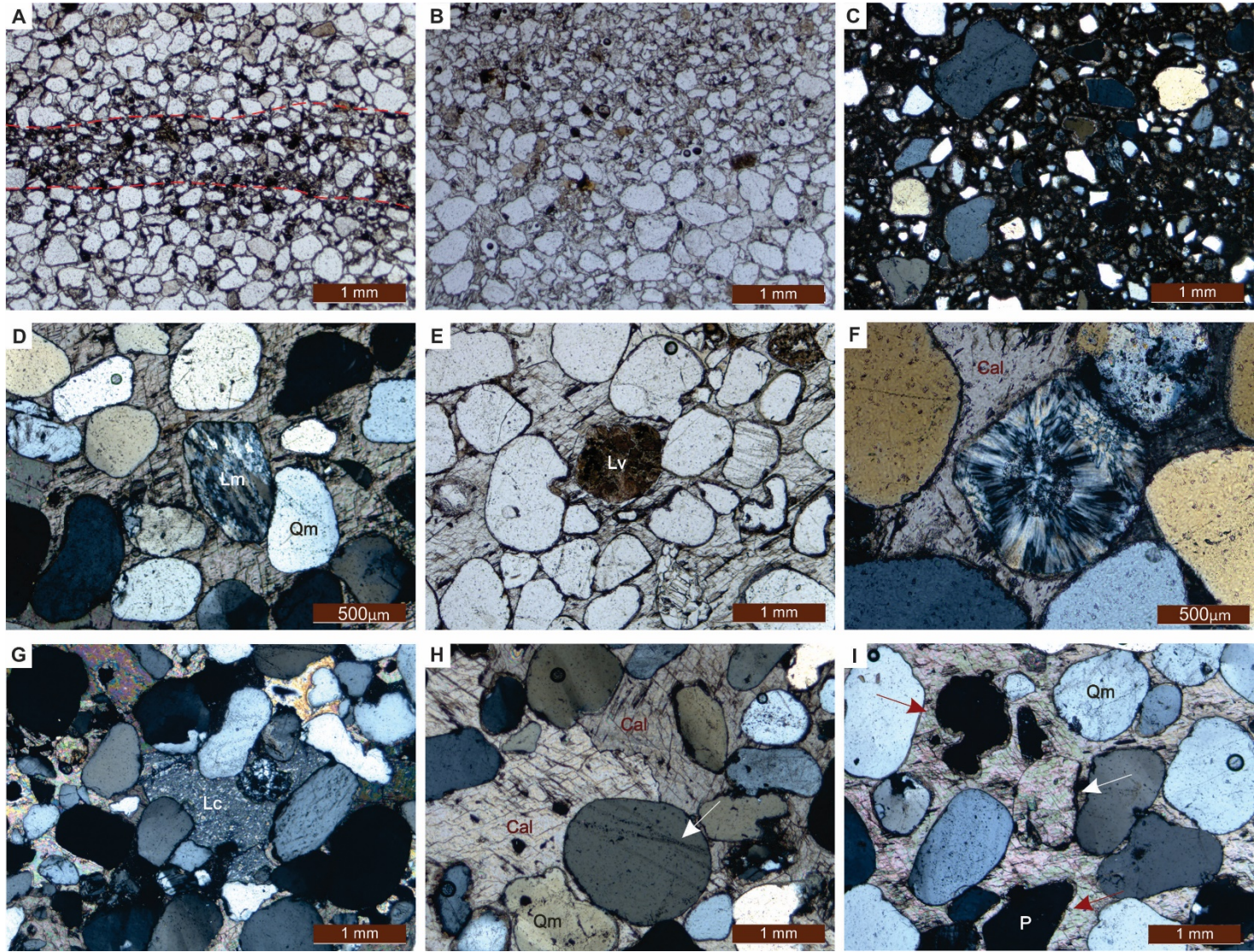


Figure 4 – Petrographic aspects of Upper Mesozoic sandstones from Parnaíba Basin. **A.** Even-parallel lamination and normal-to-reverse grading. **B.** Normal grading in quartzarenite. **C.** Greywacke, with poorly sorted and subangulose grains floating in clayey matrix. This lithotype do not present cementation. **D.** Quartzite lithic fragment in rectilinear contact with monocrystalline quartz. Grains float in poikilotopic calcite cement, in open framework rocks. **E.** Rounded volcanic rock fragment, with alteration to clayminerals. Monocrystalline quartz grain with vacuole (left). **F.** Rounded chert fragment (chalcedony) in rectilinear to punctual contacts with quartz grains. Grain-no grain contacts are also frequent. **G.** Deformed chert fragment in concave-convex contacts with the adjacent depositional constituents. **H.** Compromise contacts between poikilotopic calcite crystals. Arrow indicates fluid inclusions in monocrystalline quartz. **I.** Grain completely replaced by calcite cement (white arrow). The morphology is indicated due to the preservation of clay films. Moldic porosity occur locally (red arrows) (Qm = monocrystalline quartz; Lm = metamorphic lithic fragment; Lv = volcanic lithic fragment; Lc = chert fragment; Cal = calcite cement; P = moldic porosity).

4.1 PETROGRAPHIC FEATURES OF QUARTZ GRAINS

Based on quartz characteristics and features, these grains were assembled in four groups, namely A, B, C and D groups, associated with volcanic, felsic plutonic, low metamorphic and high metamorphic grade sources, respectively. This analysis followed Oliveira *et al* (2017) methodology and was complemented by cathodoluminescence imaging.

4.1.1 Lacustrine Succession (Pastos Bons Formation)

The lacustrine succession presents, mainly, monocrystalline, homogeneous quartz grains with weak to absent undulose extinction, which were associated with the Group A. Embayment features and vacuoles are common in these grains, as well as fluid inclusion trails and healed fractures (Fig. 6a). Quartz grains from Group B are clear, monocrystalline, with absent to weak undulose extinction ($\sim 5^\circ$). Randomly oriented bright patches are common (Fig. 6b), whereas grains with open and healed fractures are rare. Group C presents mono to polycrystalline quartz grains, which exhibit preferential orientation, moderate undulose extinction ($5\text{-}10^\circ$) and subgrains with rectilinear contacts. Quartz grains from Group D are predominantly monocrystalline and present strong ($>10^\circ$) undulose extinction, mosaic quartz, deformation lamellae and subgrains with sutured internal contacts (Fig. 6c-e).

4.1.2 Aeolian Succession (Corda Formation)

Group A quartz grains are also predominant in these deposits. These are homogeneous, monocrystalline, with weak to absent undulose extinction (Fig. 6f). Embayment features are common (Fig. 6g), whereas fluid inclusion trails and healed fractures occur locally. Group B quartz grains are monocrystalline, clear, with absent to weak undulose extinction ($\sim 5^\circ$). Polycrystalline quartz grains, with subgrains characterized by sutured

internal contacts and moderately to strong ($>10^\circ$) undulose extinction were assemblage in Group D. Grains with inherited silica overgrowth, drag and impact marks are common (Fig. 6h-i). Deformation lamellas and mosaic quartz occur punctually. There are no grains from Group C in these deposits.

4.2 QUARTZ CATHODOLUMINESCENCE

Quartz grains generally compose great part of sandstones framework and modern siliciclastic sediments. Despite that, grain modifications occurring during transport, deposition, burial and diagenesis may difficult sandstones classification and identification of source areas only by petrographic criteria (Omer, 2015). According to the conditions of formation, mainly temperature and pressure, quartz grains properties may be distinguished and source areas may be more precisely tracked (Augustsson and Bahlburg, 2003). This property has been associated with replacement of Si by Al, variation in trace elements content and/or intracrystalline defects (Perny *et al*, 1992; Watt *et al*, 1997; Ramseyer and Mullis, 2000; Stevens-Kalceff *et al*, 2000). In hot cathodoluminescence imaging, lacustrine and aeolian sandstones from Mesozoic of Parnaíba Basin exhibited dark red, dark blue and bright blue colored quartz grains (Fig. 7a-f). These were associated, respectively, with volcanic, metamorphic and plutonic sources (Bernet and Basset, 2005; Augustsson and Rekker, 2012; Oliveira *et al*, 2017). According to Bernet and Basset (2005) discrimination diagram, the analyzed quartz grains were plotted, preferentially, in the volcanic sourced field (Fig. 8).

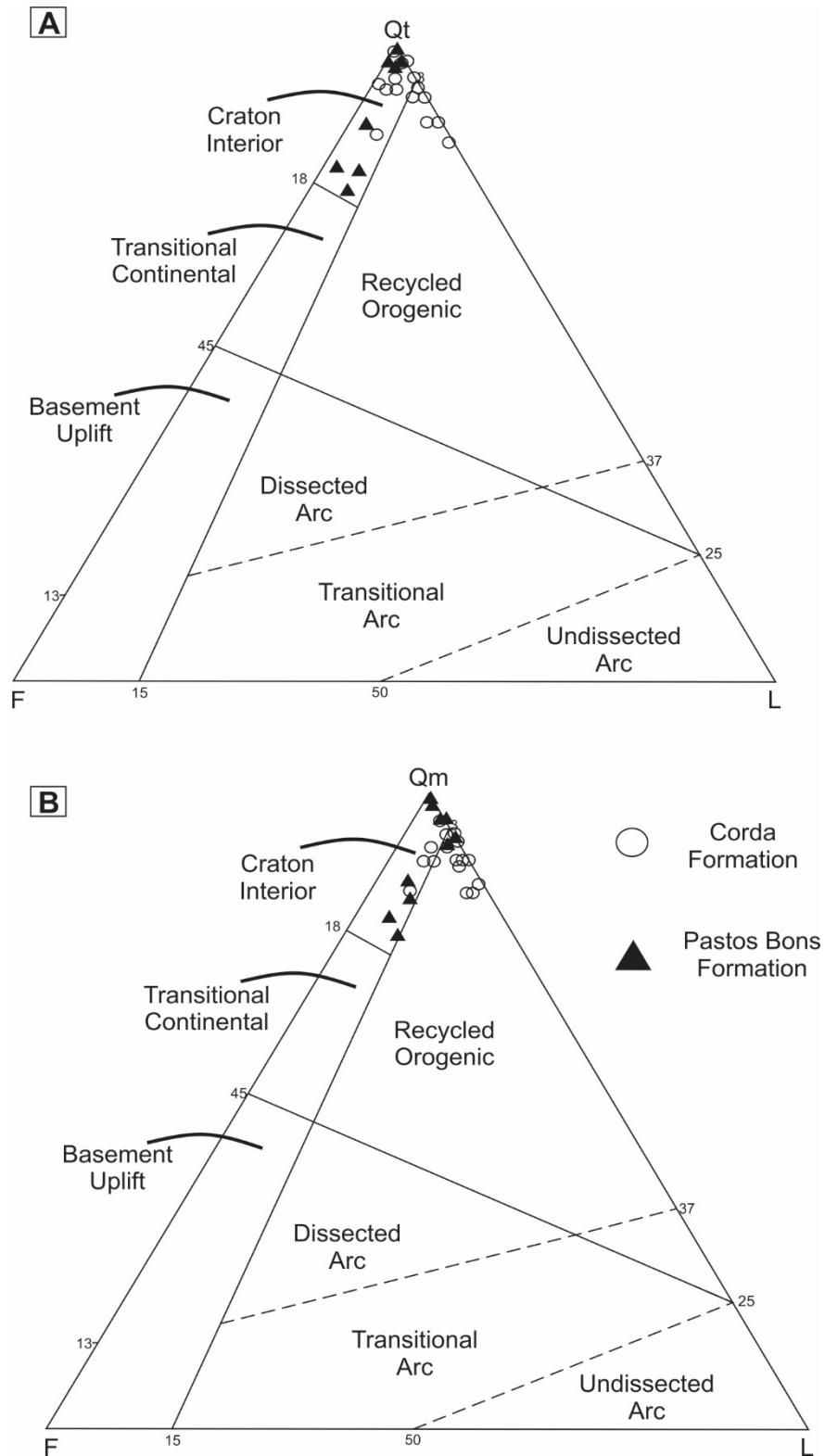


Figure 5 – Tectonic discrimination diagrams for Upper Mesozoic sandstones of the Parnaíba Basin. A. QtFLt triangular diagram. B. QmFLt triangular diagram. Both lacustrine and aeolian sandstones plot in Craton Interior and Recycled Orogenic fields in Dickinson diagrams (Dickinson, 1985). Data were plotted with support of the TriPlot software.

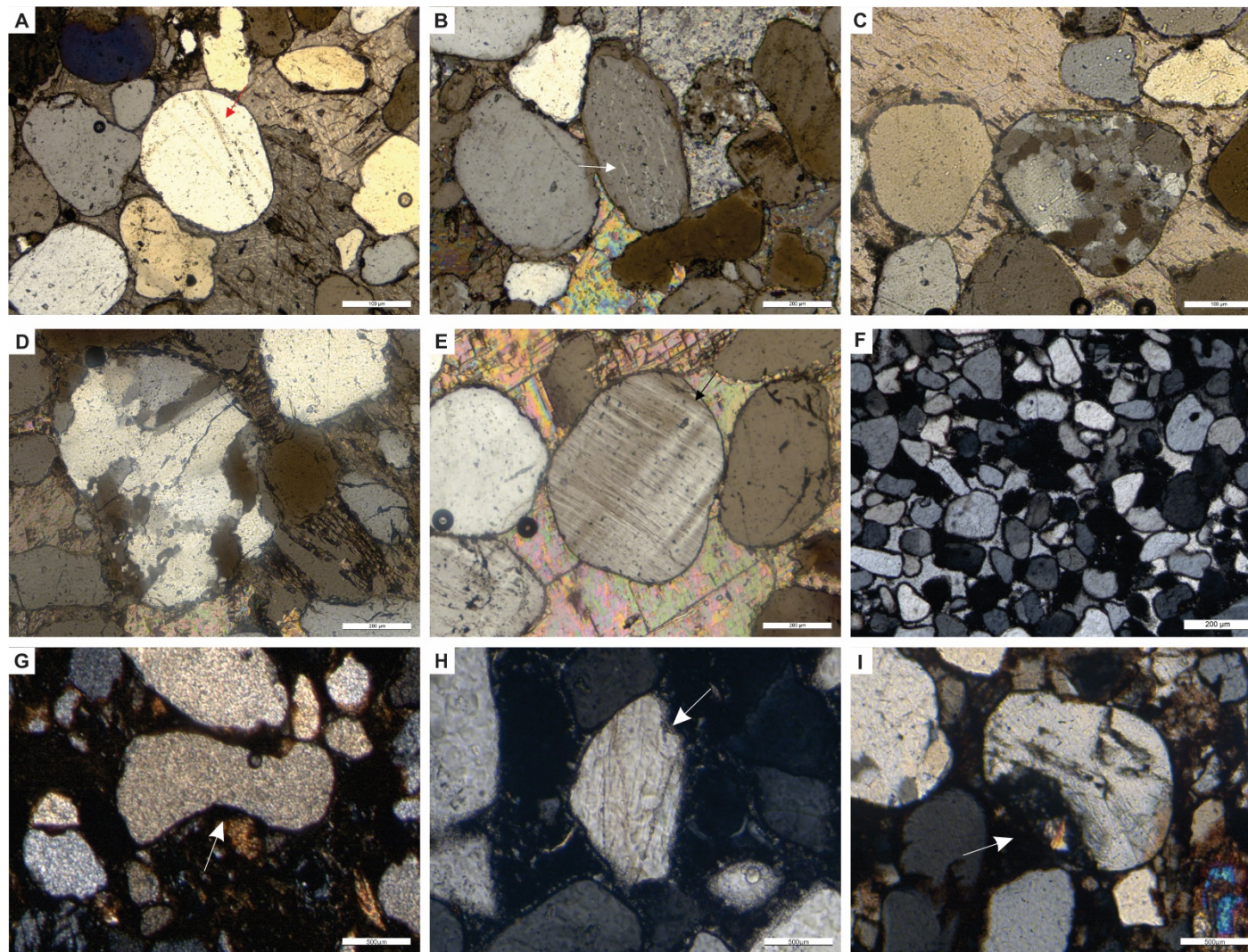


Figure 6 – Petrographic aspects of quartz grains from lacustrine (A-E) and aeolian (F-I) deposits. A. Healed fractures (red arrow). **B.** Bright patches (white arrow). **C.** Mosaic quartz. **D.** Polycrystalline quartz grain with sutured internal contacts. **E.** Deformation lamellae. **F.** Predominance of homogeneous, non-undulose quartz grains in aeolian sandstones. **G.** Embayed grain (white arrow). **H.** Dragging marks in quartz grain (white arrow) **I.** Impact mark (white arrow).

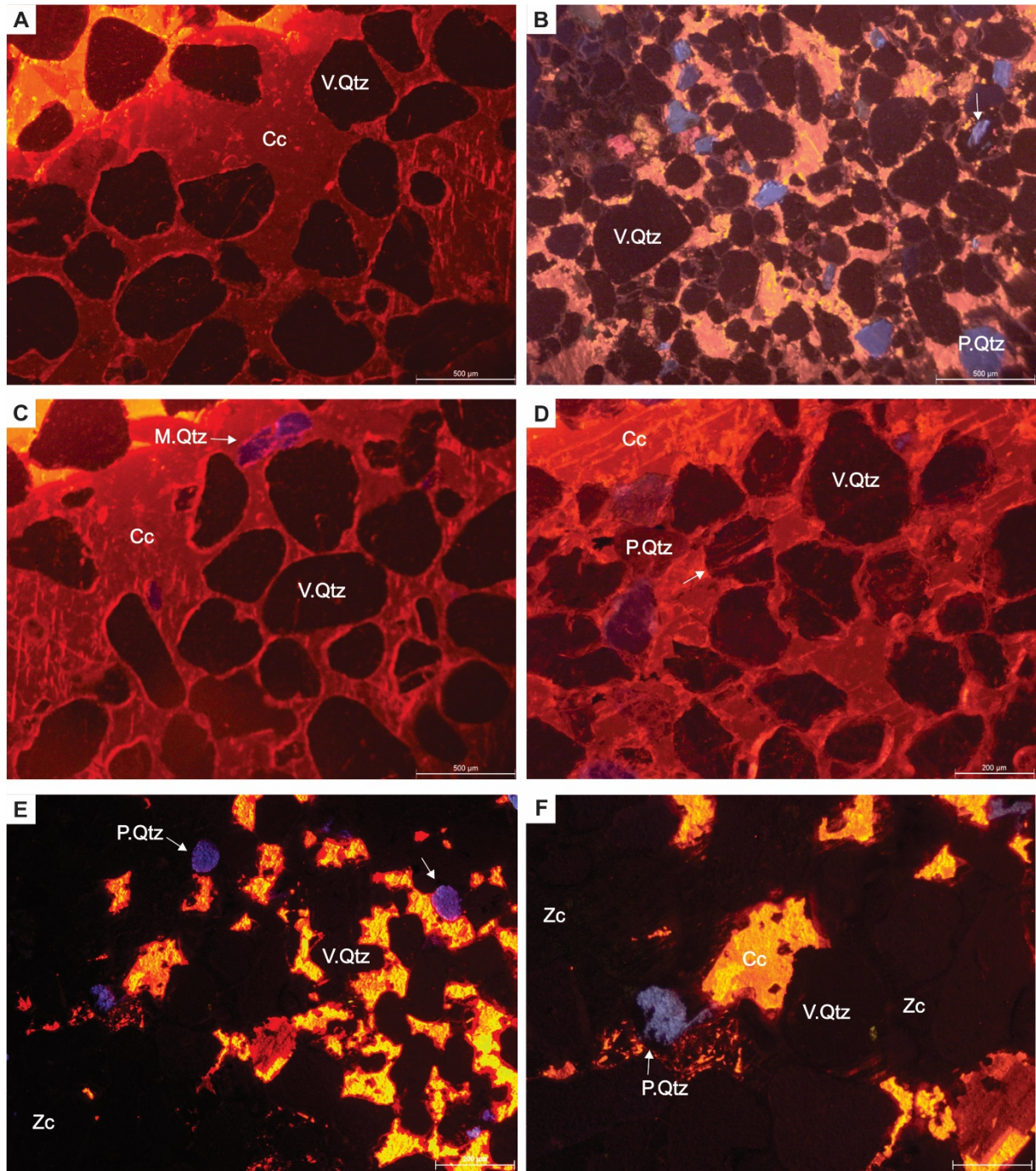


Figure 7 – Quartz cathodoluminescence from lacustrine (A-D) and aeolian (E-F) deposits. A. Dark red quartz grains floating in calcite cement. B. Dark red and, subordinately, bright blue quartz (white arrows). C. Blue colored metamorphic quartz grains. D. Volcanic and plutonic quartz grains. Dissolution features occur locally (white arrow). E-F. Predominance of dark red and blue colored grains in aeolian sandstones. V.Qtz = volcanic quartz; P.Qtz = plutonic quartz; M.Qtz = metamorphic quartz; Cc = calcite cement; Zc = zeolite cement.

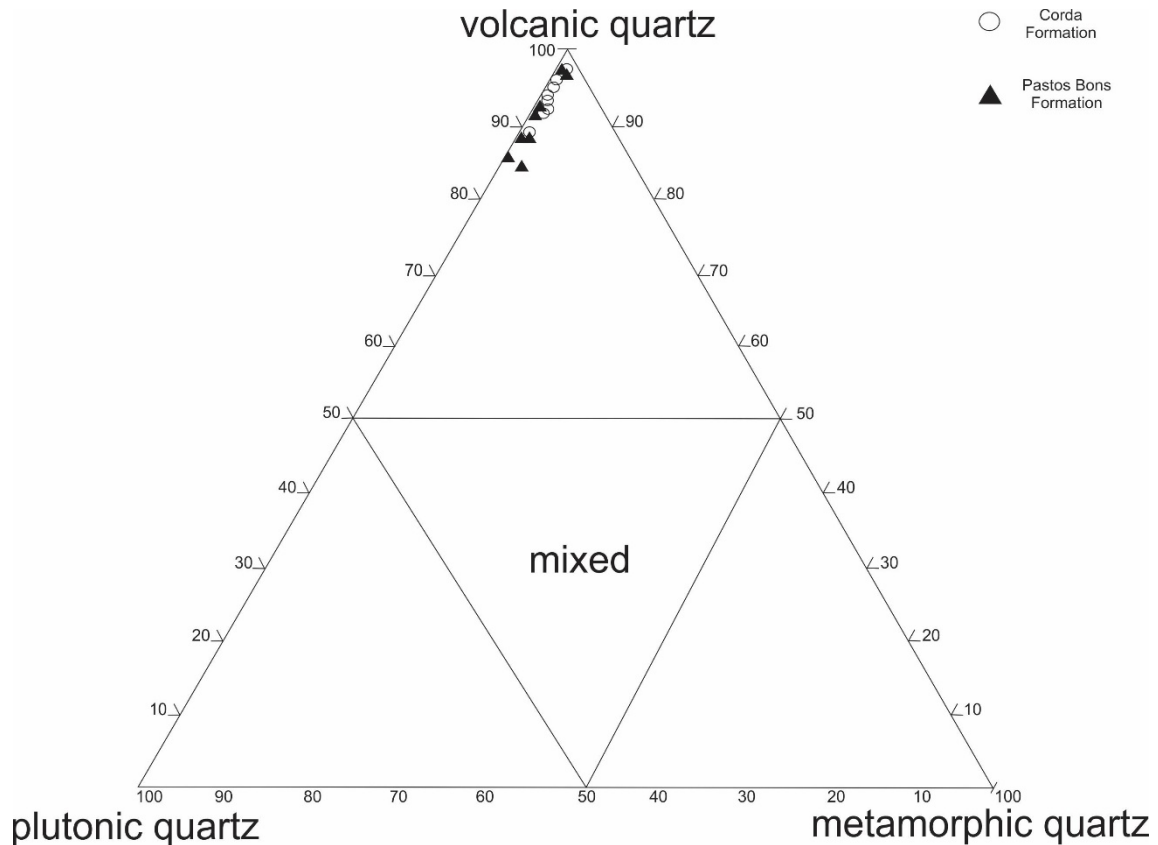


Figure 8 - Quartz provenance of lacustrine and eolian deposits, according to ternary provenance discrimination diagram (Bernet and Basset, 2005).

5 HEAVY MINERALS OF THE UPPER MEZOSOIC PARNAÍBA BASIN

5.1 HEAVY MINERALS OF THE MEARIM GROUP

5.1.1 Lacustrine Succession (Pastos Bons Formation)

The heavy mineral assemblage of lacustrine deposits from Pastos Bons Formation is composed by tourmaline, zircon, rutile, garnet and, subordinately, epidote, andalusite, staurolite and hornblende (Table 1).

Tourmaline is the dominant mineral in the succession, mainly in fine-grained fraction, with 17-77% modal proportion. This is characterized by rounded and anhedral grains, with dark green, pale green and, subordinately, reddish and blue colors (Fig. 9a). These are easily distinguished due to pleochroic halos, reverse pleochroism and, less commonly, basal divisibility. Tourmaline may be subdivided in three groups: Tur1 presents subrounded to rounded grains, rutile inclusions, as well as fluid and opaque minerals inclusions, sometimes with acicular habit. Conchoidal fractures, impact marks and abrasion borders are common, whereas zoning occur rarely. Tur2 group includes tabular and subrounded grains, which

contain apatite and opaque minerals inclusions. This group presents abrasion borders and, occasionally, corrosion features. Tur3 group includes clear, euhedral, subangulose to angulose grains, with prismatic habit. These grains may be fragmented, whereas fractures, abrasion and dissolution features are rare to absent.

Zircon presents 6-62.60% content and occurs as anhedral to subhedral, colorless to slightly yellowish grains (Fig. 9b). These may be subdivided in two groups: Zr1, which contains subangulose, occasionally fragmented grains, with impact marks, corroded edges, opaque inclusions and, rarely, concentric zoning. The Zr2 group contains grains with prismatic habit, subangulose, sometimes bipyramidal terminations, with acicular apatite inclusions, as well as rutile and opaque minerals inclusions. Additionally, this group exhibits features such as impact marks, conchoidal fractures and metamitic grains. Rutile grains occur in proportions of 1-18% and comprise brownish to reddish-brown grains, predominantly anhedral, subrounded and, sometimes, fragmented (Fig. 9c). Prismatic and subrounded grains with impact marks occur rarely.

Garnet grains occur with 0-54% modal content, inversely proportional to tourmaline. These are colorless to pale pink, rounded to subrounded grains and present mammillae and impact marks (Fig. 9d). Andalusite grains are present mainly in the fine-grained fraction (0.125-0.062 mm), in 0-7% modal content. These constituents are colorless to pale brown, clear, angulose, absent to weakly pleochroic, with strong birefringence and common fluid inclusions. Andalusite grains are frequently fragmented or present impact marks (Fig. 9e). Epidote grains have 0-8% modal content, with colorless to yellow-greenish, angulose to subrounded grains, often fragmented. These exhibit abrasion edges, fluid inclusions and corroded edges (Fig. 9f). Staurolite occurs restricted to fine-grained sandstones with low modal content (<1%). This is characterized by yellowish, weakly pleochroic, subhedral and subangulose to angulose grains, sometimes with “cockscomb” terminations and corroded edges (Fig. 9g). Hornblende occurs as trace mineral (<1%), with greenish, angulose and strongly pleochroic grains (Fig. 9h).

Table 1 – Heavy minerals content and mineralogical indexes of Upper Mesozoic sandstones from Parnaíba Basin (xxx = abundant >30%; xx = frequent 10-30%; x = rare <10%).

	Samples	Zr	Tur	Rt	Grt	Hbl	Ep	Cpx	St	And	Sil	ZTR	GZi	RZi
Pastos	PB-11a	xxx	xxx	xx	x	-	x	-	-	-	-	86.2	14.8	34.2
Bons	PB-11d	xxx	xxx	xx	-	-	-	-	-	-	-	99	0	26.1
Formation	PB-02d(F)	x	xxx	x	xxx	x	x	-	-	-	-	56	50	87.2
	PB-02d	xxx	xxx	xx	xxx	-	-	-	x	-	-	46.5	71.9	28.9
	PB-02e	xxx	xxx	xx	xxx	-	-	x	-	x	-	59.1	53.9	16.9
	PB-06a	xx	xxx	x	x	-	-	-	-	-	-	99	3.7	4.5
	PB-06b	xxx	xxx	x	x	-	-	-	-	-	-	99	0.7	11.2
	PB-06c	xxx	xxx	x	-	-	-	-	-	-	-	99	0	8.5
	PB-04a	x	xxx	x	xx	-	-	x	-	x		86.7	53.9	16.9
Formation	AM-1a	xxx	xx	x	x	-	x	xx	-	-	-	59	15.3	4.3
	AM-2a	xx	xxx	-	xxx	-	x	x	-	x	-	63.2	58.3	0
	AM-2b	xxx	xxx	x	xx	-	xx	x	-	x	-	66.1	25.8	4.5
	AM-3a	xxx	xx	x	xx	-	x	x	x	x	-	67.1	24.2	10
	AM-4a	xx	xx	x	xx	-	xx	x	x	xx	-	50.9	45.1	12
	AM-5b	x	x	-	xxx	-	-	-	-	-	-	12	97	0
	AM-6a	x	x	xx	xxx	-	x	x	-	-	-	21.7	94.1	78
	AM-9a	xx	x	xx	xxx	-	-	x	-	-	-	35	73.2	68.9
	P2-1a	xxx	xxx	x	x	-	x	x	-	-	-	97	1.1	11.2
	P5-1b	x	xxx	-	x	-	-	-	-	-	-	96	36.3	0
Formation	PB-05j	xx	xxx	x	xxx	xx	-	x	x	x	x	47.2	45.7	25
	PB-05i	xxx	xxx	x	x	xxx	-	x	x	x	-	41.2	18.5	18.8

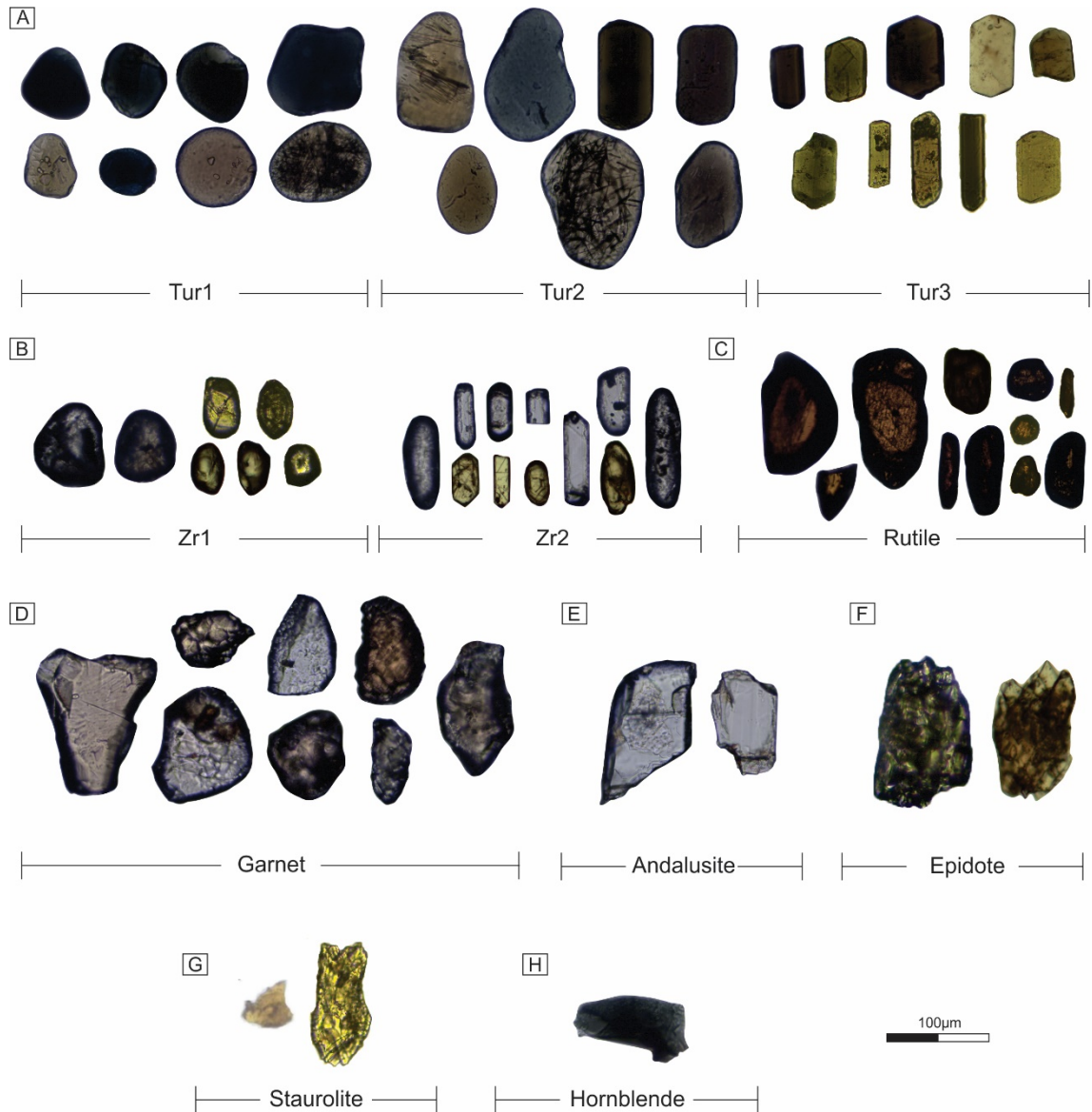


Figure 9 – Heavy minerals from lacustrine succession (Pastos Bons Formation). A. Tourmaline, divided in three groups according to the morphological and textural aspects. B. Zircon, divided in two groups according to the morphological and textural aspects. C. Rutile. D. Garnet. E. Andalusite. F. Epidote. G. Staurolite. H. Hornblende.

5.1.2 Aeolian Succession (Corda Formation)

The heavy minerals assemblage of the aeolian succession from Corda Formation is constituted by tourmaline, zircon, rutile, garnet, epidote and, subordinately, andalusite, clinopyroxene and staurolite (Table 1).

Tourmaline is present in 1.5-89% modal ratio and may occur in two different groups (Fig. 10a): Tur1 is most frequent and comprises anhedral, rounded/subrounded, green, blue and dark brown grains; and Tur2, which is composed by greenish, euhedral and prismatic grains. These constituents are characterized by strong reverse pleochroism and medium

birefringence, sometimes with pleochroic halos. Zircon grains occur with 2.6-51.1% frequency and are subdivided in two types (Fig. 10b): Zr1, which includes rounded to well-rounded constituents, with abrasion marks; and Zr2, with prismatic grains and rarely bipyramidal terminations. These grains present rutile, apatite and opaque minerals inclusions, as well as fluid inclusions. Impact marks and conchoidal fractures are frequent. Rounded to subrounded brownish rutile grains occur in 0-15.8% modal proportions (Fig. 10c).

Garnet group exhibits 0.5-71.2% frequency, with pink or brownish colored to colorless grains. These components are, generally, homogeneous, with impact marks and rare marks of surface solution features (corrosion facets) and mammillae marks (Fig. 10d). Epidote presents 0-16.8% modal content and may be colorless or exhibit yellowish and greenish colors. It presents rounded to subrounded grains, commonly with anomalous interference colors (Fig. 10e). Clinopyroxene grains are concentrated, mainly, in fine-grained sandstones, in 0-8.9% modal proportions. The constituents are colorless to slightly greenish, angulose, with clear appearance, weak to absent pleochroism and strong birefringence (Fig. 10f). Andalusite presents low concentrations (0-2.4%), with subrounded to angulose grains (Fig. 10g). Yellowish, rounded to subrounded staurolite grains occur as trace components (<0.5%) and present common dissolution features (Fig. 10h).

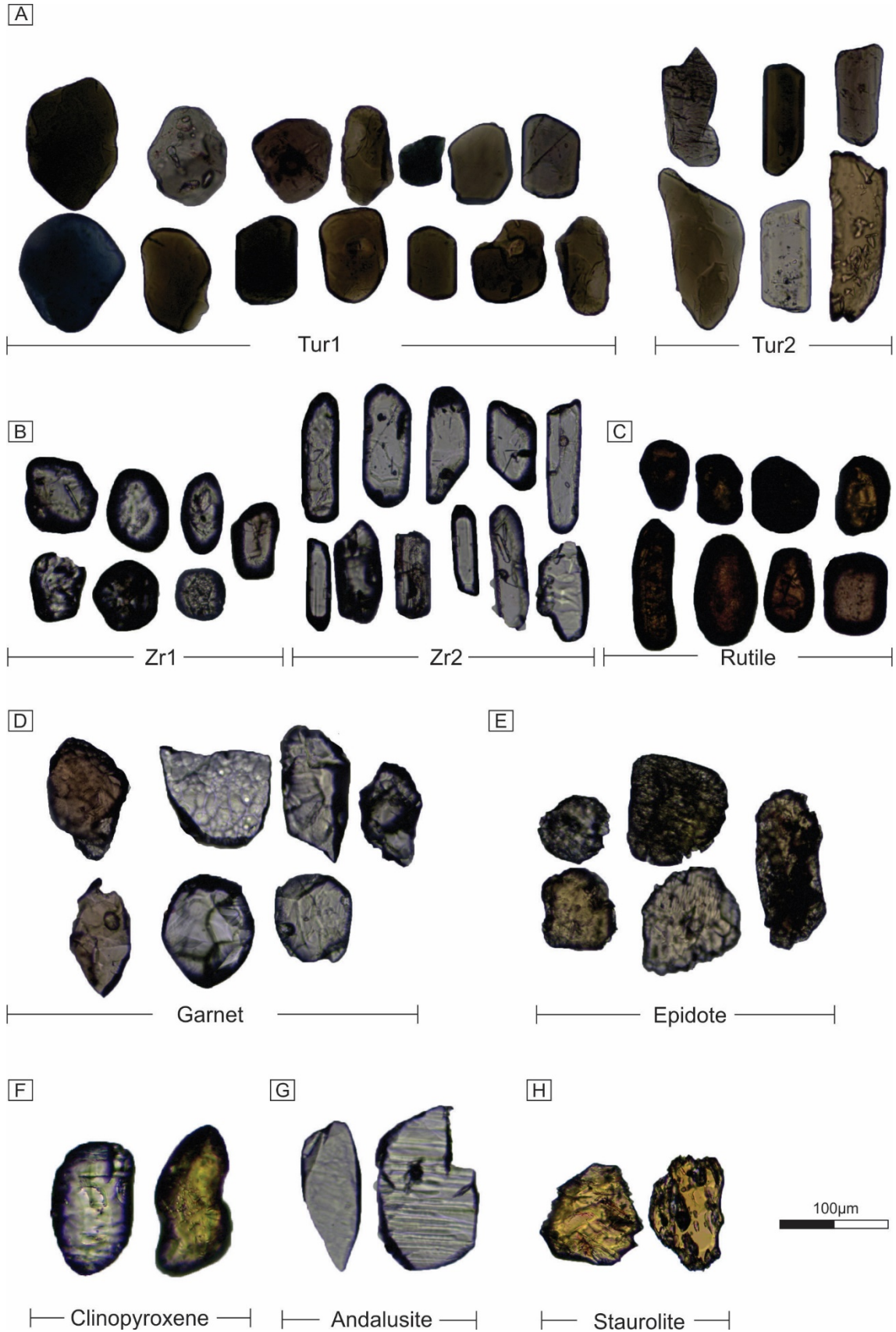


Figure 10 - Heavy minerals from aeolian succession (Corda Formation). A. Tourmaline, divided in two groups according to the morphological and textural aspects. B. Zircon, divided in two groups according to the morphological and textural aspects. C. Rutile. D. Garnet. E. Epidote. F. Clinopyroxene. G. Andalusite. H. Staurolite.

5.2 FLUVIAL SUCCESSION (GRAJAÚ FORMATION)

Fluvial sandstones from Grajaú Formation contain a heavy mineral assemblage composed by tourmaline, zircon, rutile, hornblende, garnet, clinopyroxene, andalusite and sillimanite (Table 1).

Tourmaline occurs in 13-31% modal content, and is distinguished in two groups (Fig. 11a): Tur1, with greenish, brownish, bluish, predominantly anhedral grains, which exhibit pleochroic halos and reverse pleochroism. Fluid inclusions and opaque minerals inclusions are frequent, whereas impact marks and basal divisibility rarely occur. Tur2 group presents euhedral, angulose, clear, greenish grains. Zircon grains are present in 12.90-22.90% modal content, with anhedral, rounded to subrounded constituents, which exhibit tourmaline, apatite, opaque minerals and fluid inclusions. Euhedral, bipyramidal and concentric zoned grains occur rarely (Fig. 11b). Rutile grains occur in 4.5-5.2% modal content, brown to dark brown colored, with rounded to angulose grains, sometimes, with bipyramidal terminations (Fig. 11c). Hornblende grains occur in 15.70-52.60% modal content, with prismatic subhedral, greenish grains, which are strongly pleochroic and contain well-developed cleavage (Fig. 11d). Garnet is colorless or pink with subrounded to angulose, anhedral grains, which may be fragmented. Impact marks, mammillae marks and opaque inclusions occur locally (Fig. 11e).

Clinopyroxene includes colorless to slightly yellowish/greenish, weakly pleochroic grains, with well-defined and closely spaced cleavage (Fig. 11f). Andalusite (0.4-1.7%) includes yellow to golden colored, predominantly angulose and weakly pleochroic grains (Fig. 11g). Sillimanite (0-1%) is colorless to slightly orange, represented by subhedral, angulose grains, characterized by well-developed cleavage, parallel extinction, moderate interference color and birefringence (Fig. 12g).

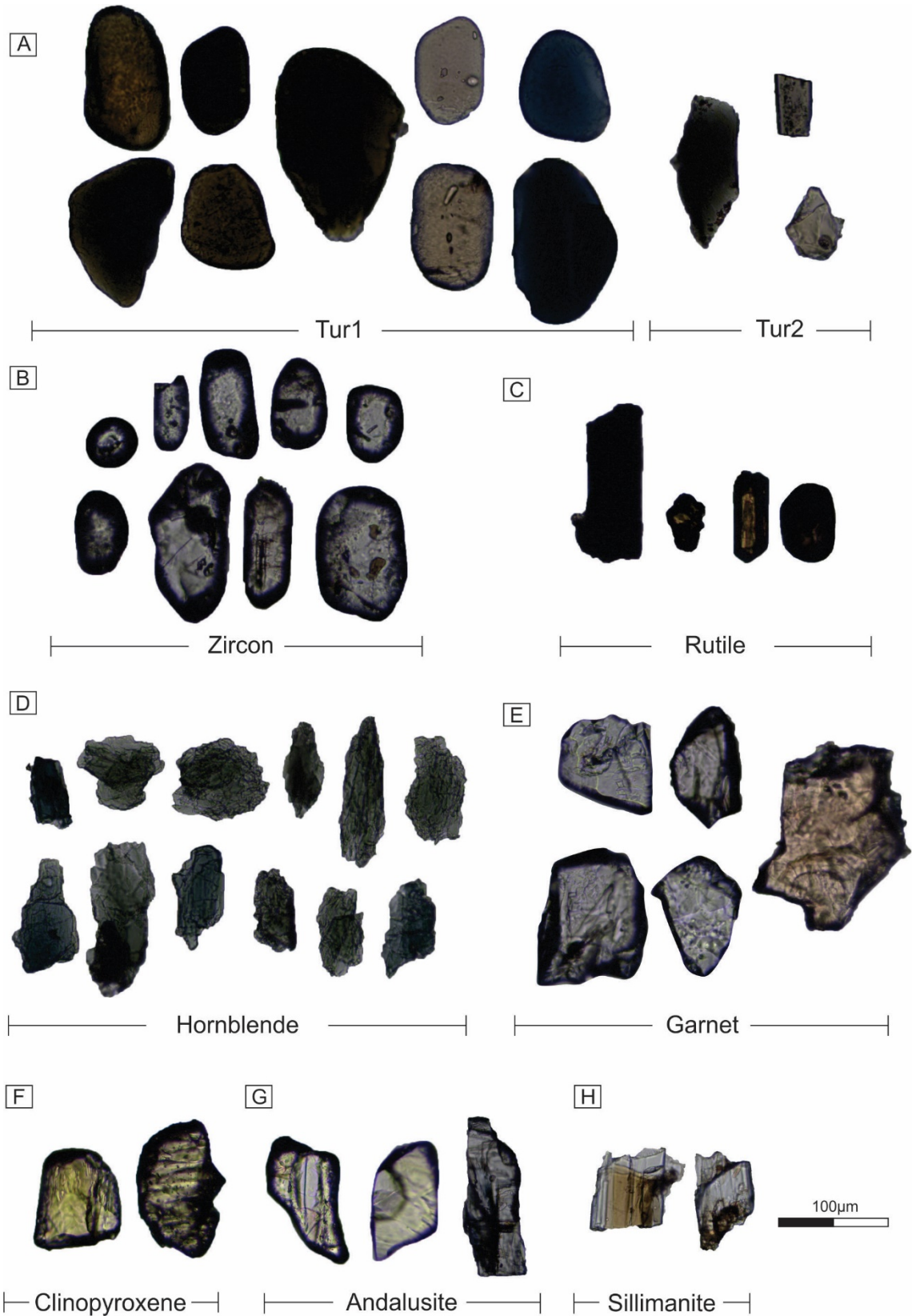


Figure 11 - Heavy minerals from fluvial deposits (Grajaú Formation). A. Tourmaline, divided in two subgroups according to the morphological and textural aspects. B. Zircon. C. Rutile. D. Hornblende. E. Garnet. F. Clinopyroxene. G. Andalusite. H. Sillimanite.

5.3 ZTR and GZi x RZi Indexes

Compositional maturity analysis of the heavy mineral assemblage was based on ZTR index (Morton, 1985), although, this analysis may be vulnerable to diagenetic modifications and distinct hydraulic behaviors between minerals (Morton and Hallsworth, 1994). In this sense, GZi and RZi indexes were also utilized to improve and constrain provenance analysis of the studied sandstones (Table 1).

Lacustrine succession presents ZTR values between 46.5 and 99, with higher values (>80) in central lake and flysch-like delta front facies associations, whereas lakeshore portions contain lower values (<60) (Fig. 12). The aeolian succession exhibits the most diverse ZTR indexes values, ranging from 11 up to 97 (Fig. 12). Dune field and wadi sandstones present higher content (>30), whereas sand sheet sandstones presented lower concentration (<25). Fluvial sandstones exhibited ZTR values lower than 49 (Fig. 12).

The GZi index values are, generally, inversely proportional to ZTR index. Lacustrine sandstones present 0-87.2 GZi index values, with lower ratios in flysch-like delta front and central lake deposits. Conversely, aeolian sandstones presented the highest values between the three studied units, mainly in wadi deposits (up to 97). RZi indexes is higher for aeolian sandstones (0-78), followed by lacustrine (4.5-50) and fluvial sandstones (≤ 25) (Fig. 13).

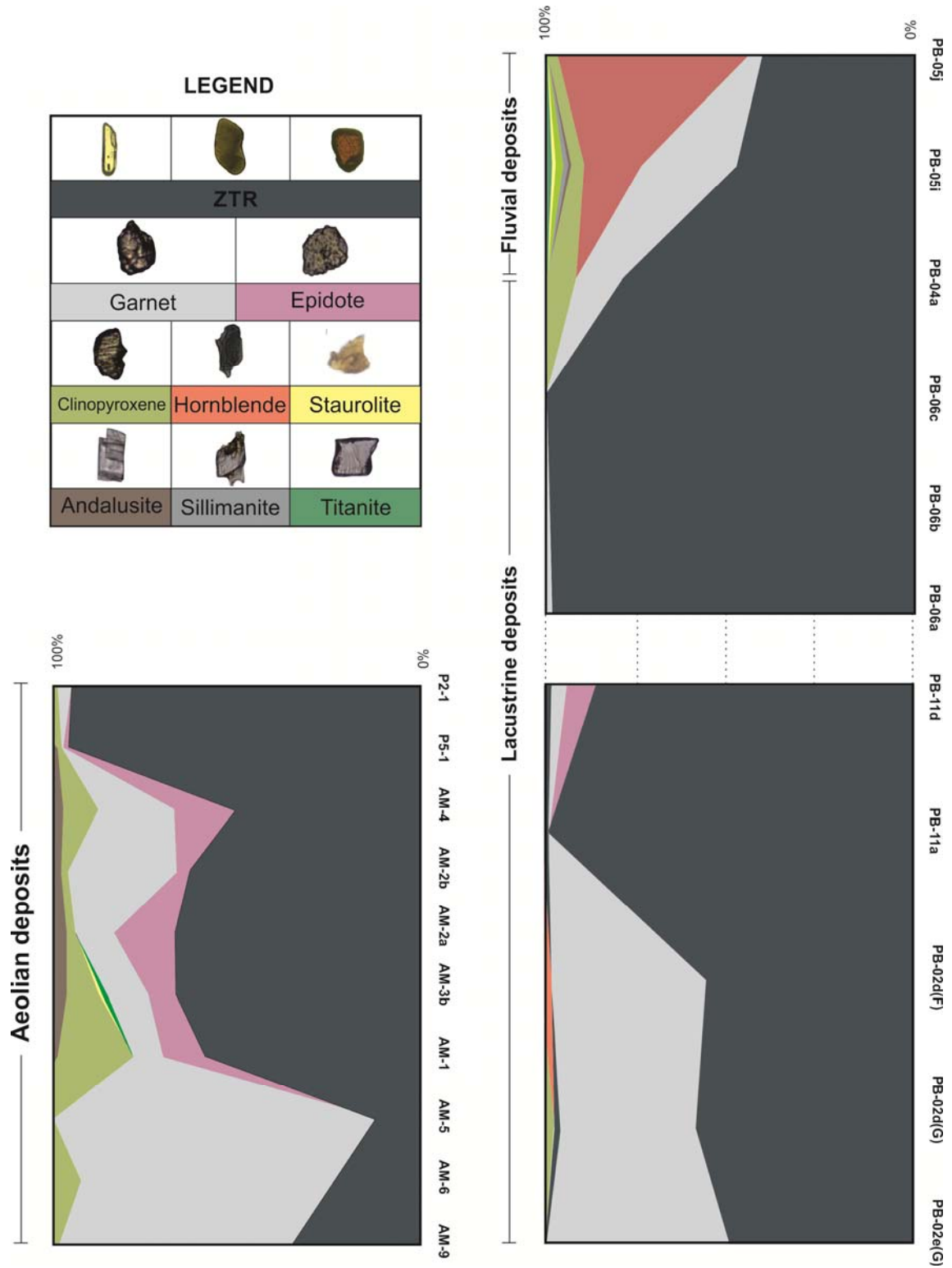


Figure 12 - ZTR index of aeolian, lacustrine and fluvial deposits from Upper Mesozoic Parnaíba Basin.

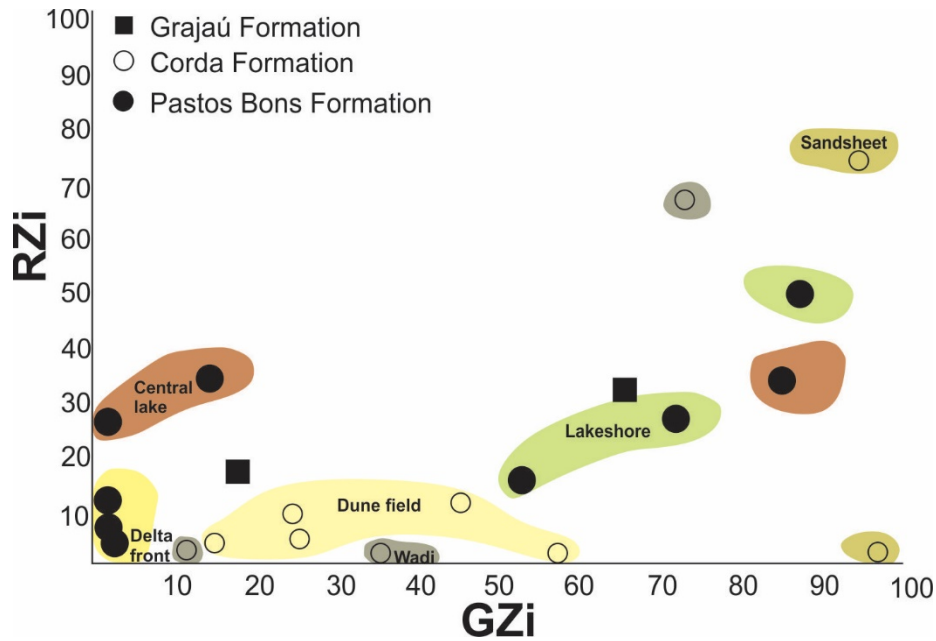


Figure 13 – Proportion between GZi and RZi indexes according to the facies associations in the lacustrine, aeolian and fluvial deposits.

6 HEAVY MINERAL ASSEMBLAGES OF THE UPPER MEZOSOIC SANDSTONES

Provenance analyses are frequently used to solve stratigraphic problems, perform stratigraphic correlations and to construct geological and geodynamic models (Mange *et al*, 2003; Morton *et al*, 2011; Morton and Hurst, 2016; Schneider *et al*, 2016; Zimmermann and Hall, 2016). The Upper Mesozoic succession of the Parnaíba Basin consists in volcanic lava flows, fluvial-lacustrine and fluvial-aeolian deposits, whose stratigraphy is still troublesome. This complexity is, mainly, a result of the intermittent exposure, denudation processes and fault displacements. In this sense, provenance data based on framework petrography, quartz cathodoluminescence, petrographic aspects of quartz grains and heavy minerals analysis were applied in order to compare and interpret the provenance of the Jurassic-Cretaceous sandstones of the Parnaíba Basin.

Sandstones from the Mearim Group plotted in recycled orogenic and interior craton provenance fields (e.g. Dickinson, 1985). The predominance of volcanic quartz, indicated by hot cathodoluminescence imaging, is coherent with the presence of massive basaltic flows over the western Parnaíba Basin. These rocks were probably one of the main source areas of the Mesozoic deposits, since this group was installed over Lower Jurassic basalts. The

decrease of volcanic lithic fragments content and increasing roundness grade of rock fragments lakeward indicate higher reworking towards the lake environment.

Additionally, sandstones from the Mearim Group exhibit higher ZTR index values, with predominantly superabundance to abundance of stable minerals in lacustrine succession (80.5 average) and equivalence of stable and unstable minerals in aeolian succession (56.8 average). The fluvial deposits exhibited lower heavy minerals content, as well as lower ZTR index values (44.4 average), with similarity in unstable and stable heavy minerals content (Fig. 12). Lacustrine sandstones exhibit higher values of tourmaline, whereas aeolian sandstones presented higher garnet, clinopyroxene and epidote content. The lacustrine and aeolian successions presented similar contents of zircon, rutile, andalusite, clinopyroxene and staurolite, whereas hornblende occurs only in the lacustrine succession. The fluvial deposits differ, mainly, by the high hornblende content (15.70-52.60%) and the presence of sillimanite. Another difference is the lower textural maturity of garnet grains, predominantly angulose and coarse-grained, compared to garnet grains in Mearim Group sandstones.

One might expect that the heavy minerals assemblages should contain high percentages of pyroxenes, due to the provenance carried out by basic volcanic rocks. The low content of these minerals is interpreted as consequence of the instability of ferromagnesian minerals in arid desertic conditions (Morton and Hallsworth, 1999), which may have enhanced dissolution processes. The high textural and compositional maturity of the Mearim Group mineral assemblage, with rounded zircon, tourmaline and rutile, indicates polycyclic character and long-standing abrasion processes, with reworking of sediments and/or sedimentary rocks (e.g. Tsikouras *et al*, 2011; Zimmermann and Hall, 2016). Mechanical surface textures in heavy minerals (e.g. abrasion borders, impact marks, conchoidal fractures) corroborate this interpretation (Andò *et al*, 2012).

In the other minerals, mainly staurolite and garnet, dissolution features controlled by the crystalline structure are commonest (e.g. “cockscomb” terminations and mammillae marks). The relatively lower garnet content in Pastos Bons Formation in comparison to the Corda Formation may be a result of the complex burial history of the lacustrine deposits, since that the burial diagenesis results in garnet solution (Morton and Hallsworth, 1999). This process is favored by the formation of acid organic gases through the alteration of organic matter in temperatures $\geq 80^{\circ}\text{C}$ (Hansley, 1987). Black shales and fossiliferous material are present in the lacustrine deposits, which may have provided the necessary source for organic gases formation. The absence/reduction of less stable minerals and consequently higher ZTR values in the lacustrine succession reflects the granulometric and mineralogical fractioning

towards the lake setting, which represent the depocenters of Parnaíba Basin during the Jurassic-Cretaceous transition. This fractioning is common in environments with distinct hydraulic behavior and may be enhanced by burial diagenesis, which results in the changing physical-chemical conditions and further dissolution of unstable minerals (Morton and Hallsworth, 1994; 1999).

6.1 UPPER MESOZOIC PROVENANCE EVOLUTION OF THE PARNAÍBA BASIN

Data from framework petrography, hot cathodoluminescence and petrography of quartz grains and heavy mineral assemblages indicate that the lacustrine (Pastos Bons) and aeolian (Corda) deposits were supplied by similar sources, which suggest possibly concomitant deposition. This assertion is coherent with sedimentological (Cunha and Carneiro, 1972; Góes and Feijó, 1994; Bállen, 2013; Rabelo and Nogueira, 2015; Cardoso *et al*, 2017), palynological (Lima and Campos, 1980; Bernardes-de-Oliveira *et al*, 2007) and paleontological (Gallo, 2005; Petra, 2006; Montefeltro *et al*, 2013; Valais *et al*, 2015) evidences, which suggest exclusively continental deposition during the sedimentation of the Mearim Group.

Single-mineral characterization indicating mainly volcanic quartz provenance and heavy minerals assemblage mainly supplied by metamorphic rocks suggest multiple source areas (e.g. Jian *et al*, 2013; Zimmermann and Hall, 2016). Minerals such as Al_2O_3 polymorphs, staurolite and garnet are commonest in metasedimentary rocks from greenschist to lower amphibolite metamorphic facies (Morton, 1985; 2012; Winter, 2001). In this sense, Mearim Group sediments were probably supplied by Paleoproterozoic to Neoproterozoic basement rocks from Borborema Province, as well as volcanic rocks within the Parnaíba Basin. In Borborema Province, the most likely areas include the Ceará Central Domain, due to the geographical proximity and predominantly metasedimentary lithologies, mainly the metapelitic supracrustal cover of the Ceará Group. Pre-Cambrian basement sources are suggested for Paleozoic sedimentary rocks, based on detrital zircon geochronology (Hollanda *et al*, 2018), which implies intrabasinal recycling. Epeirogenic uplifts triggered by magmatic emplacements related to the Central Atlantic Magmatic Province (CAMP) (Klöcking *et al*, 2018) may have played an important role in the Mesozoic provenance history of the Parnaíba Basin. Intrabasinal highs generated by this event probably renewed autogenic source areas and were strongly affected by denudation processes.

Conversely, high hornblende content in fluvial deposits of Grajaú Formation indicates intermediate-acid igneous source (e.g. Jian *et al*, 2013; Schneider *et al*, 2016), probably I-type Brazilian granites. The exact lithostratigraphic units are hard to define without geochronological data. However, Neoproterozoic Brazilian granites from Ceará Central Domain include the Tamboril – Santa Quitéria Complex (Souza Neto *et al*, 2008) and may compose an important source area. The occurrence of andalusite and sillimanite suggest high grade metamorphic source rocks (upper amphibolite to granulite facies) for these sandstones (Winter, 2001), without equivalence with the Mearim Group deposits. Different heavy mineral assemblages of the fluvial succession in comparison to the aeolian and lacustrine deposits may indicate shifts in provenance or unroofing of common source areas (e.g. Mange *et al*, 2003; Jian *et al*, 2013). Regional data are needed to support one of these hypotheses and to constrain source areas. However, outcrop-based data and heavy minerals analyses evidence an unconformity between the Mearim Group and fluvial deposits from Grajaú Formation, such that the stratigraphic positioning previously suggested for the Upper Mesozoic Parnaíba Basin (Vaz *et al*, 2007) is no longer supported.

The unconformity between Grajaú and Pastos Bons formations evidences the necessity of reevaluation of the Alpercatas Basin, since that the studied area in this work is located >200 km away from the limits proposed for this basin, trespassing the horsts suggested by Góes (1995) (Xambioá and Itapecuru highs). Moreover, the distinction between Parnaíba and Alpercatas basins are based on the recognition of depocenters migration hypothetically due to the displacement of large faults and uplift of the basin borders (Góes, 1995; Pedreira da Silva *et al*, 2003). Nevertheless, these features do not support this individualization, since that these are intrinsic processes of sedimentary basins evolution. The uplift of the Parnaíba Basin borders, as well as the depocenter migration during the Triassic-Jurassic transition may be explained by the post-magmatic cooling and subsequent thermal readjustment of the sedimentary deposits (Köckling *et al*, 2018). Filling dykes of Grajaú Formation in lacustrine beds indicate sin-sedimentary tectonics during the Aptian. In this sense, we do not consider the Alpercatas Basin as a geotectonic unit and interpret that the evolution of Parnaíba Basin extended from Silurian to the Upper Cretaceous.

7 CONCLUSIONS

This work investigated the provenance of Mesozoic deposits from a debatable stratigraphic succession in the Parnaíba Basin. A set of techniques was applied to avoid the

effects of transport, depositional and diagenetic processes, as well as to minimize the influence of the grain size chosen and sedimentary recycling. We focused on bulk sediment (sandstone petrography), multi-mineral (heavy minerals) and single-mineral (quartz petrography and quartz cathodoluminescence) analyses. The stratigraphic succession studied consists in the Mearim Group, defined by lacustrine shales and sandstones of the Pastos Bons Formation, and aeolian sandstones of the Corda Formation. These beds are unconformably overlaid by conglomerates and sandstones of the Grajaú Formation.

The sandstones plotted in recycled orogenic and interior craton fields, whereas quartz petrography and hot cathodoluminescence data evidenced volcanic sources. Heavy minerals assemblages from lacustrine and aeolian deposits are highly similar; nevertheless, both differ from the fluvial deposits, mainly due to the high hornblende content. In addition, ZTR, GZi and RZi indexes are higher in lacustrine and aeolian beds, and lower for fluvial strata. This dataset evidences multiple source areas for Mesozoic sandstones of the Parnaíba Basin, with quartz provenance mainly from volcanic rocks and heavy minerals supplied by low to medium-grade metapelitic rocks (greenschist to medium amphibolite facies). The increasing ZTR index and roundness towards the lacustrine beds reflect the hydraulic fractioning and the influence of depositional processes in this environment. The high hornblende content in fluvial deposits, as well as the lower roundness, indicate texturally immature components for sandstones of the Grajaú Formation, without equivalence with the Mearim Group. In this sense, the Mearim Group was probably supplied by Neoproterozoic rocks of the Ceará Central Domain (Ceará Group?), in addition to intrabasinal recycling of the Paleozoic basement and lava flows related to the CAMP event. Conversely, the Grajaú Formation was supplied by acid sources, such as I-type Brazilian granites. The provenance data presented for Mesozoic sandstones of the Parnaíba Basin reflect the geological evolution of this region and resulted from the unroofing of common sources or shifts in provenance areas. Geochronological data are fundamental to unravel these questions and to better constrain source units.

Acknowledgements

We are very grateful to National Council for Scientific and Technological Research (CNPq) for funding this research with a master scholarship (CNPq - 130823/2017-1) conceded to the first author, and to the Programa de Pós-Graduação em Geologia e Geoquímica (PPGG) of the Federal University of Pará (UFPA). We also thank Raíza Renné and Hudson Santos for hot cathodoluminescence analysis and Everaldo Cunha and Joelma Lobo for facilitating the heavy minerals separation.

REFERENCES

- AGUIAR, G.A. de. Bacia do Maranhão: geologia e possibilidades de petróleo. Belém: PETROBRAS, 1969, p. 55-106. (Relatório Técnico, n. 371).
- AGUIAR, G.A. de. Revisão geológica da bacia paleozoica do Maranhão. In: CONGRESSO BRASILEIRO DE GEOLOGIA, 25, 1971, São Paulo. Anais... São Paulo: SBG, 1971. v.3, p. 113-122.
- ANDÒ, S.; GARZANTI, E.; PADOAN, M.; LIMONTA, M. Corrosion of heavy minerals during weathering and diagenesis: a catalog for optical analysis. *Sedimentary Geology*, v. 280, p. 165-178, 2012.
- AUGUSTSSON, C.; BAHLBURG, H., 2003. Cathodoluminescence spectra of detrital quartz as provenance indicators for Paleozoic metasediments in southern Andean Patagonia. *Journal of South American Earth Sciences*, 16: 15-26.
- AUGUSTSSON, C., REKER, A., 2012. Cathodoluminescence spectra of quartz as provenance indicators revisited. *J. Sedimentary Research*, 82 (8): 559-570.
- BATISTA, A. M. N., 1992. Caracterização paleoambiental dos sedimentos Codó-Grajaú, Bacia de São Luís (MA). Dissertação (Mestrado). Belém: Instituto de Geociências – UFPA.
- BERNET, M., BASSETT, K., 2005. Provenance analysis by single quartz grain SEM-CL/optical microscopy. *J. Sedimentary Research*, 3: 496–504.
- BERNARDES-DE-OLIVEIRA, M.E.C.; MOHR, B.; DINO, R.; GUERRA-SOMMER, M.; GARCIA, M.J.; SUCERQUIA, P.A., 2007. As flores mesofíticas brasileiras no cenário paleoflorístico mundial. Editora Interciência. 40p.
- BOGGS JR., S. *Petrology of sedimentary rocks*. Nova Iorque: Cambridge University Press, 2009.
- CALDASSO, A. L. S. O problema Pastos Bons na estratigrafia da Bacia do Parnaíba. Recife: Companhia de Pesquisa de Recursos Minerais, Recife: 1978. Não paginado (Relatório Interno).
- CAPUTO, M.V. Stratigraphy, tectonics, paleoclimatology and paleogeography of Northern Basins of Brazil. 1984. xx, 583f. Tese (Doutorado) - University of California, Santa Barbara, USA: 1984.
- CARDOSO, A. R.; NOGUEIRA, A. C. R.; ABRANTES JR, F. R. A.; RABELO, C. E. N., 2017. Mesozoic lacustrine system in the Parnaíba Basin, northeastern Brazil: paleogeographic implications for West Gondwana. *Journal of South American Earth Science*. 74: 41-53.
- CASTRO, D.L., FUCK, R.A., PHILLIPS, J.D., VIDOTTI, R.M., BEZERRA, F.H.R., DANTAS, E.L., 2014. Crustal structure beneath the Paleozoic Parnaíba basin revealed by airborne gravity and magnetic data, Brazil. *Tectonophysics* 614, 128–145.
- CUNHA, F.B.; CARNEIRO, R.G. Interpretação fotogeológica do centro-oeste da Bacia do Maranhão. In: XXVI CONGRESSO BRASILEIRO DE GEOLOGIA. Anais... Belém, 1972, v. 3, p. 64-80.
- DALY, M. C.; ANDRADE, V.; BAROUSSE, C. A.; COSTA, R.; MCDOWELL, K.; PIGGOTT, N.; POOLE, A. J., 2014. Brasileiro crustal structure and the tectonic setting of the Parnaíba basin of NE Brazil: results of a deep seismic reflection profile. *Tectonics*, 33: 1-19.
- DE VALAIS, S.D.E; CANDEIRO, C.R.; TAVARES, L.F.; ALVES, Y.M.; CRUVINEL, C. Current situation of the ichnological locality of São Domingos from the Corda Formation (Lower Cretaceous), northern Tocantins state, Brazil. *Journal of South American Earth Sciences*, 61: 142-146.
- DICKINSON, W.R., 1985. Interpreting provenance relations from detrital modes of sandstones. In: Zuffa, G.G. (Ed.), *Provenance of arenites*. Reidel, Dordrecht, NATO ASI Series 148, pp. 333–361.
- FOLK, R. L. *Petrology of sedimentary rocks*. Ed. Hemphil's Public., Austin, Texas, 107p, 1968.
- GALEHOUSE, J. S. Sedimentation analysis. In: Carver, R. E. (ed.), *Procedures in sedimentary petrology*: John Wiley and Sons, New York, NY, p. 69–94, 1971.
- GALLO V. Redescription of *Lepidotes Piauhyensis* Roxo and Löefgren, 1936 (Neopterygil, Semionotiformes, Semionotidae) from the ?Late Jurassic-Early Cretaceous of Brazil. *Journal of Vertebrate Paleontology*, v. 25, n. 4, p. 757-769, 2005.
- GARZANTI, E., 2016. From static to dynamic provenance analysis – Sedimentary petrology upgraded. *Sedimentary Geology*, 336: 3-13.
- GÓES A.M., 1995. A Formação Poti (Carbonífero Inferior) da Bacia do Parnaíba. PhD Thesis, Universidade de São Paulo, São Paulo, 145p.
- GÓES, A. M.; ROSSETTI, D. F. 2001. Gênese da Bacia de São Luís-Grajaú, Meio-Norte do Brasil. In: O Cretáceo na Bacia de São Luís-Grajaú (eds. D. F. Rossetti, A. M. Góes and W. Truckenbrodt), pp. 15–29. Coleção Friedrich Katzer. Belém: Museu Paraense Emílio Goeldi.
- GÓES, A.M.O.; FEIJÓ, F.J. A Bacia do Parnaíba. *Boletim de Geociências da Petrobras*, p. 57-67, 1994.
- GÓES, A. M. O.; TRAVASSOS, W. A. S.; NUNES, K.C. Projeto Parnaíba: Reavaliação e perspectivas exploratórias. Belém, PETROBRAS, v. 1, 358p. (circulação restrita).
- HANSLEY, P.L., 1987. Petrologic and experimental evidence for the etching of garnets by organic acids in the Upper Jurassic Morrison Formation, northwestern New Mexico. *J. Sediment. Petrol.* 57, 666–681.

- HASUI, Y.; COSTA, J.B.S.; BORGES, M.S.; ASSIS, J.F.P.; PINHEIRO, R.V.L.; BARTORELLI, A.; PIRES NETO, A.G.; MIOTO, J.A. A borda sul da Bacia do Parnaíba no Mesozóico. In: 3° Simpósio Nacional De Estudos Tectônicos, Rio Claro. Boletim, Rio Claro, SBG – Núcleo de São Paulo: v. 8, n. 1, p. 93-95, 1991.
- HOLLANDA, M. H. B. M.; GÓES, A. M.; NEGRI, F. A., 2018. Provenance of sandstones in the Parnaíba Basin through detrital zircon geochronology. In: DALY, M. C., FUCK, R. A., JULIÀ, J., MACDONALD, D. I. M. & WATTS, A. B., (eds) Cratonic Basin Formation: A Case Study of the Parnaíba Basin of Brazil. Geological Society, London, Special Publications, 472.
- JIAN, X.; GUAN, P.; ZHANG, D.; ZHANG, W.; FENG, F.; LIU, R.; LIN, S., 2013. Provenance of Tertiary sandstones in the northern Qaidan Basin, northeastern Tibetan Plateau: Integration of framework petrography, heavy minerals analysis and mineral chemistry. *Sedimentary Geology*, 290: 109-125.
- KLÖCKING, M.; WHITE, N.; MACLENNAN, J., 2018. Role of basaltic magmatism within the Parnaíba cratonic basin, NE Brazil. In: DALY, M. C., FUCK, R. A., JULIÀ, J., MACDONALD, D. I. M. e WATTS, A. B. (eds) Cratonic Basin Formation: A Case Study of the Parnaíba Basin of Brazil. Geological Society, London, Special Publications, 472.
- LIMA, E. A. M.; LEITE, J. F. Projeto de estudo global dos recursos minerais da Bacia Sedimentar do Parnaíba. Integração Geológico-Metalogenética: Relatório Final da Etapa III. Companhia de Pesquisa de Recursos Minerais. Recife, 212p, 1978.
- LIMA, M.R.; CAMPOS, D.de A. Palinologia dos folhelhos da fazenda Muzinho, Floriano, Piauí. *Geodiversitas - USP, São Paulo*: v. 11, p. 149-154, 1980.
- MANGE, A. M.; DEWEY, J. F.; WRIGHT, D. T., 2003. Heavy minerals solve structural and stratigraphic problems in Ordovician strata of the western Irish Coaledonides. *Geological Magazine*, 140 (1): 25-30.
- MONTEFELTRO, F. C.; LARSSON, H. C. F.; FRANÇA, M. A. G., LANGER, M. C. A new neosuchian with Asian affinities from the Jurassic of northeastern Brazil. *Naturwissenschaften*, v. 100, p. 835–841, 2013.
- MORTON, A. C. Heavy minerals in provenance studies. In: G. G. ZUFFA (eds). *PROVENANCE OF ARENITES*. Reidel, Dordrecht, p. 249-277, 1985.
- MORTON, A.C., 2012. Value of heavy minerals in sediments and sedimentary rocks for provenance, transport history and stratigraphic correlation. In: Sylvester, P. (Ed.), *Quantitative mineralogy and microanalysis of sediments and sedimentary rocks*. Mineralogical Association of Canada Short Course Series, 42: 133–165.
- MORTON, A.C.; HALLSWORTH, C.R., 1994. Identifying provenance-specific features of detrital heavy mineral assemblages in sandstones. *Sedimentary Geology*, 90, 241-256.
- MORTON, A.C.; HALLSWORTH, C.R., 1999. Processes controlling the composition of heavy minerals assemblage in sandstones. *Sedimentary Geology*, 124: 3-29.
- MORTON, A.; HURST, A.; 2016. Correlation of sandstones using heavy minerals: an example from the Staffjord Formation of the Snorre Field, northern North Sea. *Geological Society Special Publication*, 89: 3-22.
- MORTON, A.; MEINHOLD, G.; HOWARD, J. P.; PHILLIPS, R. J.; STROGEN, D.; ABUTARRUMA, Y.; ELGADRY, M.; THUSU, B.; WHITMAN, A. G., 2011. A heavy minerals study from the eastern Murzuq Basin, Libya: Constraints on provenance and stratigraphic correlation. *Journal of African Earth Sciences*, 61: 308-330.
- NAJMAN, Y., 2006. The detrital record of orogenesis: a review of approaches and techniques used in the Himalayan sedimentary basins. *Earth-Science Reviews*, 74: 1-72.
- NICHOLS, G. *Sedimentary and stratigraphy*. Chichester, Ed. Wiley-Blackwel, Oxford. 2. ed., 2009.
- OLIVEIRA, C.E.S.; PE-PIPER, G.; PIPER, D.J.W.; ZHANG, Y.; CORNEY, R., 2017. Integrated methodology for determining provenance of detrital quartz using optical petrographic microscopy and cathodoluminescence (CL) properties. *Marine and Petroleum Geology*, 88: 41-53.
- OLIVEIRA, D. C.; MOHRIAK, W. U. Jaibaras Trough: an important element in the early tectonic evolution of the Parnaíba interior sag Basin, Northeastern Brazil. *Marine and Petroleum Geology*, Guildford, n. 20, p. 351-383, 2003.
- OMER, M.F., 2015. Cathodoluminescence petrography for provenance studies of the sandstones of Ora Formation (Devonian-Carboniferous), Iraqi Kursditan Region, northern Iraq. *Journal of South African Earth Sciences*, 109: 195-210.
- PAZ, J.D.S.; ROSSETTI, D.F., 2005. Linking lacustrine cycles with syn-sedimentary tectonic episodes: an example from the Codó Formation (late Aptian), northeastern Brazil. *Geol. Mag.*, 142(3): 269-285.
- Pedreira da Silva A.J.; Cunha Lopes R.; Vasconcelos M.; Bahia R.B.C., 2003. Bacias sedimentares Paleozóicas e Meso-Cenozóicas interiores. In: Bizzi L.A., Schobbenhaus C., Vidotti R.M., Gonçalves J.H., eds., *Geologia, tectônica e recursos minerais do Brasil*: Brasília, Brasil, Companhia de Pesquisa de Recursos Minerais, p. 55–85.
- PERNY, B.; EBERHARDT, P.; RAMSEYER, K.; MULLIS, J.; PANKRATH, R., 1992. Microdistribution of Al, Li, and Na in alpha quartz: Possible causes and correlation with short-lived cathodoluminescence: *American Mineralogist*, v. 77, p. 534-544.

- PETRA, M.S. Paleoiçtiofauna da Formação Pastos Bons (Bacia do Parnaíba) – Reconstituição Paleoambiental e Posicionamento Cronoestratigráfico. 2006. Dissertação (de Mestrado). Universidade do Estado do Rio de Janeiro, xvii, 141 f., 2006.
- PORTO, A.; DALY, M.C.; LA TERRA, E.; FONTES, S., 2018. The pre-Silurian Riachão Basin: a new perspective on the basement of the Parnaíba Basin, NE Brazil. In: DALY, M. C., FUCK, R. A., JULIÀ, J., MACDONALD, D. I. M. & WATTS, A. B. (eds) Cratonic Basin Formation: A Case Study of the Parnaíba Basin of Brazil. Geological Society, London, Special Publications, 472.
- RABELO, C.N.; NOGUEIRA, A.C.R. O sistema desértico úmido do Jurássico Superior da Bacia do Parnaíba, na região entre formosa da Serra Negra e Montes Altos, Estado do Maranhão, Brasil. *Geol. USP, Séries Científicas*, v. 15, p. 3-21, 2015.
- RABELO, C.E.N.; CARDOSO, A.R.; NOGUEIRA, A.C.R.; GÓES, A.M.; SOARES, J.L.S., 2018. Poikilotopic zeolite in the Late Mesozoic eolian sandstones of the Parnaíba Basin, northern Brazil: a post-continental magmatic reconstitution for the West Gondwana. Submitted.
- RAMSEYER, K.; MULLIS, J., 2000, Geologic application of cathodoluminescence of silicates, in Pagel, M., Barbin, V., Blanc, P., and Ohnenstetter, D., eds., *Cathodoluminescence in Geosciences*: Berlin, Springer-Verlag, p. 177-191.
- REZENDE, N.G.A.M., 1998. Reordenamento estratigráfico do Mesozoico da Bacia do Parnaíba. XL Congresso Brasileiro de Geologia, Belo Horizonte, Anais... SBG-MG, p. 111.
- ROMERO BALLÉN, O. A. R. As sucessões sedimentares interderrames da Formação Mosquito, exemplo de um sistema eólico úmido, Província Parnaíba. Dissertação (de Mestrado). USP – Universidade de São Paulo, xix, 85 f, 2012.
- ROXO, M.; LÖFGREN, A. *Lepidotus piauhyensis*, sp. nov. Notas Preliminares e Estudos. Divisão de Geologia e Mineralogia/DNPM, v. 1, p. 7–12, 1936.
- SANTOS M. E. C. M., CARVALHO M. S. S. Paleontologia das Bacias do Parnaíba, Grajaú e São Luís, Ed. 2, CPRM, Rio Janeiro, 212p, 2004.
- SANTOS, R. da S. Peixes triássicos dos folhelhos da Fazenda Muzinho, estado do Piauí. Notas Preliminares e Estudos. Rio de Janeiro, Departamento Nacional de Produção Mineral. DNPM, v. 82, p. 170-178, 1953.
- SCHNEIDER, S.; HORNUNG, J.; HINDERER, M., 2016. Evolution of the western East African Rift System reflected in provenance changes of Miocene to Pleistocene synrift sediments (Albertine Rift, Uganda). *Sedimentary Geology*, 343: 190-205.
- SCHOBENHAUS, C., CAMPOS, D.A., QUEIROZ, E.T., WINGE, M., BERBERTBORN, M. (eds.). *Sítios Geológicos e Paleontológicos do Brasil*. Brasília, DNPM/CPRM, 1984.
- SEVASTJANOVA, I.; HALL, R.; ALDERTON, D., 2012. A detrital heavy mineral viewpoint on sediment provenance and tropical weathering in SE Asia. *Sedimentary Geology*, 280: 179-194.
- SOUZA NETO, J.A., LEGRAND, J.M., VOLFINGER, M., PASCAL, M. & SONNET, P. 2008. W–Au skarns in the Neo- Proterozoic Seridó Mobile Belt, Borborema Province in northeastern Brazil: an overview with emphasis on the Bonfim deposit. *Mineralium Deposita*, 43: 185–205.
- STEVENS-KALCEFF, M.A.; PHILLIPS; M.R.; MOON, A.R.; KALCEFF, W., 2000, Cathodoluminescence microcharacterisation of silicon dioxide polymorphs, in Pagel, M., Barbin, V., Blanc, P., and Ohnenstetter, D., eds., *Cathodoluminescence in Geosciences*: Berlin, Springer-Verlag, p. 193-224.
- TISIKOURAS, B.; PE-PIPER, G.; PIPER, D.; SCHAFFER, M., 2011. Varietal heavy minerals analysis of sediment provenance, Lower Cretaceous Scotian Basin, eastern Canada. *Sedimentary Geology*, 237: 150-165.
- TUCKER. M. E. *Sedimentary petrology: an introduction the origin of sedimentary rocks*. Ed. Oxford: Blackwell Science. 2. Ed, 1991. 260p.
- VAZ, P.T.; REZENDE, N.G.A.M.; WANDERLEY FILHO, J.R.; TRAVASSOS, W.A.S. Bacia do Parnaíba. *Boletim de Geociências da Petrobras*, v. 15, n. 2, p. 253-263, 2007. VAIL, P.R., 1987. Seismic stratigraphy interpretation using sequence stratigraphy. In: Bally, W.A. (Ed.), *Atlas of Seismic Stratigraphy*. V 1, AAPG Studies Geology, 27: 1-10.
- VICTOR ZALÁN, P. Influence of pre-Andean orogenies on the Paleozoic intracratonic basins of South America. IV Simpósio Bolivariano, Bogotá, v. 1, n. 7, p. 17-29, 1991.
- WATT, G.R.; WRIGHT, P.; GALLOWAY, S.; MCLEAN, C., 1997, Cathodoluminescence and trace element zoning in quartz phenocrysts and xenocrysts: *Geochimica et Cosmochimica Acta*, v. 61, p. 4337-4348.
- WINTER, J.D.; 2001. *An Introduction to Igneous and Metamorphic Petrology*. Prentice-Hall, New Jersey.
- ZIMMERMANN, S.; HALL, R., 2016. Provenance of Triassic and Jurassic sandstones in the Banda Arc: Petrography, heavy minerals and zircon geochronology. *Gondwana Research*, 37: 1-19.

CONCLUSÕES

Este trabalho inclui dados estratigráficos, faciológicos e mineralógicos inéditos referentes à porção central da Bacia do Parnaíba, com enfoque na Formação Pastos Bons, além de unidades adjacentes, como os arenitos eólicos da Formação Corda e os arenitos fluviais da Formação Grajaú. A Formação Pastos Bons é constituída por depósitos siliciclásticos lacustres, subdivididos em quatro associações de fácies: lacustre central (AF1), *sheet-like delta front* (AF2), lacustre marginal (AF3) e canais fluviais efêmeros (AF4), organizados principalmente em ciclos de raseamento ascendente. Esta sucessão inclui quatro ciclos deposicionais, limitados por discordâncias ou superfícies de inundação, cujo arcabouço estratigráfico exhibe um padrão retrogradacional-progradacional-retrogradacional. O aumento ascendente do espaço de acomodação é interpretado como resultado de uma subsidência térmica que afetou a Bacia do Parnaíba após o extravasamento massivo de lava associado a *Central Atlantic Magmatic Province* (CAMP). A proveniência desta unidade foi investigada a partir de petrografia de arenitos, petrografia e catodoluminescência de quartzo, além da análise de minerais pesados. Os arenitos da Formação Pastos Bons plotam nos campos de orógenos reciclados e interior cratônico, enquanto que dados de catodoluminescência de quartzo e petrografia de quartzo indicam fontes vulcânicas. No entanto, a assembleia de minerais pesados desta unidade exhibe fontes metapelíticas com paragênese das fácies xisto verde a anfíbolito médio. Estas análises também foram aplicadas nas formações Corda e Grajaú e constata-se que, embora os depósitos eólicos sejam muito similares, os arenitos fluviais diferem por apresentarem grãos predominantemente imaturos e alto teor de hornblenda. O aumento dos índices ZTR, GZi e RZi e o maior grau de arredondamento nos depósitos lacustres refletem o fracionamento hidráulico e os processos deposicionais atuantes neste ambiente. Os dados supracitados indicam múltiplas áreas fonte para as formações Pastos Bons e Corda (Grupo Mearim), com grãos de quartzo supridos por rochas vulcânicas possivelmente associadas ao CAMP. Os minerais pesados, no entanto, foram provavelmente influenciados por coberturas proterozoicas do Domínio Ceará Central (Grupo Ceará?), além da ocorrência de retrabalhamentos intrabaciais. Contrariamente, a assembleia de minerais pesados da Formação Grajaú apresenta influência de rochas intermediárias a ácidas, provavelmente granitos Brasileiros tipo-I. Esta evolução geológica reflete a exumação de áreas fontes em comum ou a mudança de áreas fonte, contudo, dados geocronológicos são necessários para melhor responder esta questão.

REFERÊNCIAS

- Abrantes Jr. F. R. & Nogueira A. C. R., 2012. Reconstituição paleoambiental das formações Motuca e Sambaíba, Permo-Triássico da Bacia do Parnaíba no sudoeste do Estado do Maranhão, Brasil. *Geol. USP, Sér. Cient.*, **13**(3): 65-82.
- Abrantes Jr. F. R., Nogueira A. C. R., Soares J. L., 2016. Permian paleogeography of West-Central Pangea: reconstruction using sabkha-type gypsum-bearing deposits of Parnaíba Basin, Northern Brazil. *Sedimentary Geology*, n. 341, p. 175-188.
- Aguiar G.A. de., 1969 Bacia do Maranhão: geologia e possibilidades de petróleo. Belém: Petrobras, p. 55-106. (*Relatório Técnico*, n. 371).
- Aguiar G.A. de., 1971. Revisão geológica da bacia paleozoica do Maranhão. *In: Congresso Brasileiro de Geologia*, 25, São Paulo. *Anais...* São Paulo: SBG, 1971. v.3, p. 113-122.
- Almeida F. F. M., Hasui, Y., Brito Neves B. B., 1976. The upper pre-cambrian of South América. *Boletim IG Instituto de Geociências, USP*, v. 7, p. 45-80.
- Andò S., Garzanti E., Padoan M., Limonta M., 2012. Corrosion of heavy minerals during weathering and diagenesis: a catalog for optical analysis. *Sedimentary Geology*, v. 280, p. 165-178.
- Andrade L.S., Nogueira A.C.R., Bandeira J., 2014. Evolução de um Sistema Lacustre Árido Permiano, parte Superior da Formação Pedra de Fogo, Borda Oeste da Bacia do Parnaíba. *Geol. USP: Série Científica* 14 (4): 39–60.
- Augustsson C & Bahlburg H. 2003. Cathodoluminescence spectra of detrital quartz as provenance indicators for Paleozoic metasediments in southern Andean Patagonia. *Journal of South American Earth Sciences*, 16: 15-26.
- Augustsson C. & Reker A. 2012. Cathodoluminescence spectra of quartz as provenance indicators revisited. *J. Sedimentary Research*, 82 (8): 559-570.
- Bardet N., Falconnet J., Fischer V., Houssaye A.; Jouve S.; Suberbiola X.P.; Pérez-García A.; Rage J.C., Vincent P., 2014. Mesozoic marine reptile palaeobiogeography in response to drifting plates. *Gondwana Research*, 869-887.
- Baksi A.K. & Archibald D. A., 1997. Mesozoic igneous activity in the Maranhão province, northern Brazil: 40Ar/39Ar evidence for separate episodes of basaltic magmatism. *Earth and Planetary Sciences Letters*, v. 151, p. 139-153.
- Batista A. M. N., 1992. Caracterização paleoambiental dos sedimentos Codó-Grajaú, Bacia de São Luís (MA). Dissertação (Mestrado). Belém: Instituto de Geociências – UFPA.
- Benvenuti M., 2003. Facies analysis and tectonic significance of lacustrine fan-deltaic successions in the Pliocene–Pleistocene Mugello Basin, Central Italy. *Sedimentary Geology* 157: 197–203.
- Bernet M. & Bassett K., 2005. Provenance analysis by single quartz grain SEM-CL/optical microscopy. *J. Sedimentary Research*, 3: 496–504.
- Beurlen K., 1954. Um novo gênero de conchostráceo da família Limnadiidae. *Notas Preliminares e Estudos*, Rio de Janeiro, Departamento Nacional de Produção Mineral DNPM, n. 83, p. 23-28.
- Bernardes-De-Oliveira M.E.C., Mohr. B., Dino R., Guerra-Sommer M., Garcia M.J & Sucerquia P.A., 2007. As flores mesofíticas brasileiras no cenário paleoflorístico mundial. Editora Interciência. 40p.

- Boggs Jr. S., 2009. *Petrology of sedimentary rocks*. Nova Iorque: Cambridge University Press.
- Bohacs K.M., 1999. Sequence stratigraphy of lake basins; unraveling the influence of climate and tectonics: *American Association of Petroleum Geologists Bulletin*, v. 83, p. 1878.
- Bohacs K.M., Carroll A.R., Neal J.E., 2003. Lessons from large lake systems – Thresholds, nonlinearity, and strange attractors: *Geological Society of America Abstracts with Programs*, v. 32, no. 7, p. A-312.
- Bohacs K.M., Carroll A.R., Neal J.E., Mankiewicz P.J., 2000. Lake-basin type, source potential, and hydrocarbon character: An integrated sequence stratigraphic – geochemical framework. In: Gierlowski-Kordesch, E., and Kelts, K., eds., *Lake basins through space and time: American Association of Petroleum Geologists Studies in Geology* v. 46, p. 3–37.
- Bosence D., Procter E., Aurrel M., Kahla A.B., Boudagher-Fadel M., Casaglia F., Cirilli S., Mehdie M., Nieto L., Rey J., Scherreiks R., Soussi M., Waltham D., 2009. A dominant tectonic signal in high-frequency, peritidal carbonate cycles? A region analysis of Liassic platforms from western Thetys. *J. Sediment. Res.* 79, 389-475.
- Bouma A. H., 1962. Sedimentology of some flysch deposits: a graphic approach to facies interpretation. *Sedimentology*.
- Bouma A. H., 2008. Coarse-grained and fine-grained turbidite systems as end-member models: applicability and dangers. *Marine and Petroleum Geology*; 17: 137 – 143.
- Brazil J.J., 1948. Zona Sul da Bacia do Maranhão. Rio de Janeiro: Conselho Nacional de Petróleo. p.71-78. (*Relatório Interno*).
- Caldasso A. L. S., 1978. O problema Pastos Bons na estratigrafia da Bacia do Parnaíba. Recife: Companhia de Pesquisa de Recursos Minerais, Recife. Não paginado (*Relatório Interno*).
- Callegaro S., Baker D.R., Min A.D., Marzoli A., Geraki K., Bertrand H., Viti C., Nertola, F. 2014. Microanalyses link sulfur from large igneous provinces and Mesozoic mass extinctions. *Geology*, 42(10): 895-898.
- Ccampbell D. F., 1949. Bacia do Maranhão. Conselho Nacional de Petróleo. Rio de Janeiro: Cons. Nac. de Petról., p. 68-74 (*Relatório Interno*. N. 153).
- Caputo M.V., 1984. Stratigraphy, tectonics, paleoclimatology and paleogeography of Northern Basins of Brazil. 1984. xx, 583f. Tese (Doutorado) - University of California, Santa Barbara, USA.
- Cardoso A. R., Nogueira A. C. R., Abrantes Jr F. R. A., Rabelo C. E. N. 2017. Mesozoic lacustrine system in the Parnaíba Basin, northeastern Brazil: paleogeographic implications for West Gondwana. *Journal of South American Earth Science*. 74: 41-53.
- Carroll A.R. & Bohacs, K.M. Stratigraphic classification of ancient lakes: balancing tectonic and climatic controls. *Geology*, v. 27, p. 99-102, 1999.
- Castro D.L., Fuck R.A., Phillips J.D., Vidotti R.M., Bezerra F.H.R., Dantas, E.L., 2014. Crustal structure beneath the Paleozoic Parnaíba basin revealed by airborne gravity and magnetic data, Brazil. *Tectonophysics* 614, 128–145.
- Catuneanu O., 2006. *Principles of sequence stratigraphy*. (1ed.) Elsevier, 375p.

- Catuneanu O., Abreu, V., Battacharya J.P., Blum, M.D., Dalrymple R.J., Eriksson P.G.; Fielding C.R., Fisher W.L., Galloway W.E., Gibling M.R., Giles K.A., Holbrook J.M., Jordan R., Kendall C.G.St.C., Macurda B., Martinsen O.J., Miall A.D., Neal J.E., Nummedal J., Pomar L., Posamentier H.W., Pratt B.R., Sarg J.F., Sharley K.W., Steel R.J., Strasser A., Tucker M.E., Winker C. 2009. Towards the standardization of sequence stratigraphy. *Earth-Science Reviews*, 92: 1-33.
- Catuneanu O., Galloway W.E., Kendall C.G.St.C., Miall A.D., Posamentier H.W., Strasser A., Tucker M.E.; 2010. Sequence Stratigraphy: methodology and nomenclature. *Newsletter on Stratigraphy*, v. 44(3): 173-245.
- Catuneanu O. & Zecchin M. 2013. High-resolution sequence stratigraphy of clastic shelves II: controls on sequence development. *Marine and Petroleum Geology*, 39: 26-38.
- Changsong L., Kenneth E., Sitian L., Yongxian W., Jianye R., Yanmei Z., 2001. Sequence architecture depositional systems, and controls on development of lacustrine basin fills in part of the Erlian basin, northeast China. *AAPG Bulletin*, 85(11): 2017-2043.
- Cunha F.B. & Carneiro R.G. Interpretação fotogeológica do centro-oeste da Bacia do Maranhão. In: XXVI Congresso Brasileiro de Geologia. *Anais...* Belém, 1972, v. 3, p. 64-80.
- Currie B.S. 1997. Sequence stratigraphy of nonmarine Jurassic-Cretaceous rocks, central Cordilleran foreland-basin system. *GSA Bulletin*, 109(9): 1206-1222.
- Daly M. C., Andrade V., Barousse C. A., Costa R., McDowell K., Piggott N., Poole A. J. 2014. Brasiliano crustal structure and the tectonic setting of the Parnaíba basin of NE Brazil: results of a deep seismic reflection profile. *Tectonics*, 33: 1-19.
- Davis, R. A., 1992. *Depositional systems: an introduction to sedimentology and stratigraphy*. Englewood Cliffs, NJ, Ed. Prentice Hall.
- Della Fávera J. C., 2001. *Fundamentos de estratigrafia moderna*. Ed. Moderna. Rio de Janeiro.
- De Ros L.F. & Moraes M.A.S. 1984. Sequência diagenética em arenitos: Uma discussão inicial. *Anais do XXXIII Congresso Brasileiro de Geologia*, Rio de Janeiro.
- De Valais S.D.E, Candeiro C.R., Tavares L.F., Alves Y.M., Cruvinel, C. Current situation of the ichnological locality of São Domingos from the Corda Formation (Lower Cretaceous), northern Tocantins state, Brazil. *Journal of South American Earth Sciences*, 61: 142-146.
- Dickinson W.R. 1985. Interpreting provenance relations from detrital modes of sandstones. In: Zuffa, G.G. (Ed.), *Provenance of arenites*. Reidel, Dordrecht, NATO ASI Series 148, pp. 333-361.
- Dumas S., Arnott R.W.C., Southard J.B. 2005. Experiments on oscillatory flow and combined-flow bed forms: implications for interpreting parts of the shallow marine sedimentary record. *Journal of Sedimentary Research*, 75, 501-513.
- Feng Y., Jiang S., Hu S., Changsong L., Xie X. 2016. Sequence stratigraphy and importance of syndepositional structural slope-break for architecture of Paleogene syn-rift lacustrine strata, Bohai-Bay Basin, E. China. *Marine and Petroleum Geology*, 69: 183-204.
- Fischer A.G. 1964. The Lofer cyclothems of the Alpine Triassic. In: Merriam, D.F. (Ed.), *Symposium on Cyclic Sedimentation*, 169: 107-149. Kansas Geological Survey, Bulletin.
- Folk R. L., 1968. *Petrology of sedimentary rocks*. Ed. Hemphill's Public., Austin, Texas, 107p.

- Galehouse J. S., 1971. Sedimentation analysis. In: Carver, R. E. (ed.), *Procedures in sedimentary petrology*: John Wiley and Sons, New York, NY, p. 69–94.
- Gallo V., 2005. Redescription of *Lepidotes Piauhyensis* Roxo and Löefgren, 1936 (Neopterygil, Semionotiformes, Semionotidae) from the ?Late Jurassic-Early Cretaceous of Brazil. *Journal of Vertebrate Paleontology*, v. 25, n. 4, p. 757-769.
- Gallo V. & Figueiredo, F. J., 2004. A new teleost fish from the Early Cretaceous of Northeastern Brazil. *Boletim do Museu Nacional*. Rio de Janeiro, n. 27, p. 65-73.
- Garzanti E., 2016. From static to dynamic provenance analysis – Sedimentary petrology upgraded. *Sedimentary Geology*, 336: 3-13.
- Góes A.M., 1995. A Formação Poti (Carbonífero Inferior) da Bacia do Parnaíba. PhD Thesis, Universidade de São Paulo, São Paulo, 145p.
- Góes A. M. & Rossetti D. F. 2001. Gênese da Bacia de São Luís-Grajaú, Meio-Norte do Brasil. In: *O Cretáceo na Bacia de São Luís-Grajaú* (eds. D. F. Rossetti, A. M. Góes & W. Truckenbrodt), pp. 15–29. Coleção Friedrich Katzer. Belém: Museu Paraense Emílio Goeldi.
- Góes A.M.O. & Feijó F.J. A Bacia do Parnaíba. *Boletim de Geociências da Petrobras*, p. 57-67, 1994.
- Góes A. M. O., Travassos W. A. S., Nunes K.C. Projeto Parnaíba: Reavaliação e perspectivas exploratórias. Belém, *Petrobras*, v. 1, 358p. (circulação restrita).
- Goldhammer R.K., Lehmann P. J, Dunn, P.A. 1993. The origin of high-frequency platform carbonate cycles and third-order sequences (Lower Ordovician El Paso Group, west Texas): constraints from outcrop data and stratigraphic modeling: *Journal of Sedimentary Petrology*, v. 63, p. 318-359.
- Grogan E.D. & Lund R., 2002. The geological and biological environment of the Bear Gulch Limestone (Mississippian of Montana) and a model for its deposition. *Geodiversitas* 24: 295–315.
- Hanneman D.L & Wideman C.J, 2010. Continental sequence stratigraphy and continental carbonates. *Developments in Sedimentology*, 62: 215-273.
- Hansley P.L., 1987. Petrologic and experimental evidence for the etching of garnets by organic acids in the Upper Jurassic Morrison Formation, northwestern New Mexico. *J. Sediment. Petrol.* 57, 666–681.
- Hasui Y., Costa J.B.S., Borges M.S., Assis J.F.P., Pinheiro R.V.L., Bartorelli A., Pires Neto A.G., Miotto J.A., 1991. A borda sul da Bacia do Parnaíba no Mesozóico. In: 3º Simpósio Nacional De Estudos Tectônicos, Rio Claro. Boletim, Rio Claro, SBG – Núcleo de São Paulo: v. 8, n. 1, p. 93-95.
- Holdsworth R.E., Butler C.A., Roberts A.M. 1997. The recognition of reactivation during continental deformation. *Journal of Geological Society*, London, 54: 73-78.
- Holz M., 2015. Mesozoic paleogeography and paleoclimate – a discussion of the diverse greenhouse and hothouse conditions of an alien world. *Journal of South American Earth Sciences*, v. 61, p. 91-107.
- Hamdani Y., Mareschal J.-C., Arkani-Hamed J. 1991. Phase changes and thermal subsidence in intracontinental sedimentary basins, *Geophys. J. Int.*, 106: 657-665.
- Hamdani Y., Mareschal J.-C., Arkani-Hamed J. 1994. Phase changes and thermal subsidence of the Williston basin. *Geophys. J. Int.*, 116: 585-597.

- Husinec A., Basch D., Rose B., Read, J.F., 2008. FISCHERPLOTS: an excel spreadsheet for computing Fischer plots of accommodation change in cyclic carbonate successions in both the time and depth domains. *Comput. Geosci.* 34: 269-277.
- Keighley D., Flint S., Howell J., Moscariello A., 2003. Sequence stratigraphy in lacustrine basins: a model for part of the Green River Formation (Eocene), southwest Uinta Basin, Utah, U.S.A. *Journal of Sedimentary Research*, 73(6): 987-1006.
- Kerans C. & Tinker S.W. 1997. Sequence stratigraphy and characterization of carbonate reservoirs: *Society of Economic Paleontologists and Mineralogists Short Course Notes*, 40, 165 p.
- Ilgar A. & Nemeç W., 2005. Early Miocene lacustrine deposits and sequence stratigraphy of the Ermenek Basin, Central Taurides, Turkey. *Sedimentary Geology*, 173: 233-275.
- IUGS (International Union on Geological Sciences). *International Chronostratigraphic Chart*. International Commission on Stratigraphy, 2013. Não paginado.
- Lamb M. P., Myrow P. M., Lukens C., Houck K., Strauss, J. 2008. Deposits from wave-influenced turbidites currents: Pennsylvanian Minturn Formation, Colorado, USA. *Journal of Sedimentary Research*, 78: 480-498.
- Lima E. A. M. & Leite, J. F. Projeto de estudo global dos recursos minerais da Bacia Sedimentar do Parnaíba. *Integração Geológico-Metalogenética: Relatório Final da Etapa III*. Companhia de Pesquisa de Recursos Minerais. Recife, 212p, 1978.
- Lima M.R. & Campos D. de A., 1980. Palinologia dos folhelhos da fazenda Muzinho, Floriano, Piauí. *Geodiversitas - USP*, São Paulo: v. 11, p. 149-154.
- Lindoso R.M., Carvalho I.S., Mendes L.D. 2013. An isopod from the Codó Formation (Aptian of the Parnaíba Basin), Northeastern Brazil. *Brazilian Journal of Geology*, 43: 16-21.
- Lisboa, M. A. R., 1914. The Permian geology of northern of Brazil. *Am. Jour. Sci.*, v. 37, n. 221, p. 425-443.
- Luca P. H. V. & Basilici G. 2013. A prodeltaic system controlled by hyperpycnal flows and storm waves: reinterpretation of the Punta Negra Formation (Lower-Middle Devonian, Argentine Precordillera). *Brazilian Journal of Geology*, 43(4): 673-694.
- Martinsen O., Ryseth A., Hansen W.H., Fleshe H., Torkildsen G., Idil, S. 1999. Stratigraphic base level and fluvial architecture: Ericson Sandstone (Campanian), Rock Springs Uplift, SW Wyoming, USA. *Sedimentology* 46, 235–259.
- Mcelwain J. C. & Punyasena S. W., 2007. Mass extinction events and the plant fossil record. *Trends in Ecology and Evolution*, 22 (10): 548-557.
- Meju M. A., Fontes S.L., Oliveira M.F.B., Lima J.P.R., Ulugergerli E.U., Carrasquilla A.A. 1999. Regional aquifer mapping using combined VES-TEM-AMT/EMAP methods in the semiarid eastern margin of Parnaíba Basin, Brazil. *Geophysics*, 64(2): 337-356.
- Mesner C. J. & Wooldridge C. P. Maranhão Paleozoic basin and Cretaceous coastal basin, north Brazil. *Bulletin of the American Association of Petroleum Geologists*, v. 48, n. 9, p. 1475-1512, 1964.
- Milani E., J. & Thomaz Filho, A. Sedimentary basins of the South America. In: Cordani U. G., Milani E. J., Thomaz Filho A & Campos D. A. (eds.). *Tectonic Evolution Of South America*. Anais... Rio de Janeiro, Ed. Esp. XXXI Congresso Geológico Internacional, Rio de Janeiro, p. 389-449, 2000.

- Mitchum R.M. & Van Wagoner J.C., 1991. High frequency sequences and their stacking patterns: Sequence stratigraphic evidence of high-frequency eustatic cycles. *In: W. Schlager & K.T. Biddle (Eds.), The Record of Sealevel Fluctuation. Sediment. Geol.*, 70: p. 131-160.
- Montefeltro F. C., Larsson H. C. F., França M. A. G., Langer M. C., 2013. A new neosuchian with Asian affinities from the Jurassic of northeastern Brazil. *Naturwissenschaften*, v. 100, p. 835–841.
- Morad S., Ketzer J.M., De Ros L.F. 2000. Spatial and temporal distribution of diagenetic alterations in siliciclastic rocks: implications for mass transfer in sedimentary basin. *Sedimentology*, 47: 95-120.
- Morad S., Ketzer J.M., De Ros L.F., 2012. Linking diagenesis to sequence stratigraphy: an integrated tool for understanding and predicting reservoir quality distribution. International Association of *Sedimentology*, Special Publication, 45: 1-36.
- Morton A.C., 2012. Value of heavy minerals in sediments and sedimentary rocks for provenance, transport history and stratigraphic correlation. *In: Sylvester, P. (Ed.), Quantitative mineralogy and microanalysis of sediments and sedimentary rocks. Mineralogical Association of Canada Short Course Series*, 42: 133–165.
- Morton A. C., 1985. Heavy minerals in provenance studies. *In: G. G. ZUFFA (eds). Provenance Of Arenites.* Reidel, Dordrecht, p. 249-277.
- Morton A.C. & Hallsworth C.R. 1994. Identifying provenance-specific features of detrital heavy mineral assemblages in sandstones. *Sedimentary Geology*, 90, 241-256.
- Morton A.C. & Hallsworth, C.R. 1999. Processes controlling the composition of heavy minerals assemblage in sandstones. *Sedimentary Geology*, 124: 3-29.
- Morton A. & Hurst A. 2016. Correlation of sandstones using heavy minerals: an example from the Statfjord Formation of the Snorre Field, northern North Sea. *Geological Society Special Publication*, 89: 3-22.
- Najman Y. 2006. The detrital record of orogenesis: a review of approaches and techniques used in the Himalayan sedimentary basins. *Earth-Science Reviews*, 74: 1-72.
- Nichols, G., 2009. *Sedimentology and stratigraphy*. Chichester, Ed. Wiley-Blackwel, Oxford. 2. ed..
- North C. P. & Davidson S. K., 2012. Unconfined fluvial processes: recognition and interpretation of their deposits, and the significance for palaeogeographic reconstruction. *Earth-Science Reviews*, n. 111, p. 199-223.
- Nunes A. De B., 1973. Geologia da folha 23.SB Teresina e parte da folha 24.SB Jaguaribe. DNPM. *Projeto RADAM. Levantamento de recursos naturais.* Rio de Janeiro, v. 2, p. 1-24.
- Oliveira C.E.S., Pe-Piper G., Piper D.J.W., Zhang Y., Corney R. 2017. Integrated methodology for determining provenance of detrital quartz using optical petrographic microscopy and cathodoluminescence (CL) properties. *Marine and Petroleum Geology*, 88: 41-53.
- Oliveira D. C. & Mohriak W. U., 2003. Jaibaras Trough: an important element in the early tectonic evolution of the Parnaíba interior sag Basin, Northeastern Brazil. *Marine and Petroleum Geology*, Guildford, n. 20, p. 351-383.
- Omer M.F. 2015. Cathodoluminescence petrography for provenance studies of the sandstones of Ora Formation (Devonian-Carboniferous), Iraqi Kursditan Region, northern Iraq. *Journal of South African Earth Sciences*, 109: 195-210.

- Oviatt C.G., McCoy W.D., Nash W.P. 1994. Sequence stratigraphy of lacustrine deposits: a Quaternary example from the Bonneville basin, Utah. *Geological Society of America Bulletin*, 106: 133-144.
- Owen G., Moretti M., Alfaro, P., 2011. Recognising triggers for soft-sediment deformation: current understanding and future directions. *Sedimentary Geology*, n. 235, p. 133-140.
- Owen G. & Moretti M. Identifying triggers for liquefaction-induced soft-sediment deformation in sands. *Sedimentary Geology*, n. 235, p. 141-147, 2011.
- Paz J.D.S. & Rossetti, D.F. 2005. Linking lacustrine cycles with syn-sedimentary tectonic episodes: an example from the Codó Formation (late Aptian), northeastern Brazil. *Geol. Mag.*, 142(3): 269-285.
- Perny B., Eberhardt P., Ramseyer K., Mullis J., Pankrath R. 1992, Microdistribution of Al, Li, and Na in alpha quartz: Possible causes and correlation with short-lived cathodoluminescence: *American Mineralogist*, v. 77, p. 534-544.
- Petra M.S., 2006. Paleoictiofauna da Formação Pastos Bons (Bacia do Parnaíba) – Reconstituição Paleoambiental e Posicionamento Cronoestratigráfico. 2006. Dissertação (de Mestrado). Universidade do Estado do Rio de Janeiro, xvii, 141 f..
- Pinto I. D. & Purper Y. Observations on Mesozoic Conchostracea from the north of Brazil. Congresso Brasileiro de Geologia, 28. *Anais...* Porto Alegre, SBG, v. 2, p. 5–16, 1974.
- Plummer F. B., 1948. Estados do Maranhão e Piauí. Conselho Nacional do Petróleo, Rio de Janeiro, n. 46, p. 87-134 (*Relatório Interno*).
- Porto A., Daly M.C., La Terra E.; Fontes, S., 2018. The pre-Silurian Riachão Basin: a new perspective on the basement of the Parnaíba Basin, NE Brazil. *In: Daly, M. C., Fuck, R. A., Juliã, J., Macdonald, D. I. M. & Watts, A. B. (eds) Cratonic Basin Formation: A Case Study of the Parnaíba Basin of Brazil. Geological Society of London, Special Publications*, 472.
- Posamentier H.W. & James D.P. 1993, An overview of sequence-stratigraphic concepts: uses and abuses, *In: H.W. Posamentier, C.P. Summerhayes, B.U. Haq & G.P. Allen, eds., Sequence stratigraphy and facies associations: Oxford, Blackwell*, p. 3-18.
- Posamentier H.W., Jervey M.T., Vail, P.R., 1988. Eustatic Controls on Clastic Deposition I--Conceptual Framework: in Wilgus, *et al*, (eds.), *Sea-Level changes: an integrated approach*, SEPM *Special Publication* no. 42, p. 109-124.
- Rabelo C.N. & Nogueira A.C.R., 2015. O sistema desértico úmido do Jurássico Superior da Bacia do Parnaíba, na região entre formosa da Serra Negra e Montes Altos, Estado do Maranhão, Brasil. *Geol. USP, Séries Científicas*, v. 15, p. 3-21.
- Rabelo C. 2013. Paleambiente da Formação Mosquito e a implantação do sistema desértico úmido da Formação Corda, Jurássico Superior, Centro-Oeste da Bacia do Parnaíba. 2013. Dissertação (de Mestrado). Universidade Federal do Pará, Belém, xvi, 81 f, 2013.
- Rabelo C.E.N., Cardoso A.R., Nogueira A.C.R., Góes A.M., Soares J.L.S. 2019. Poikilotopic zeolite in the Late Mesozoic eolian sandstones of the Parnaíba Basin, northern Brazil: a post-continental magmatic reconstitution for the West Gondwana. *Submitted*.
- Rajmon D. 2009. *Impact Database* 2010.1. On-line. <http://impacts.rajmon.cz>.
- Ramseyer K. & Mullis J. 2000. Geologic application of cathodoluminescence of silicates, *In: Pagel, M., Barbin, V., Blanc, P., & Ohnenstetter, D., eds., Cathodoluminescence in Geosciences: Berlin, Springer-Verlag*, p. 177-191.

- Reading H.G. *Sedimentary environment and facies*. Blackwell Scientific Publicatoin. Oxford, 3. Ed., 1996.
- Rezende N.G.A.M. 1998. Reordenamento estratigráfico do Mesozoico da Bacia do Parnaíba. XL Congresso Brasileiro de Geologia, Belo Horizonte, *Anais...* SBG-MG, p. 111.
- Rezende N.A., 2002. A zona zeolitica da Formação Corda, Bacia do Parnaíba. Dissertação (de Mestrado), Universidade Federal do Pará, Belém, xv, 144 f.
- Ribeiro. H. J. 2001. *Estratigrafia de sequências – fundamentos e aplicações*. 1a ed.. Editora Unisinos. Porto Alegre. 428p.
- Romero Ballén O. A. R., 2012. As sucessões sedimentares interderrames da Formação Mosquito, exemplo de um sistema eólico úmido, Província Parnaíba. Dissertação (de Mestrado). USP – Universidade de São Paulo, xix, 85 f.
- Romero Ballén O. A., Góes A. M., Negri F. A., Mazivieiro M. V, Teixeira V.Z.S. Sistema eólico úmido nas sucessões sedimentares interderrames da Formação Mosquito, Jurássico da Província Parnaíba. *Brazillian Journal of Geology*, v. 43, n. 4, p. 695-710, 2013.
- Roxo M. & Löfgren A. *Lepidotus piauhyensis*, sp. nov. *Notas Preliminares e Estudos*. Divisão de Geologia e Mineralogia/DNPM, v. 1, p. 7–12, 1936.
- Retallack G. J. 2011. Exceptional fóssil preservation during CO₂ greenhouse crisis?, *Palaeogeography, Palaeoclimatology, Palaeoecology*, 307: 59-74.
- Sadler P.M., Osleger D.A., Monta~Nez, I.P., 1993. On the labeling, length, and objective basis of Fischer plots. *J. Sediment. Petrol.* 63: 360-368.
- Santos M. E. C. M. & Carvalho M. S. S., 2004. *Paleontologia das Bacias do Parnaíba, Grajaú e São Luís*, Ed. 2, CPRM, Rio Janeiro, 212p.
- Santos R. da S., 1953. Peixes triássicos dos folhelhos da Fazenda Muzinho, estado do Piauí. *Notas Preliminares e Estudos*. Rio de Janeiro, Departamento Nacional de Produção Mineral. DNPM, v. 82, p. 170-178.
- Santos R. Da S., 1974. A idade geológica da Formação Pastos Bons. *Anais da Academia Brasileira de Ciências*, Rio de Janeiro, v. 46, n.3, p. 589-592.
- Schobbenhaus C., Campos D.A., Queiroz E.T., Winge M., Berbertborn M. (eds.). *Sítios Geológicos e Paleontológicos do Brasil*. Brasília, DNPM/CPRM, 1984.
- Shanley K.W. & McCabe P.J., 1994. Perspectives on the sequence stratigraphy of continental strata. *American Association of Petroleum Geology*, 78(4): 544-568.
- Spence G.H. & Tucker M.E., 2007. A proposed integrated multi-signature model for peritidal cycles in carbonates. *J. Sediment. Res.* 77, 797-808.
- SOFTWARE Global Paleogeography. *PALEOMAP Project*. 2013. Disponível em: <<http://www.scotese.com/>>. Acesso em: 14/05/2016.
- Stevens-Kalceff M.A., Phillips M.R., Moon A.R., Kalceff W., 2000, Cathodoluminescence microcharacterisation of silicon dioxide polymorphs, *In*: Pagel, M., Barbin, V., Blanc, P., and Ohnenstetter, D., eds., *Cathodoluminescence in Geosciences*: Berlin, Springer-Verlag, p. 193-224.
- Strecker J.R., Steidtmann J.R., Smithson S.B. 1999. A conceptual tectonostratigraphic model for seismic facies migrations in a fluvio-lacustrine extensional basin: *American Association of Petroleum Geologists, Bulletin*, 83: 43-61.

Terra G.J.S., De Ros L.F., Moraes M.A.S. 1982. Porosidade secundária nos arenitos jurássicos da Bacia do Recôncavo. *Anais do XXXII Congresso Brasileiro de Geologia*, Salvador, Bahia.

Torsvik T. H. & Cocks L. R. M. Gondwana from top to base in space and time. *Gondwana Research*, n. 24, p. 999-1030, 2013.

Tucker M. E. *Sedimentary petrology: an introduction the origin of sedimentary rocks*. Ed. Oxford: Blackwell Science. 2. Ed, 1991. 260p.

Twichett R. J. 2006. The palaeoclimatology, palaeoecology and palaeoenvironmental analysis of mass extinction events. *Palaeogeography, /palaeoclimatology, palaeoclimate*, 232: 190-213.

Uchupi E. & Emery K.O. Pangean divergent margins: historical perspective. In: A.W. Meyer, T.A. Davies & S.W. Wise (eds). *Evolution of Mesozoic and Cenozoic Continental Margins. Mar. Geol*, v. 102, p. 1-28, 1991

Vaz P.T., Rezende N.G.A.M., Wanderley Filho J.R., Travassos W.A.S. Bacia do Parnaíba. *Boletim de Geociências da Petrobras*, v. 15, n. 2, p. 253-263, 2007.

Vail P.R. 1987. Seismic stratigraphy interpretation using sequence stratigraphy. In: Bally, W.A. (Ed.), *Atlas of Seismic Stratigraphy. V 1, AAPG Studies Geology*, 27: 1-10.

Vail P.R. & Posamentier H. P. 1988, Principles of sequence stratigraphy: in James, D.P., & D.A. Leckie, (eds.), *Sequences, stratigraphy, sedimentology; surface and subsurface*, CSPG Memoir 15, p. 572

Van Wagoner J.C., Mitchum R.M., Campion K.M., Rahmanian V.D. 1990. Siliciclastic sequence stratigraphy in well logs, core and outcrop: Concepts for high-resolution correlation of time and facies. *American Association of Petroleum Geology, Methods in Exploration*; No. 7, 55 p.

Veevers J. J. Gondwanaland from 650-500 Ma assembly through 320 Ma merger in Pangea to 185-100 Ma breakup: supercontinental tectonics via stratigraphy and radiometric dating. *Earth-Science Reviews*, n. 68, p. 1-132, 2004.

Victor Zalán P. Influence of pre-Andean orogenies on the Paleozoic intracratonic basins of South America. *IV Simpósio Bolivariano*, Bogotá, v. 1, n. 7, p. 17-29, 1991.

Walker R. G (ed.). Facies, facies models and modern stratigraphic concepts. In: R. G. Walker & N. P. James (eds.), *Facies Models - Response to Sea Level Change*. Ontario, Ed. Geological Association of Canada, Canada, v. 1, p. 1-14, 1992.

Watt G.R., Wright P., Galloway S. & Mclean C. 1997, Cathodoluminescence and trace element zoning in quartz phenocrysts and xenocrysts: *Geochimica et Cosmochimica Acta*, v. 61, p. 4337-4348.

Wei W., Lu Y., Xing F., Liu Z., Pan, L., Algeo T.J., 2017. Sedimentary facies associations and sequence stratigraphy of source and reservoir rocks of the lacustrine Eocene Niubao Formation (Lunpola Basin, central Tibet). *Marine and Petroleum Geology*, 86: 1273-1290.

Wincander R. & Monroe J. S. *Historical Geology*. Central Michigan University, EUA, Emeritus.7. Ed, 2013. 448p.

Winter J.D.; 2001. *An Introduction to Igneous and Metamorphic Petrology*. Prentice-Hall, New Jersey.

Zecchin M. & Catuneanu O, 2013. High-resolution of sequence stratigraphy of clastic shelves I: units and bounding surfaces. *Marine and Petroleum Geology*, 39: 1-25.

Zecchin M., Catuneanu O., Caffau M. 2017. High-resolution of sequence stratigraphy of clastic shelves V: Criteria to discriminate between stratigraphic sequences and sedimentological cycles. *Marine and Petroleum Geology*, 85: 259-271.

APÊNDICE A – TABELAS DE CONTAGEM

Tabela 2 - Contagem de pontos e índice de Kahn dos arenitos da Formação Pastos Bons.

	PB-10	PB-08c	PB-08a	PB-06b	PB-02a	PB-02b	PB-02c	PB-11c	FL-09	FL-02a
Quartzo monocristalino	203	251	245	165	270	244	266	210	215	212
Quartzo policristalino	16	13	5	6	20	9	2	13	19	3
Plagioclásio	1	0	5	2	4	1	0	41	10	14
Álcali-feldspato	0	0	0	1	3	2	1	0	3	2
Fragmento de rocha vulcânica	1	0	0	0	0	1	0	0	2	0
Fragmento de quartzito	0	0	0	0	0	0	0	1	1	0
Fragmento de arenito	1	1	0	1	1	0	0	0	0	0
Fragmento de pelito	0	0	0	2	0	1	0	1	0	0
Fragmento de chert	2	0	1	1	2	1	1	3	0	0
Cimento carbonático	76	40	50	0	0	44	30	0	23	69
Zircão	0	0	1	0	0	1	0	0	0	0
Matriz argilosa	0	0	0	143	0	0	0	31	27	3
	Quartzarenito	Quartzarenito	Quartzarenito	Grauvaca	Quartzarenito	Quartzarenito	Quartzarenito	Quartzarenito	Subarcósio	Subarcósio
Grão-grão	8	13	8	5	24	22	26	31	53	60
Grão-não grão	92	87	92	95	76	78	74	69	47	40
Empacotamento	Aberto	Aberto	Aberto	Aberto	Aberto	Aberto	Aberto	Aberto	Normal	Fechado

Tabela 3 - Contagem de minerais pesados da Formação Pastos Bons.

	PB-11d	PB-11a	PB-02d(F)	PB-02d (G)	PB-06a	PB-06b	PB-06c	PB-04a	PB-02e
Zircão	23%	51%	6%	21%	26%	62,70%	37,50%	1,90%	31,50%
Turmalina	53%	31%	44%	17%	72%	29%	59%	77%	21%
Rutilo	12%	18%	6%	8,50%	2%	7,30%	3,50%	1,00%	6,30%
Epidoto	8%	0%	1%	0%	0%	0%	0%	0,00%	0%
Granada	4%	0%	41%	54%	1%	1%	0%	12,50%	36,50%
Titanita	2%	1%	0%	0%	0%	0%	0%	0,00%	1,40%
Hornblenda	0%	0%	2%	0%	0%	0%	0%	0,00%	0%
Piroxênio	0%	0%	0%	0%	0%	0%	0%	7,70%	2,90%

Tabela 4 - Contagem de minerais pesados da Formação Corda.

	AM-1	AM-2a	AM-2b	AM-3	AM-4	AM-5	AM-6	AM-9	P2-1	P5-1
Zircão	44%	31,6%	21,7%	35,8%	25,2%	2,6%	4,4%	23,5%	51,1%	5
Turmalina	13%	34,3%	41,5%	27,3%	22,2%	9,3%	1,4%	1,5%	39,4%	91%
Rutilo	2%	1,4%	0,0%	3,9%	3,4%	0,0%	15,8%	10,0%	6,4%	0%
Epidoto	12%	16,4%	3,3%	7,4%	16,8%	0,0%	0,4%	0,0%	1,1%	0%
Granada	8%	10,9%	30,4%	11,4%	20,7%	87,9%	71,2%	64,5%	0,5%	4%
Titanita	0,0%	0,0%	0,0%	1,4%	0,4%	0,0%	0,0%	0,0%	0,0%	0%
Estaurolita	0,0%	0,0%	0,0%	0,9%	0,4%	0,0%	0,0%	0,0%	0,0%	0%
Clinopiroxênio	21%	2,4%	1,9%	8,9%	8,9%	0,0%	6,4%	0,5%	1,1%	0%
Andalusita	0%	2,4%	0,9%	2,4%	1,4%	0,0%	0,0%	0,0%	0,0%	0%

Tabela 5 - Contagem de minerais pesados da Formação Grajaú.

	PB-05i	PB-05j
Turmalina	32,90%	15,40%
Zircão	12,90%	23,80%
Rutilo	4,50%	5,20%
Hornblenda	15,70%	52,60%
Granada	27,10%	3%
Estaurolita	1%	0,00%
Estaurolita	1,70%	0,40%
Sillimanita	1,00%	0,00%
Clinopiroxênio	3,20%	2,60%

Tabela 6 - Catodoluminescência de quartzo - Diagrama de Bernet e Basset (2005).

	Quartzo vulcânico	Quartzo plutônico	Quartzo metamórfico
PB-02a	95	0	5
PB-02b	94	1	5
PB-02c	91	3	6
PB-06a	88	2	10
PB-08a	92	2	6
PB-08c	88	5	7
PB-10	97	0	3
PB-11c	91	1	8
FL-09	93	0	7
FL-02a	95	1	4
A3-8	96	4	0
A3-1	94	6	0
A1-20	91	6	3
A1-22	93	3	4
CD3-1	97	1	2
AM-1	94	2	4
AM-2	92	1	7
AM-6	98	0	2